Multispectral Remote Sensing

Lectures in Benevento
June 2007

Paul Menzel
UW/CIMSS/AOS

Applications with Multispectral Remote Sensing Data

Satellite Remote Sensing

Energy Balance

VIS, IR, and MW Radiative Transfer

EOS Terra & Aqua MODIS

Multispectral Signatures

(Ocean Color, Snow/Ice, Vegetation, Aerosols, Clouds, Moisture, Fires, Volcanic Ash)

Detecting Climate Trends

Satellite remote sensing of the Earth-atmosphere

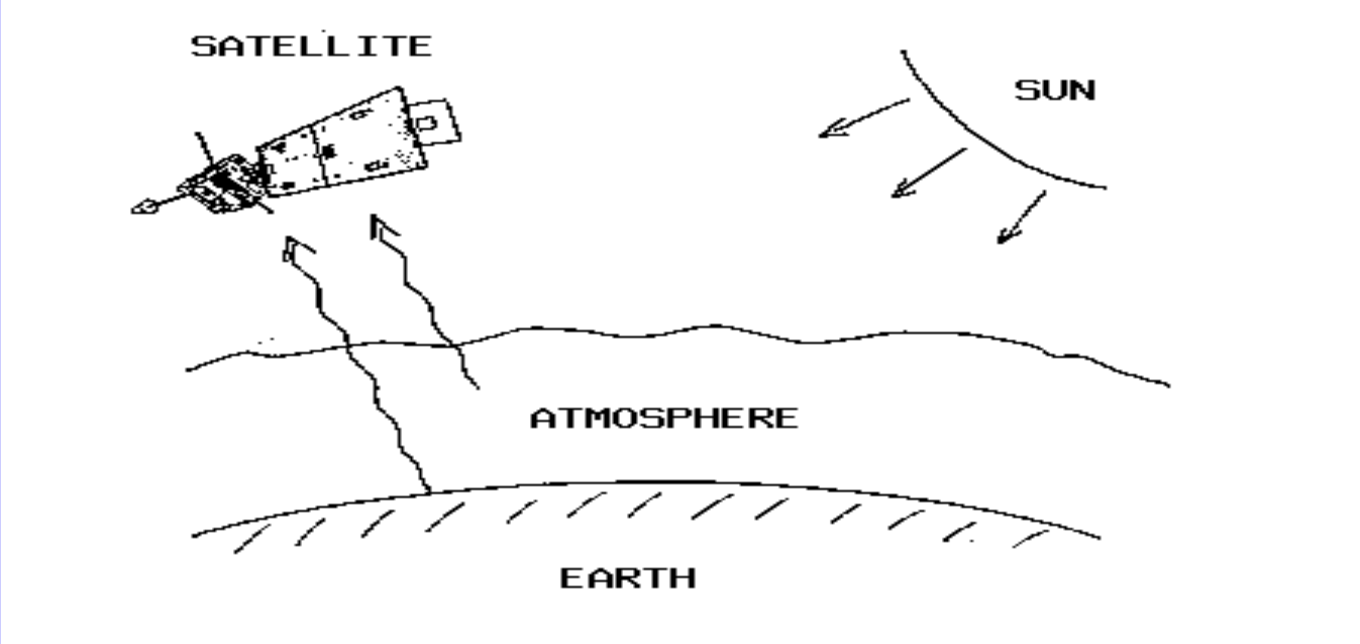

Observations depend on

telescope characteristics (resolving power, diffraction)
detector characteristics (signal to noise)
communications bandwidth (bit depth)
spectral intervals (window, absorption band)
time of day (daylight visible)
atmospheric state (T, Q, clouds)
earth surface (Ts, vegetation cover)

Remote Sensing Advantages

* provides a regional view

* enables one to observe & measure the causes & effects of climate & environmental changes (both natural & human-induced)

* provides repetitive geo-referenced looks at the same area

* covers a broader portion of the spectrum than the human eye

* can focus in on a very specific bandwidth in an image

* can also look at a number of bandwidths simultaneously

* operates in all seasons, at night, and in bad weather

Solar (visible) and Earth emitted (infrared) energy

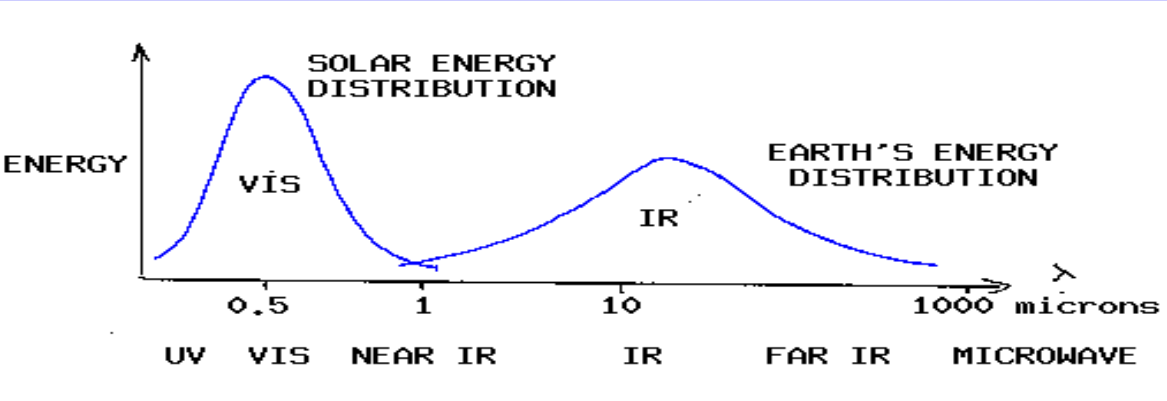

Incoming solar radiation (mostly visible) drives the earth-atmosphere (which emits infrared).

Over the annual cycle, the incoming solar energy that makes it to the earth surface (about 50 %) is balanced by the outgoing thermal infrared energy emitted through the atmosphere.

The atmosphere transmits, absorbs (by H2O, O2, O3, dust) reflects (by clouds), and scatters (by aerosols) incoming visible; the earth surface absorbs and reflects the transmitted visible. Atmospheric H2O, CO2, and O3 selectively transmit or absorb the outgoing infrared radiation. The outgoing microwave is primarily affected by H2O and O2.

Key Areas of Uncertainty in Understanding Climate & Global Change

* Earth's radiation balance and the influence of clouds on radiation and the hydrologic cycle

* Oceanic productivity, circulation and air-sea exchange

* Transformation of greenhouse gases in the lower atmosphere, with emphasis on the carbon cycle

* Changes in land use, land cover and primary productivity, including deforestation

* Sea level variability and impacts of ice sheet volume

* Chemistry of the middle and upper stratosphere, including sources and sinks of stratospheric ozone

* Volcanic eruptions and their role in climate change

Radiative Energy Balance

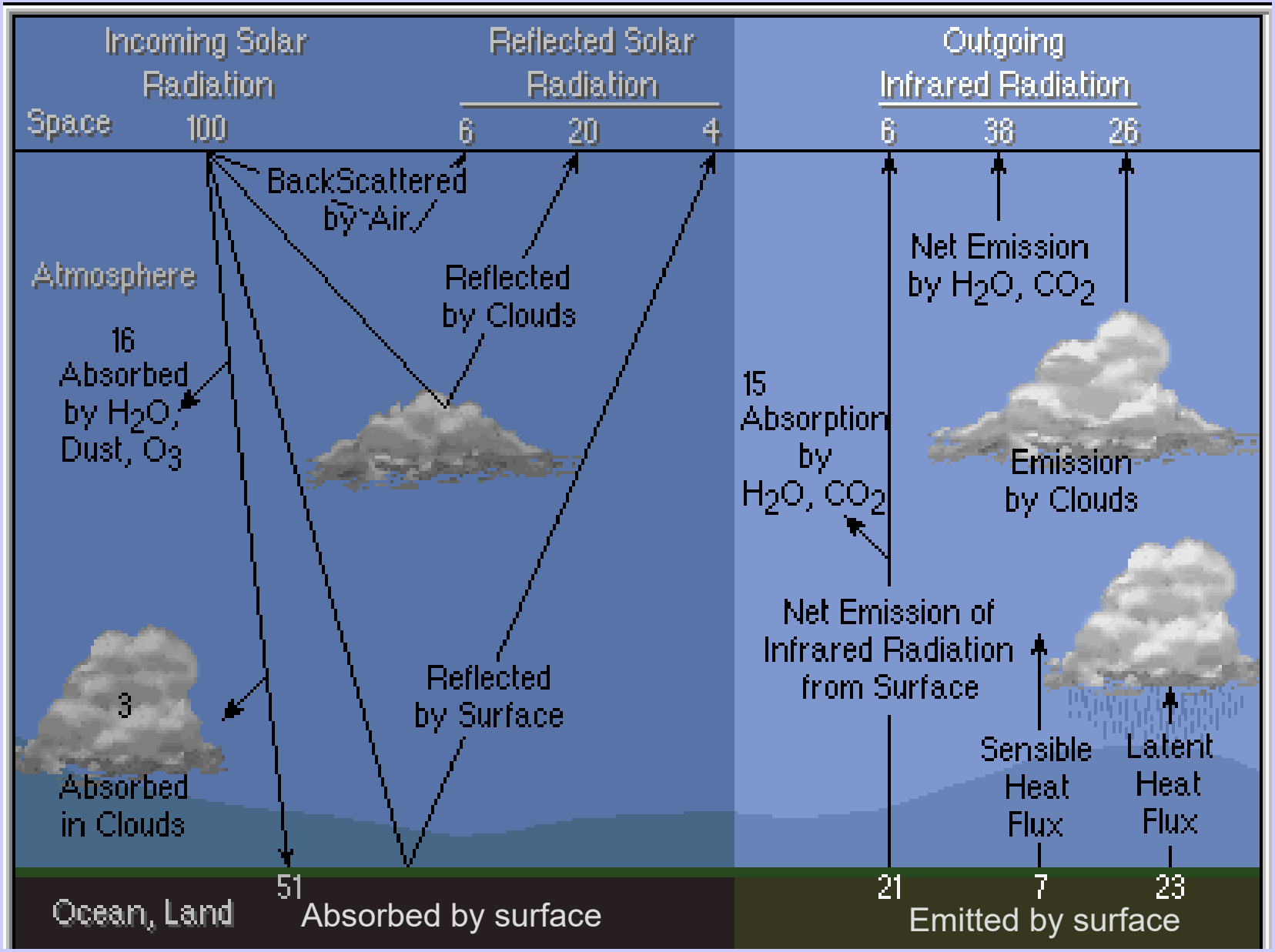

Solar Spectrum

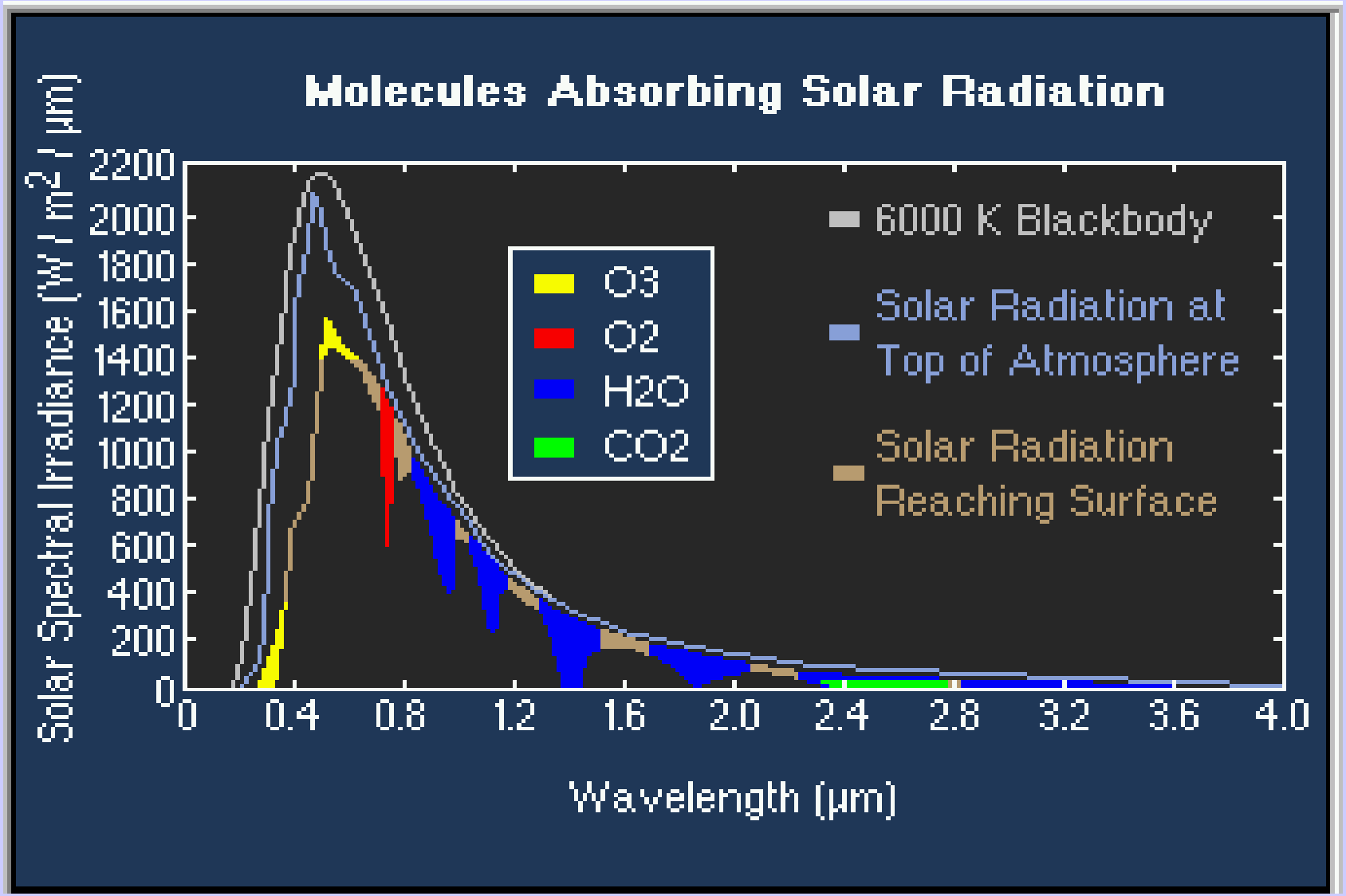

Earth emitted spectra overlaid on Planck function envelopes

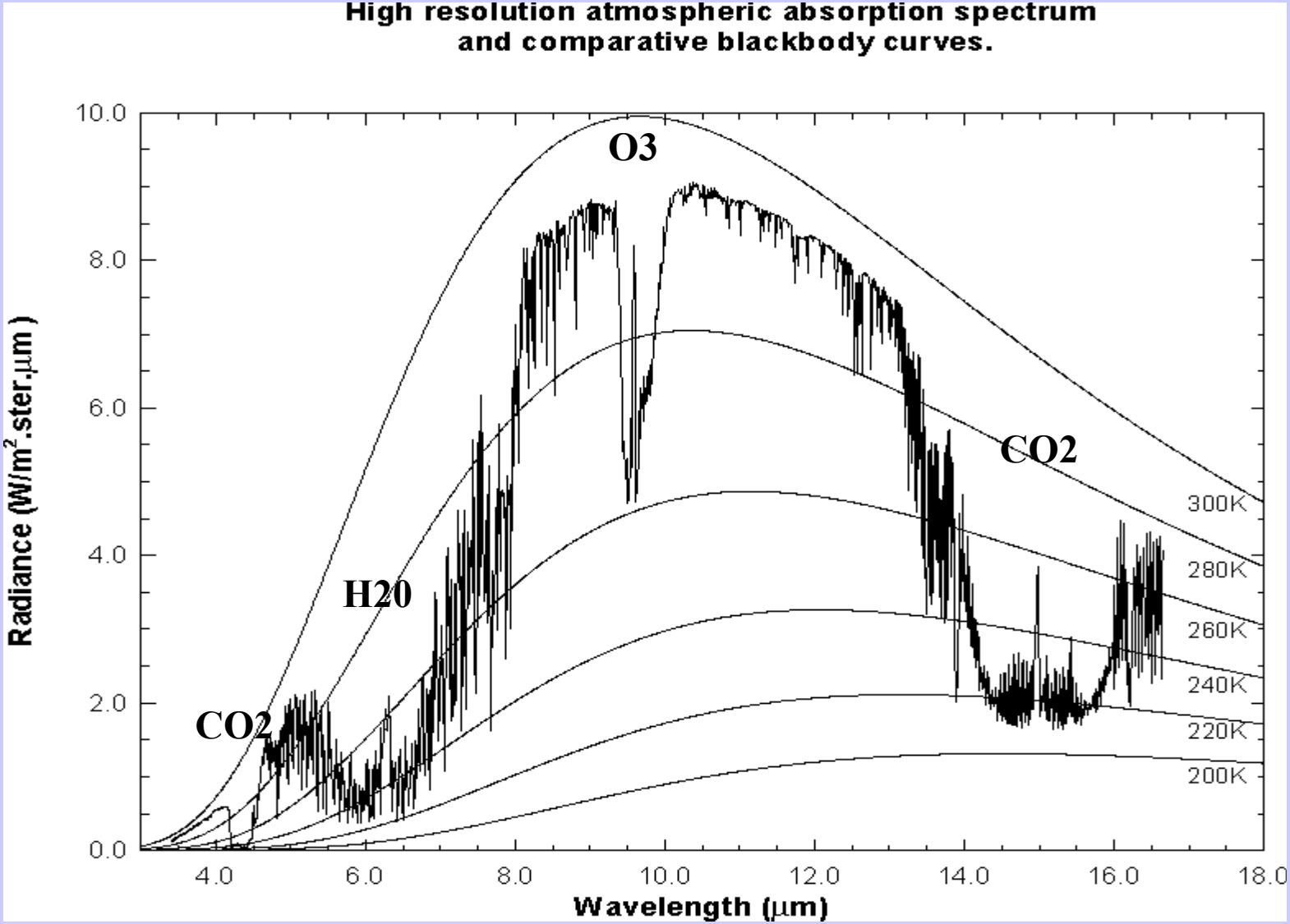

Radiative Transfer through the Atmosphere

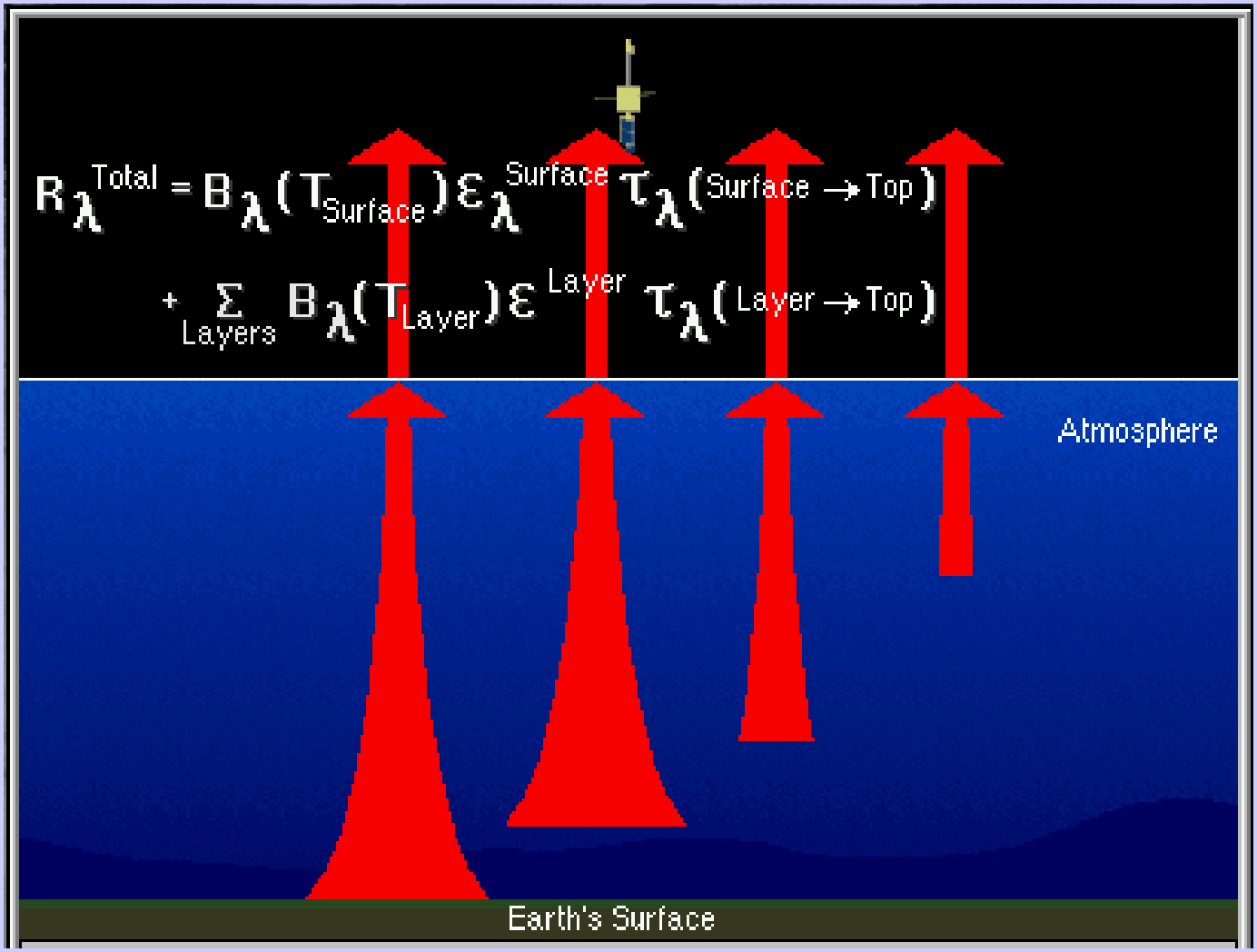

When reflection from the earth surface is also considered, the Radiative Transfer Equation for infrared radiation can be written

$$I_\lambda = \varepsilon_\lambda^{sfc} B_\lambda(T_s) \tau_\lambda(p_s) + \int_{p_s}^{o} B_\lambda(T(p)) F_\lambda(p) [d\tau_\lambda(p) / dp] dp$$

where

$$F_\lambda(p) = \{ 1 + (1 - \varepsilon_\lambda) [\tau_\lambda(p_s) / \tau_\lambda(p)]^2 \}$$

The first term is the spectral radiance emitted by the surface and attenuated by the atmosphere, often called the boundary term and the second term is the spectral radiance emitted to space by the atmosphere directly or by reflection from the earth surface.

The atmospheric contribution is the weighted sum of the Planck radiance contribution from each layer, where the weighting function is [$d\tau_\lambda(p) / dp$]. This weighting function is an indication of where in the atmosphere the majority of the radiation for a given spectral band comes from.

Including surface emissivity

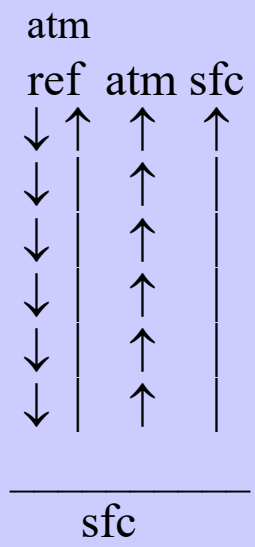

$$I^{sfc}_{\lambda} = \varepsilon_\lambda B_\lambda(T_s)\,\tau_\lambda(p_s) + (1-\varepsilon_\lambda)\,\tau_\lambda(p_s) \int_o^{p_s} B_\lambda(T(p))\,\frac{\partial \tau'_\lambda(p)}{\partial \ln p}\,d\ln p$$

$$I_\lambda = \varepsilon_\lambda B_\lambda(T_s)\,\tau_\lambda(p_s) + (1-\varepsilon_\lambda)\,\tau_\lambda(p_s) \int_o^{p_s} B_\lambda(T(p))\,\frac{\partial \tau'_\lambda(p)}{\partial \ln p}\,d\ln p + \int_{p_s}^{o} B_\lambda(T(p))\,\frac{\partial \tau_\lambda(p)}{\partial \ln p}\,d\ln p$$

using $\tau'_\lambda(p) = \tau_\lambda(p_s) / \tau_\lambda(p)$ then.

$$\frac{\partial \tau'_\lambda(p)}{\partial \ln p} = - \frac{\tau_\lambda(p_s)}{(\tau_\lambda(p))^2}\,\frac{\partial \tau_\lambda(p)}{\partial \ln p}$$

Thus

$$I_\lambda = \varepsilon_\lambda B_\lambda(T(p_s))\,\tau_\lambda(p_s) + \int_{p_s}^{o} BT(p)\,F_\lambda(p)\,\frac{\partial \tau_\lambda(p)}{\partial \ln p}\,d\ln p$$

where

$$F_\lambda(p) = \{\, 1 + (1 - \varepsilon_\lambda)\,[\frac{\tau_\lambda(p_s)}{\tau_\lambda(p)}]^2 \,\}\,.$$

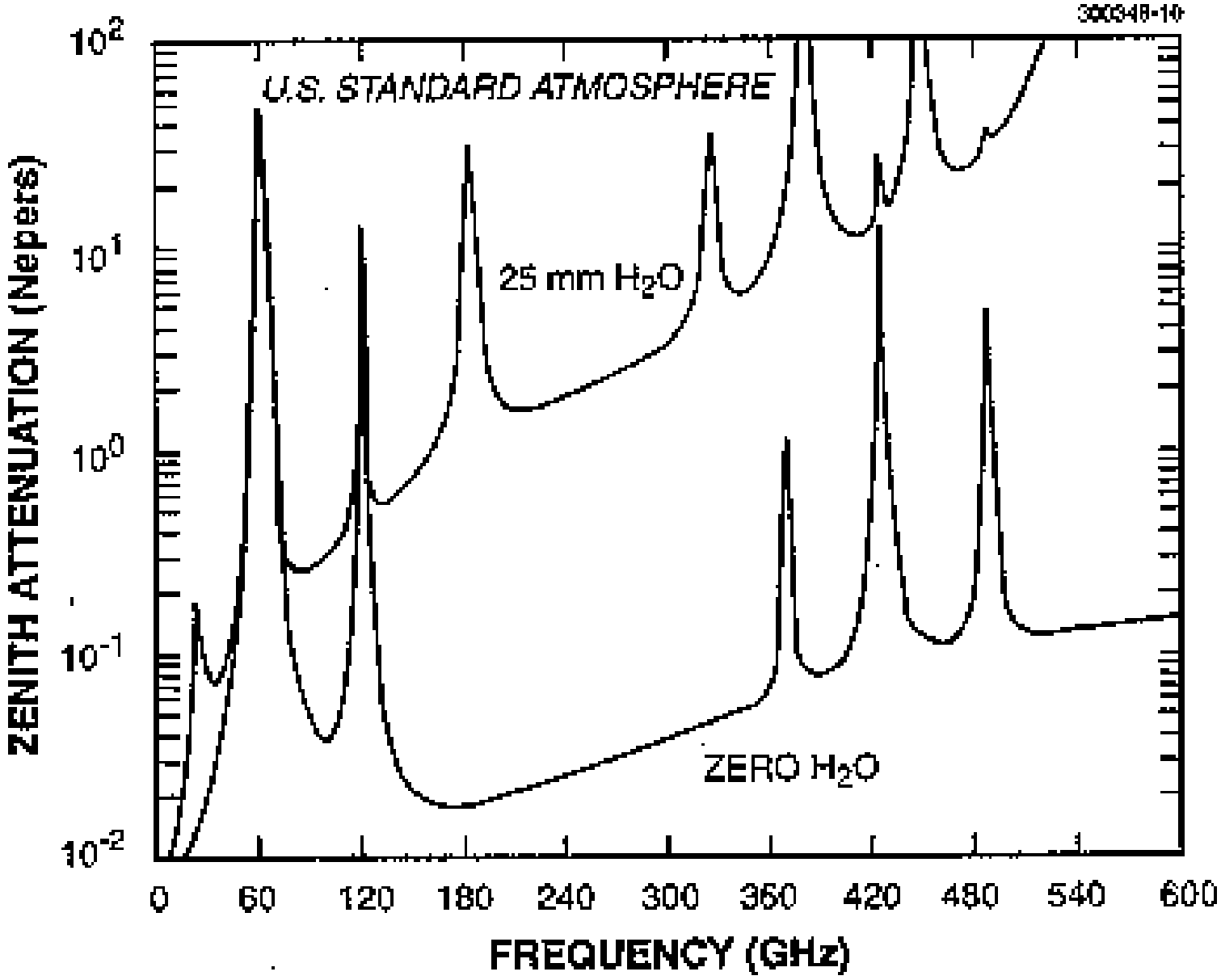
U.S. STANDARD ATMOSPHERE
25 mm H_2O
ZERO H_2O
ZENITH ATTENUATION (Nepers)
10^2
10^1
10^0
10^{-1}
10^{-2}
0
60
120
180
240
300
360
420
480
540
600
FREQUENCY (GHz)

Joint Polar System

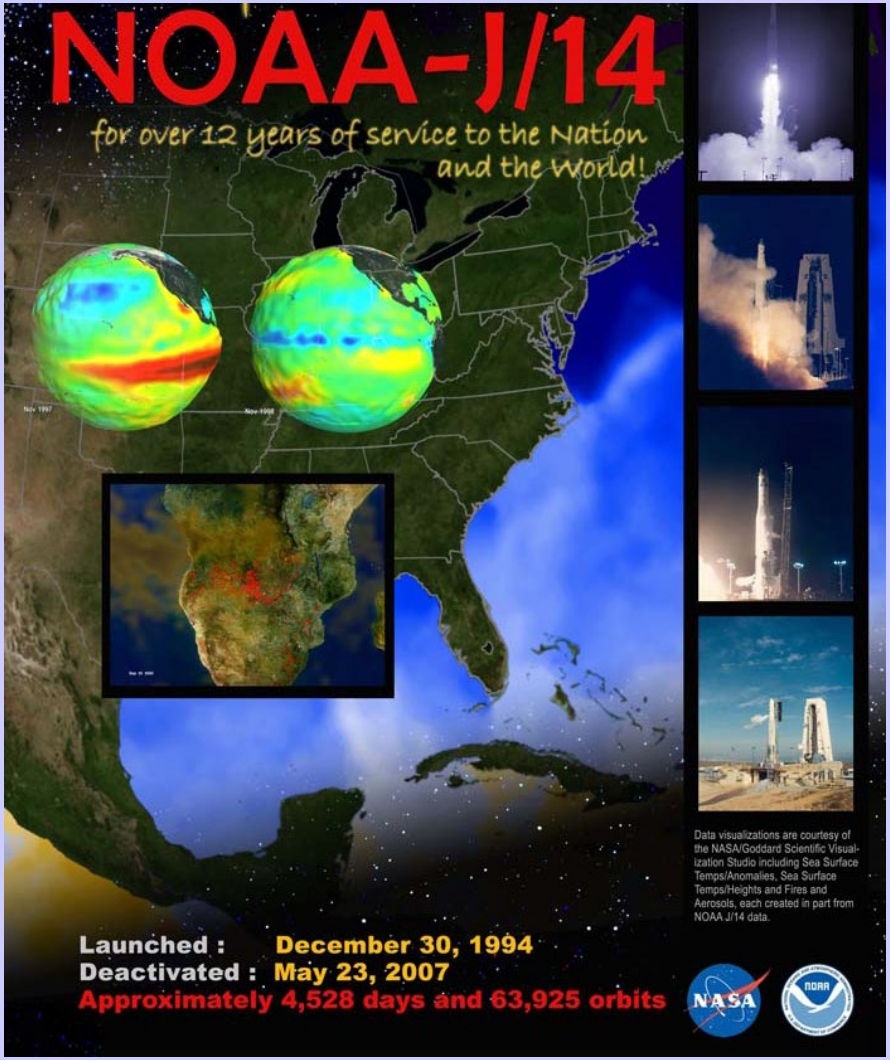

Atmospheric Products: Examples

Winds

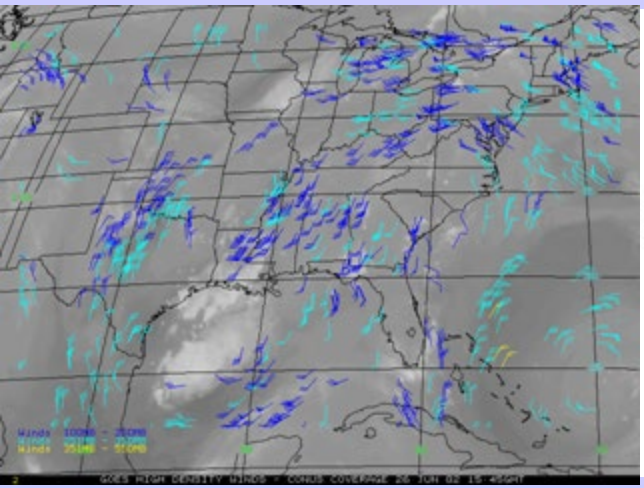

Total Water Vapor

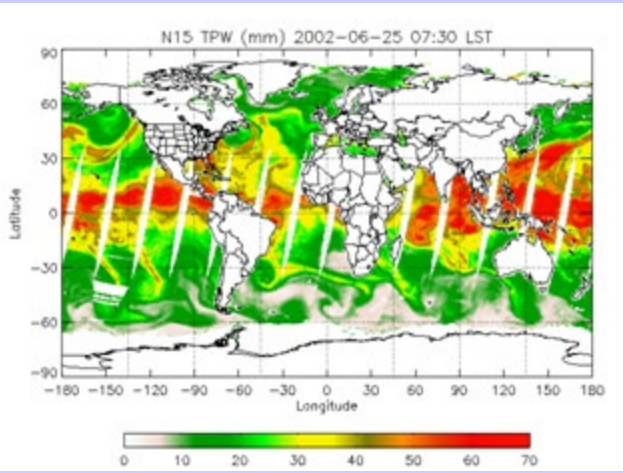

Temperature 500 mb

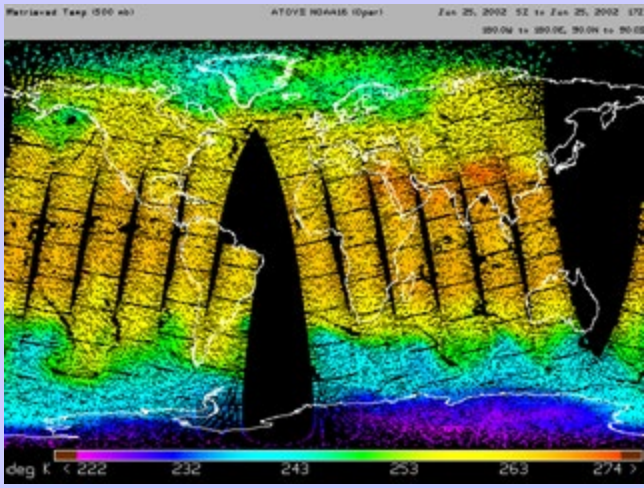

Rain Rate

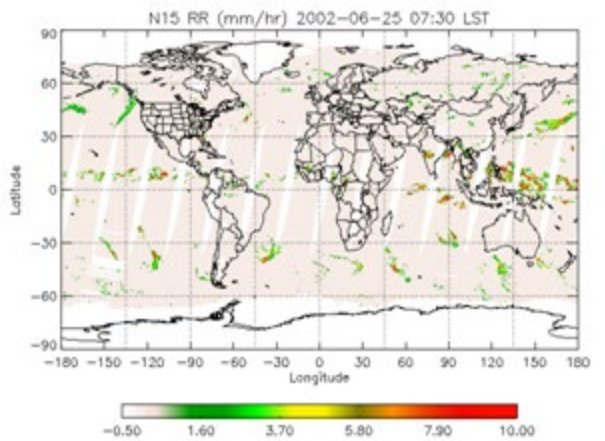

Ozone

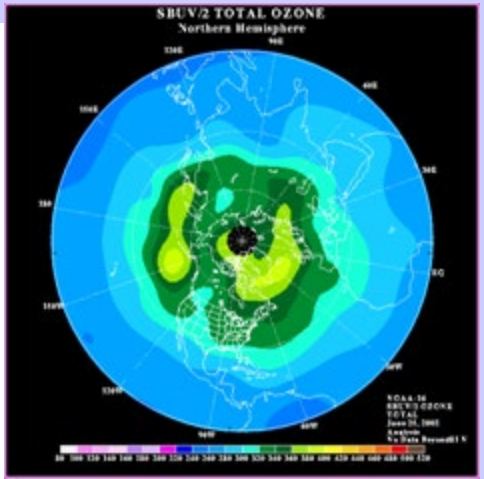

Aerosol Optical Thickness

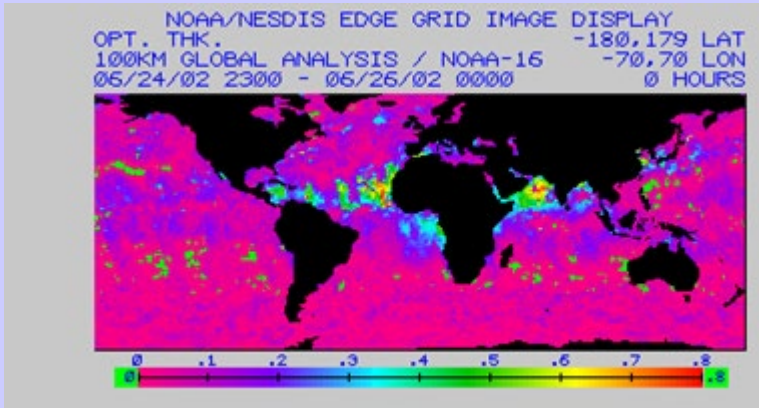

Land Surface Products: Examples

Vegetation Health

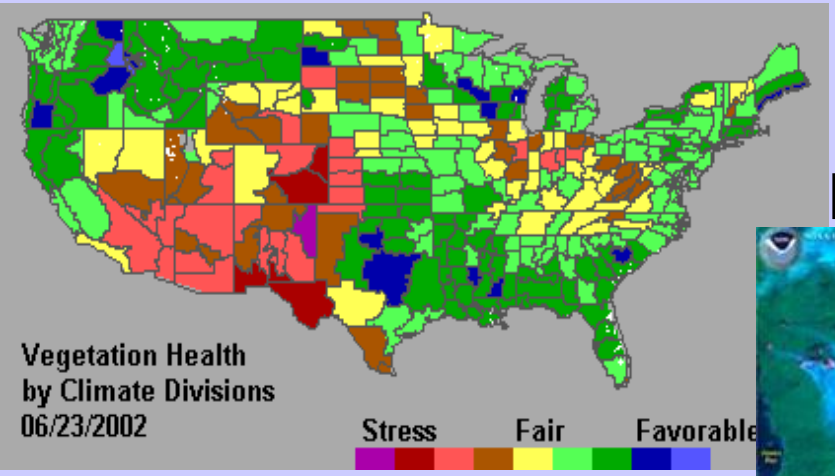

Quebec Fires/Smoke

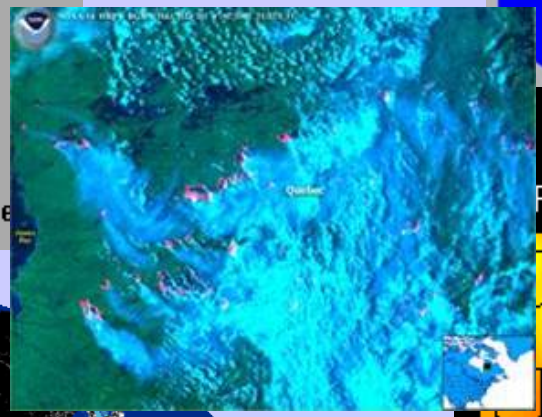

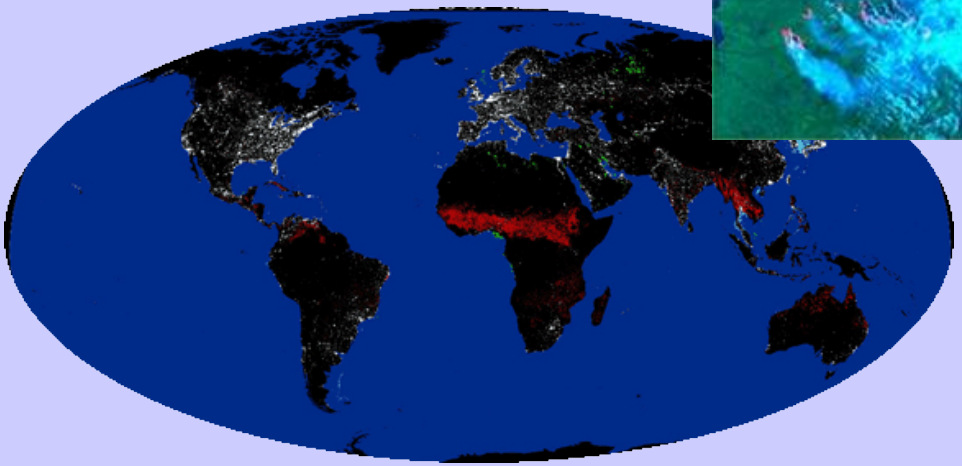

Global Lights/Fires

Solar Radiation

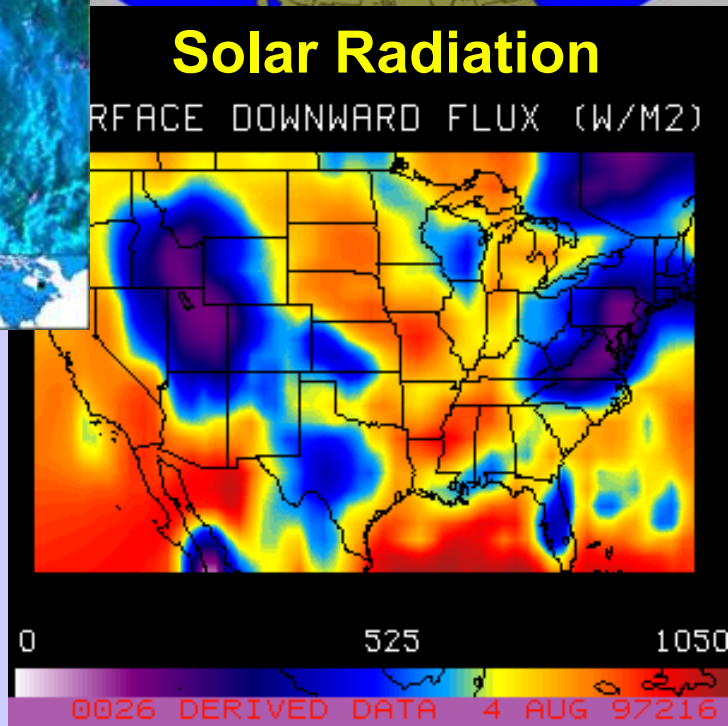

Ocean Products: Examples

SST Anomalies

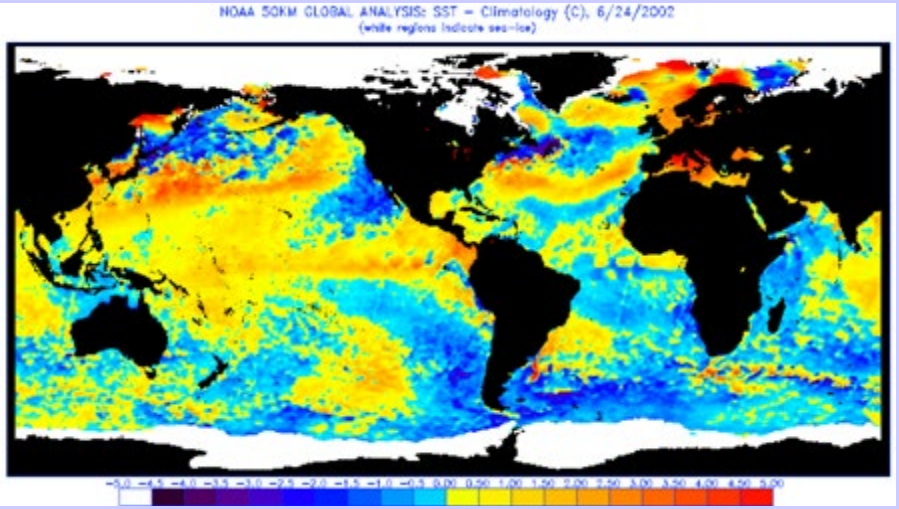

Hot Spots: Potential Coral Bleaching

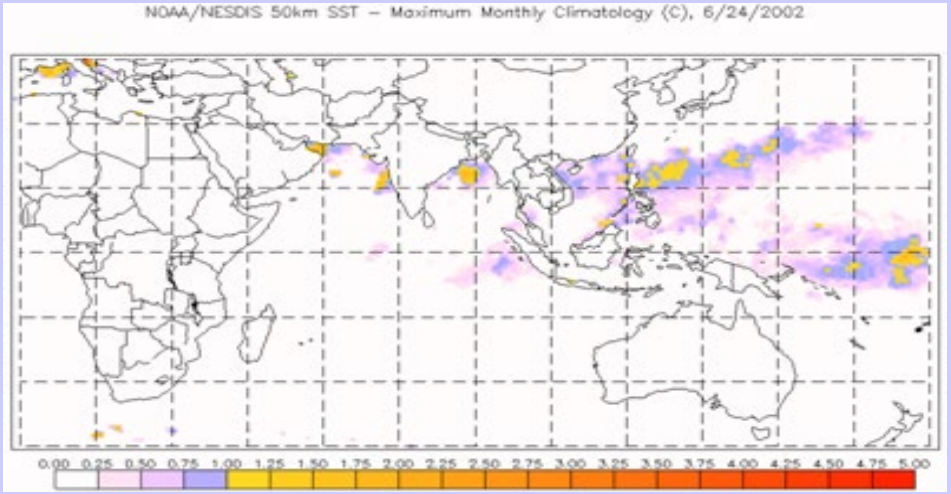

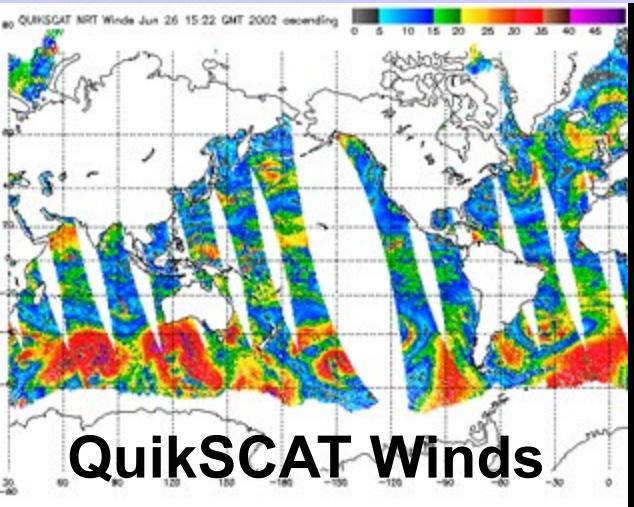

QuikSCAT Winds

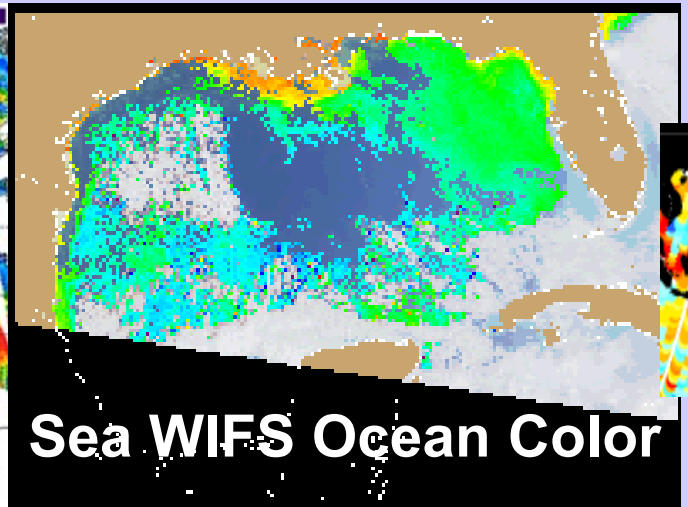

Sea WIFS Ocean Color

TOPEX Sea Level

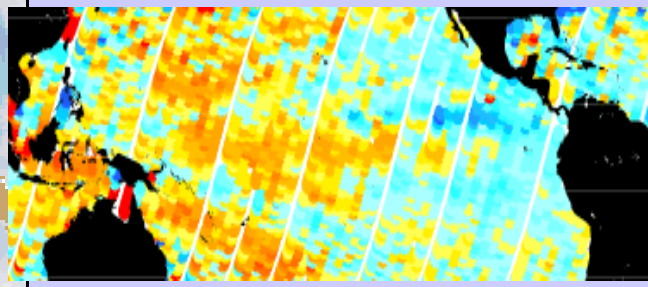

Applications with Multispectral Remote Sensing Data

Satellite Remote Sensing

Energy Balance

VIS, IR, and MW Radiative Transfer

EOS Terra & Aqua MODIS

Multispectral Signatures

(Ocean Color, Snow/Ice, Vegetation, Aerosols, Clouds, Moisture, Fires, Volcanic Ash)

Detecting Climate Trends

Evolution of Leo Obs

Terra was launched in 1999 and the EOS Era began

MODIS, CERES, MOPITT, ASTER, and MISR reach polar orbit

Aqua and ENVISAT followed in 2002

MODIS and MERIS to be followed by VIIRS
AIRS and IASI to be followed by CrIS
AMSU leading to ATMS

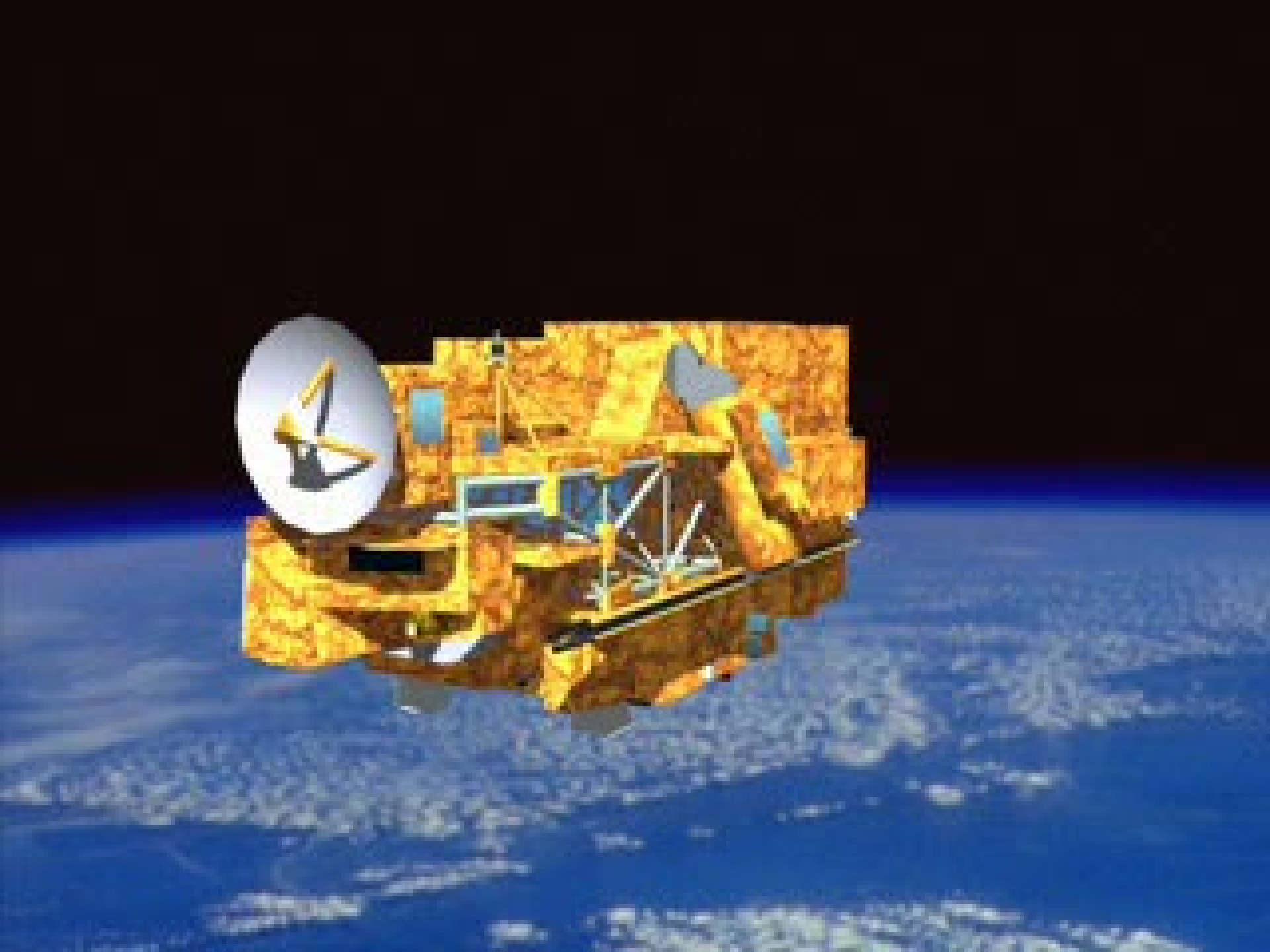

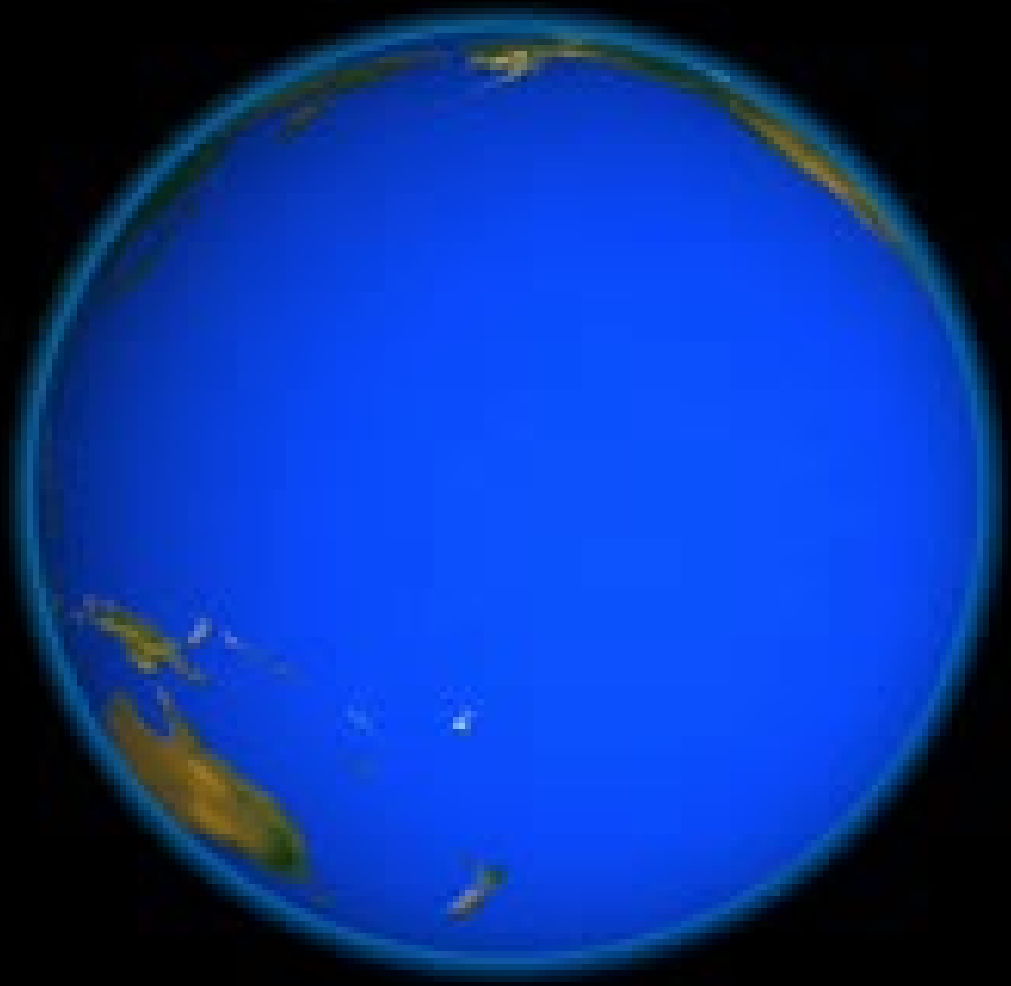

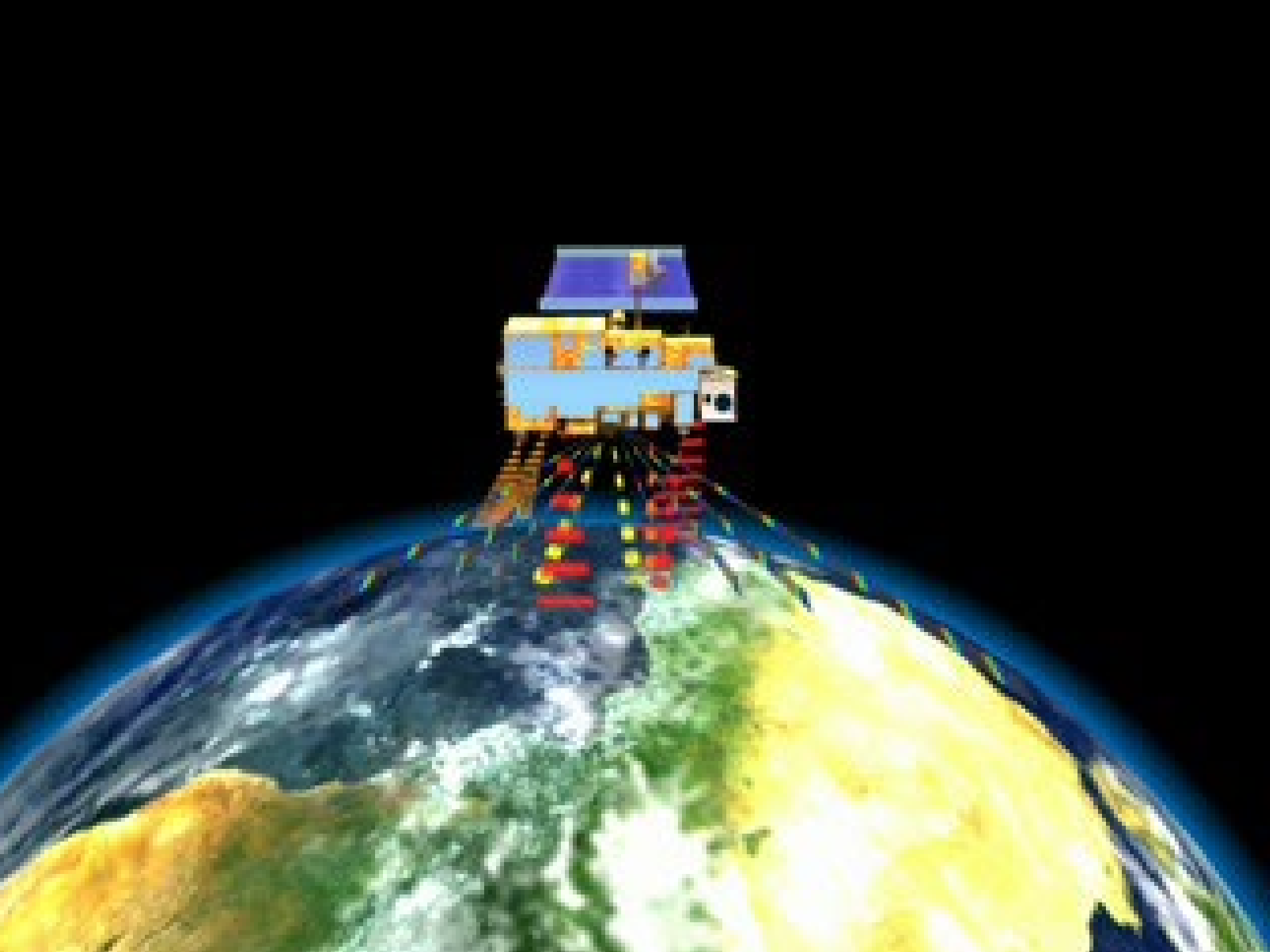

All Sats on NASA J-track

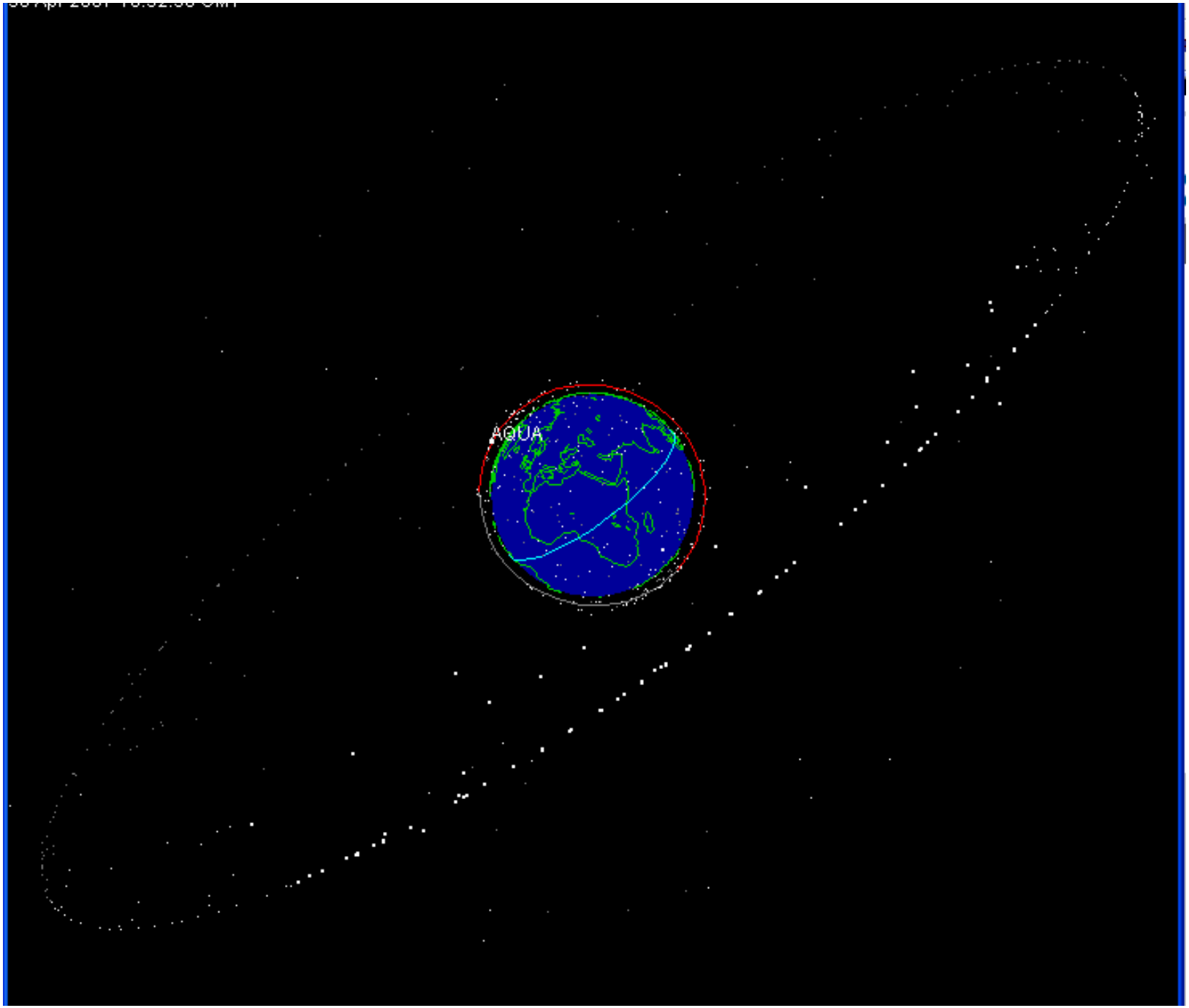

Launch of EOS-Terra (EOS-AM) Satellite - A New Era Begins

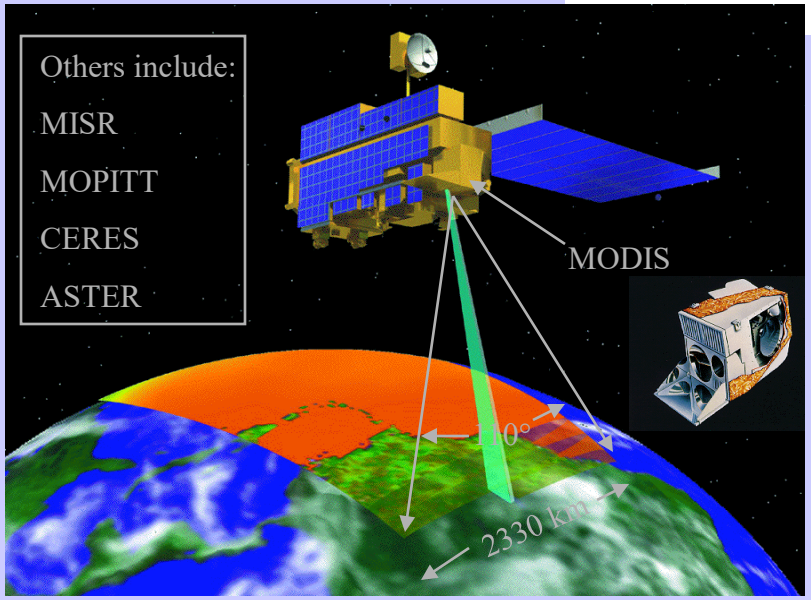

MODIS instrument Specifications:

Bands 1-2 (0.66,0.86 μm): 250 m

Bands 3-7 (0.47, 0.55, 1.24, 1.64, 2.13 μm): 500 m

Bands 8-36: 1 km

Launch date: December 18, 1999, 1:57 PT
Earth viewdoor open date: February 24, 2001

Allen Chu/NASA GSFC

Followed by the launch of EOS-Aqua (EOS-PM) Satellite

“ ”

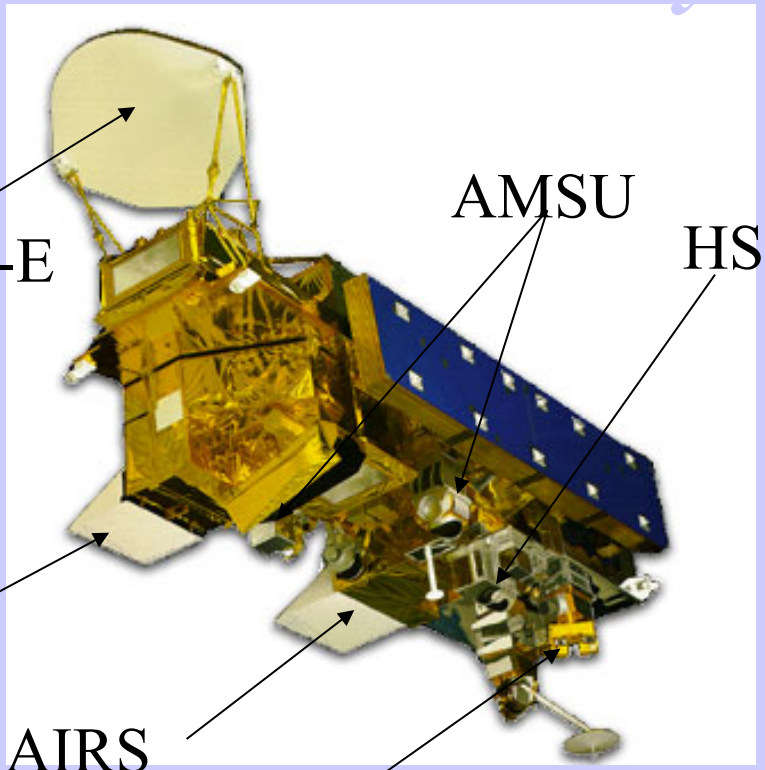

Launch date: May 4, 2002, 2:55 PDT
Earth view door open date: June 25, 2002

VIIRS, MODIS, FY-1C, AVHRR

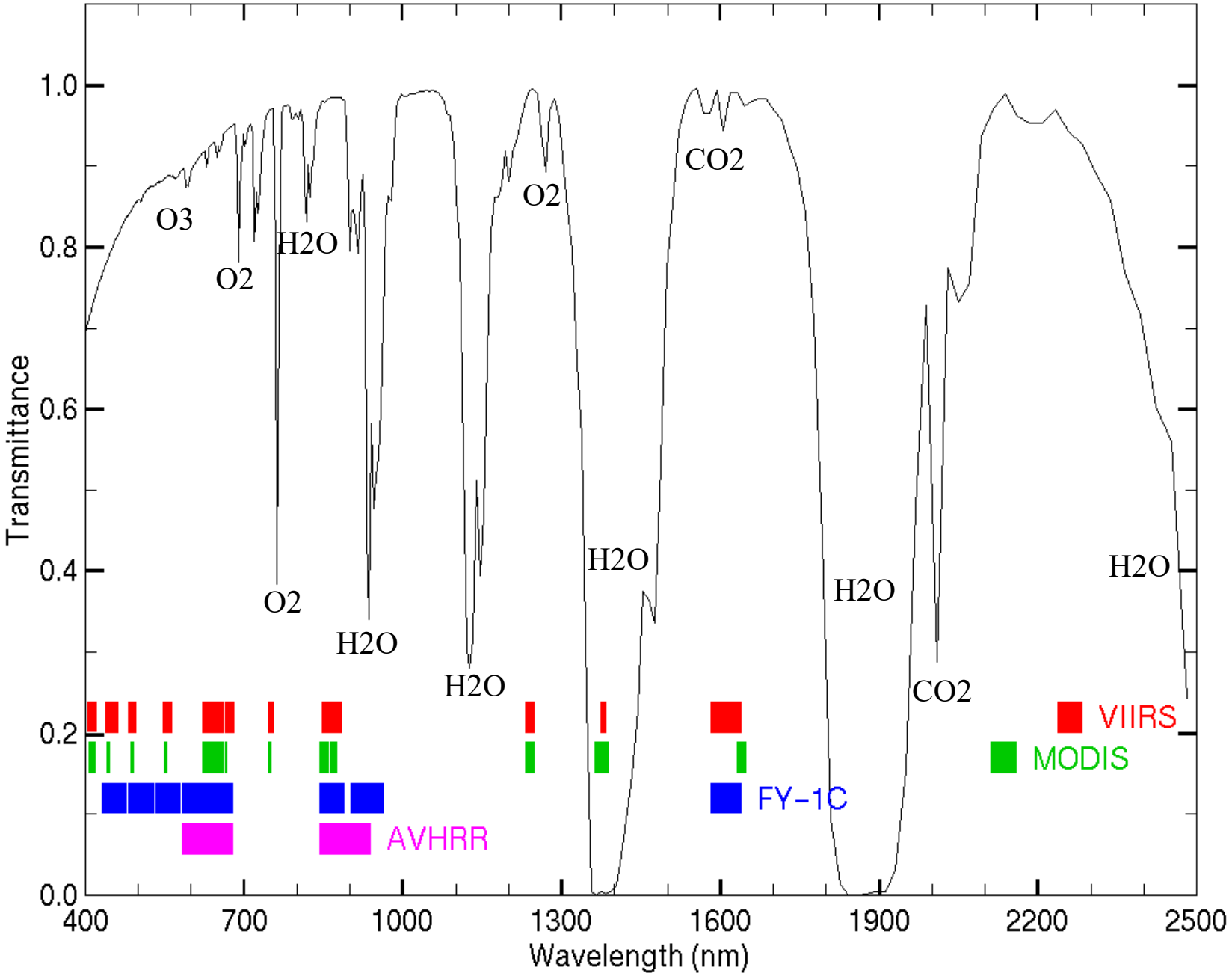

MODIS IR Spectral Bands

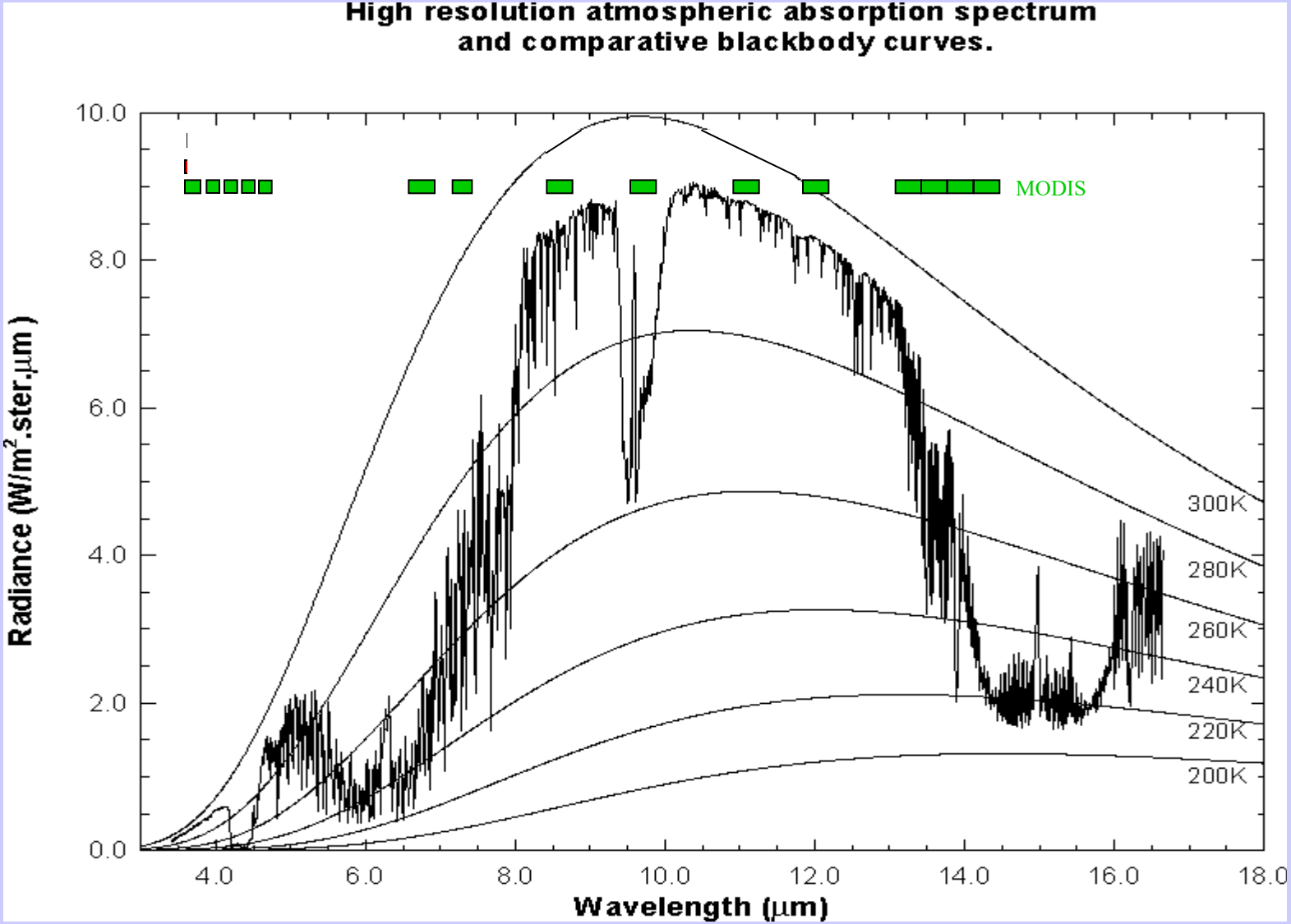

Applications with Multispectral Remote Sensing Data

Satellite Remote Sensing

Energy Balance

VIS, IR, and MW Radiative Transfer

EOS Terra & Aqua MODIS

Multispectral Signatures

*(**Ocean Color, SST**, Snow/Ice, Vegetation, Aerosols, Clouds, Moisture, Fires, Volcanic Ash)*

Detecting Climate Trends

OCEAN-SOLAR RADIATION

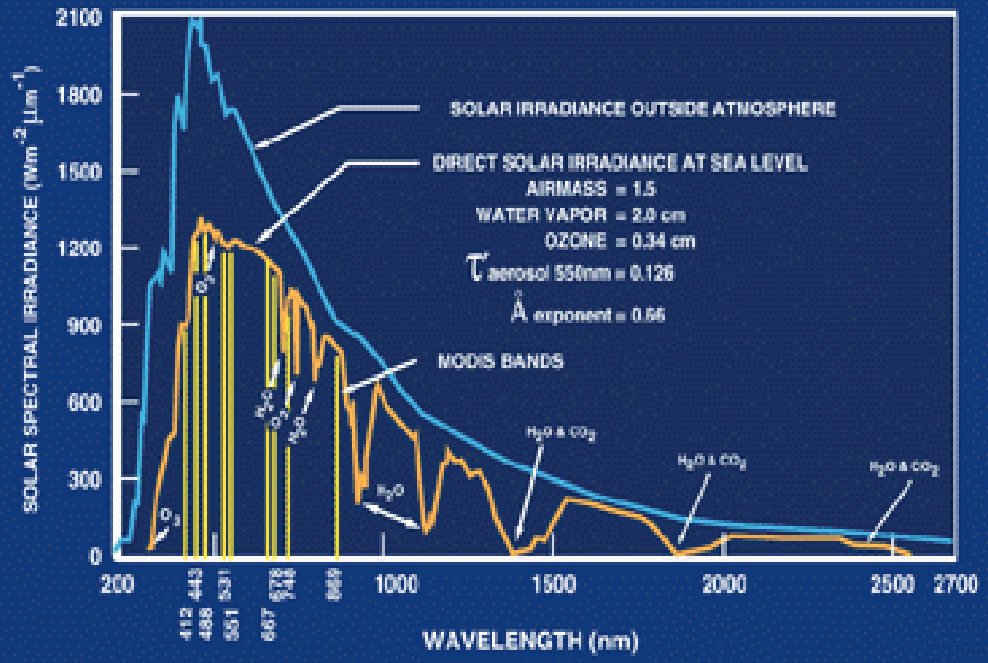

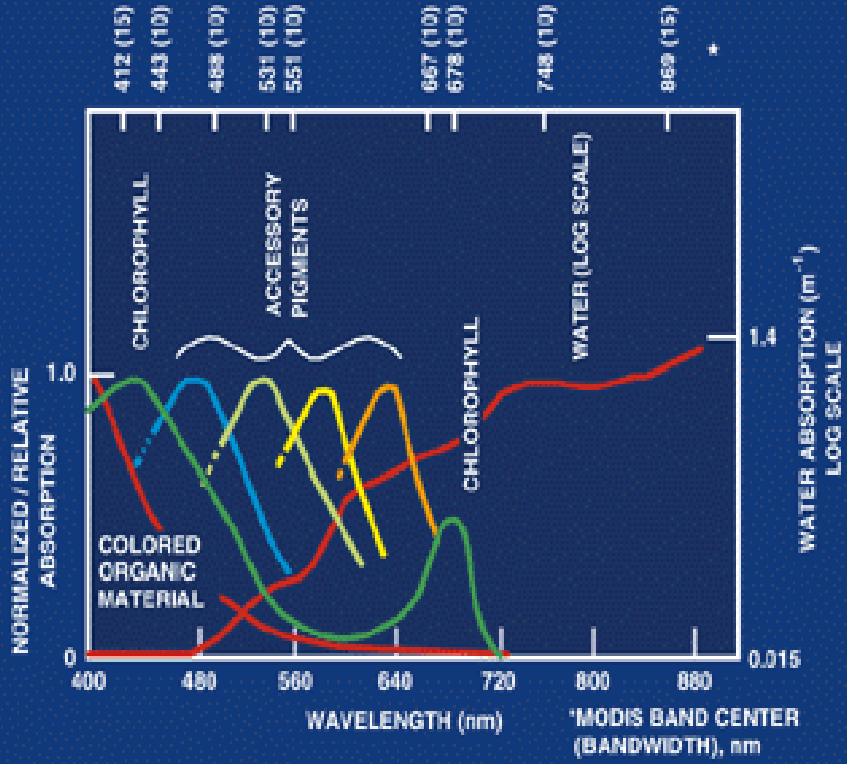

Chlorophyll - MODIS and SeaWiFS

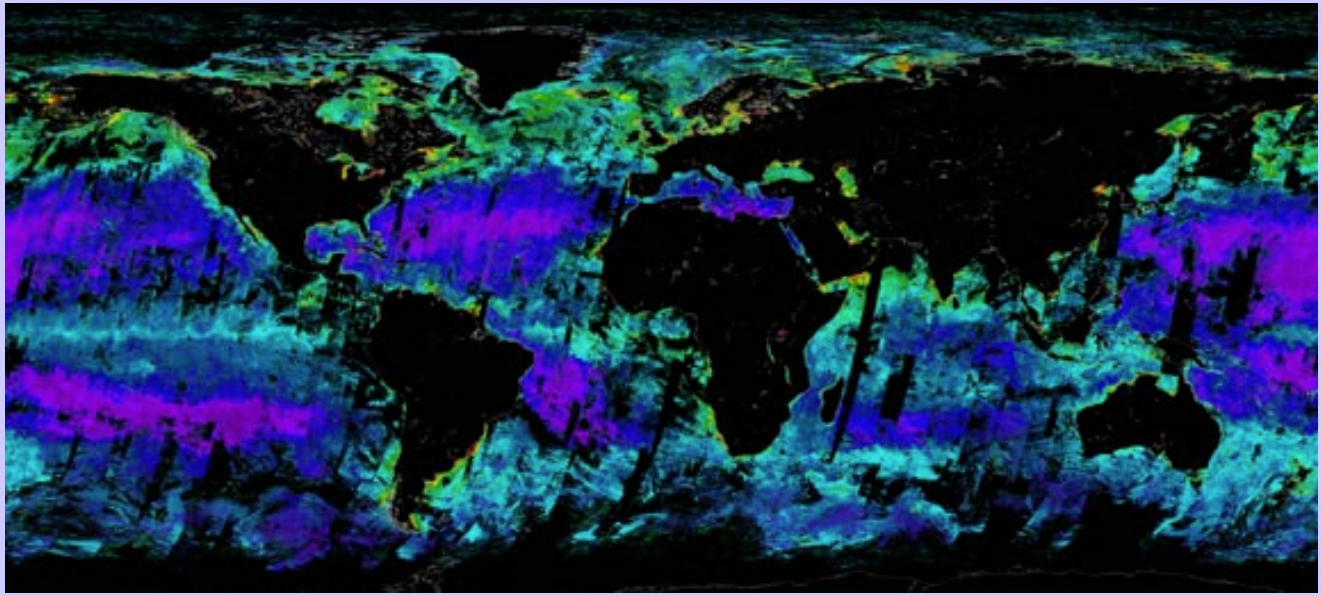

MODIS Chlor
243-250, 2000
U. Miami

MODIS tropics coverage is greater (time of day + no tilt loss). MODIS reveals global fine structure. Color scales not identical, cal not final.

SeaWiFS Chlor
241-248, 2000
SeaWIFS Project

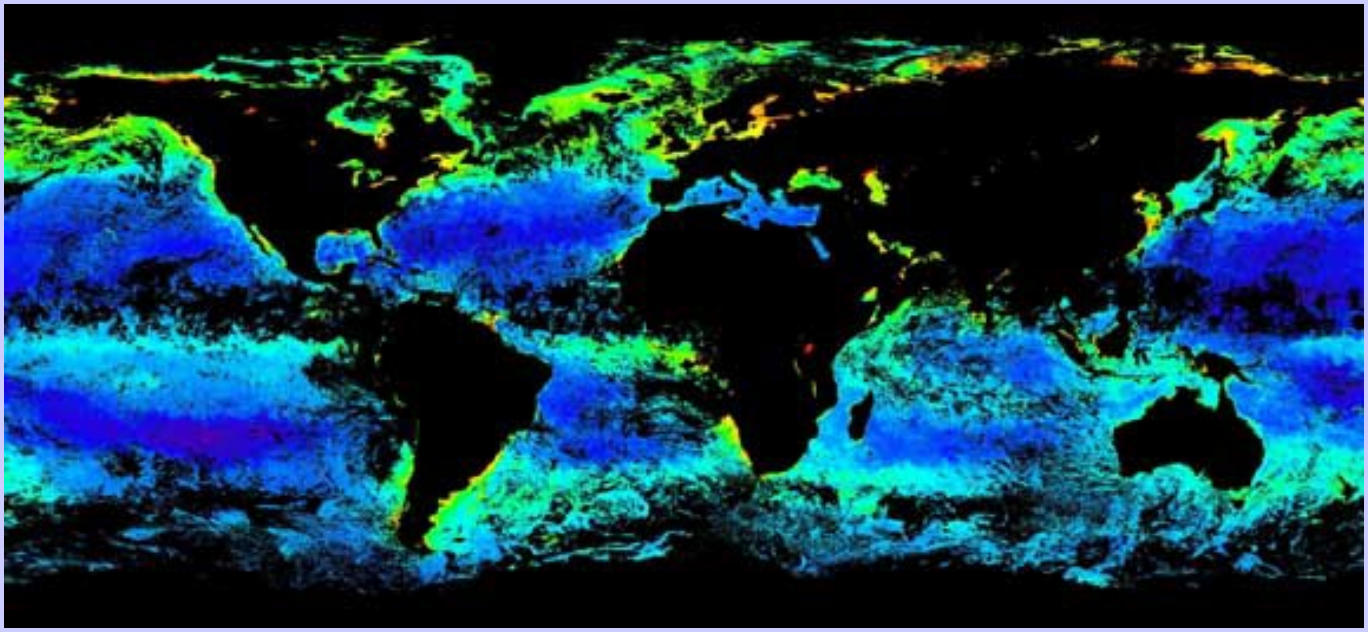

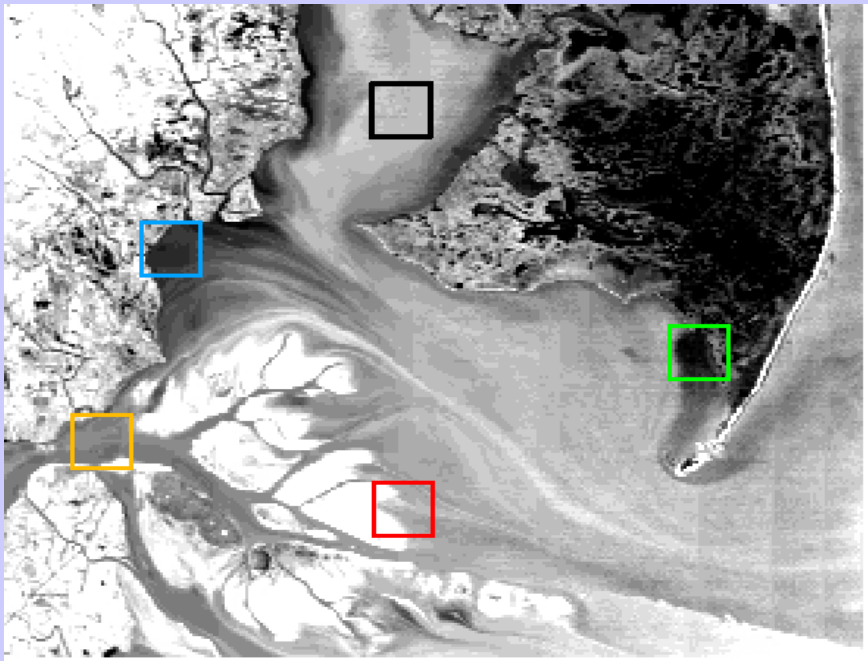

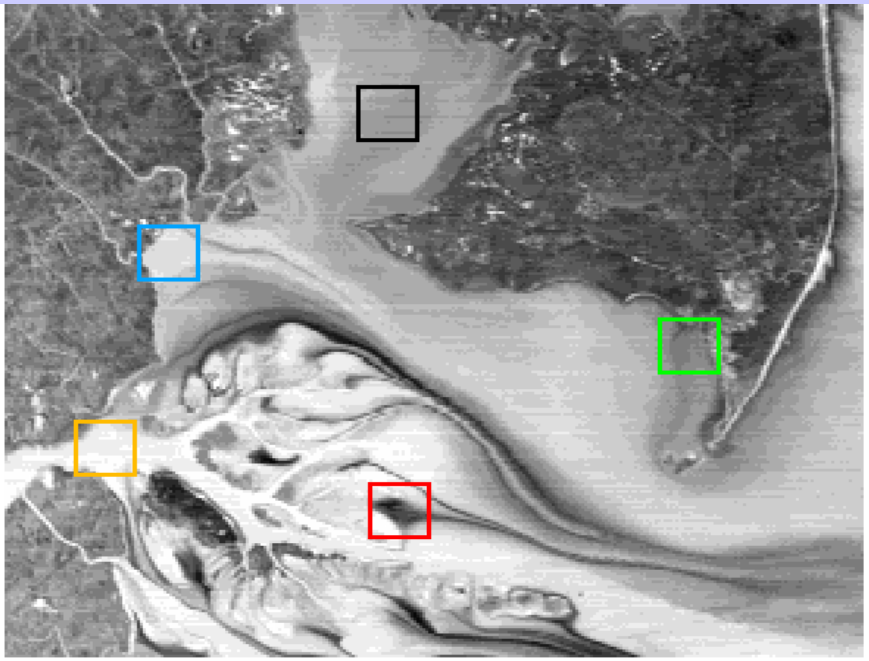

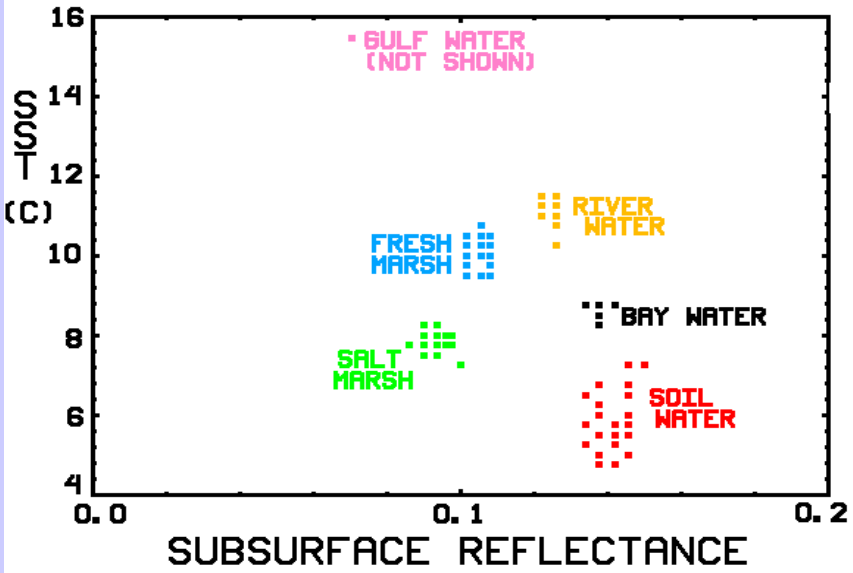

MAMS WATER TYPE ANALYSIS
DEC 4 1990

SHOWN:

* .66um REFLECTANCE (LEFT)
* SPLIT WINDOW SST (RIGHT)

First Order Estimation of SST

Moisture attenuation in atmospheric windows varies linearly with optical depth.

$$\tau_\lambda = e^{-k_\lambda u} = 1 - k_\lambda u$$

For same atmosphere, deviation of brightness temperature from surface temperature is a linear function of absorbing power. Thus moisture corrected SST can inferred by using split window measurements and extrapolating to zero k_λ

$$T_s = T_{bw1} + [\, k_{w1} / (k_{w2} - k_{w1}) \,] \, [T_{bw1} - T_{bw2}] \; .$$

Moisture content of atmosphere inferred from slope of linear relation.

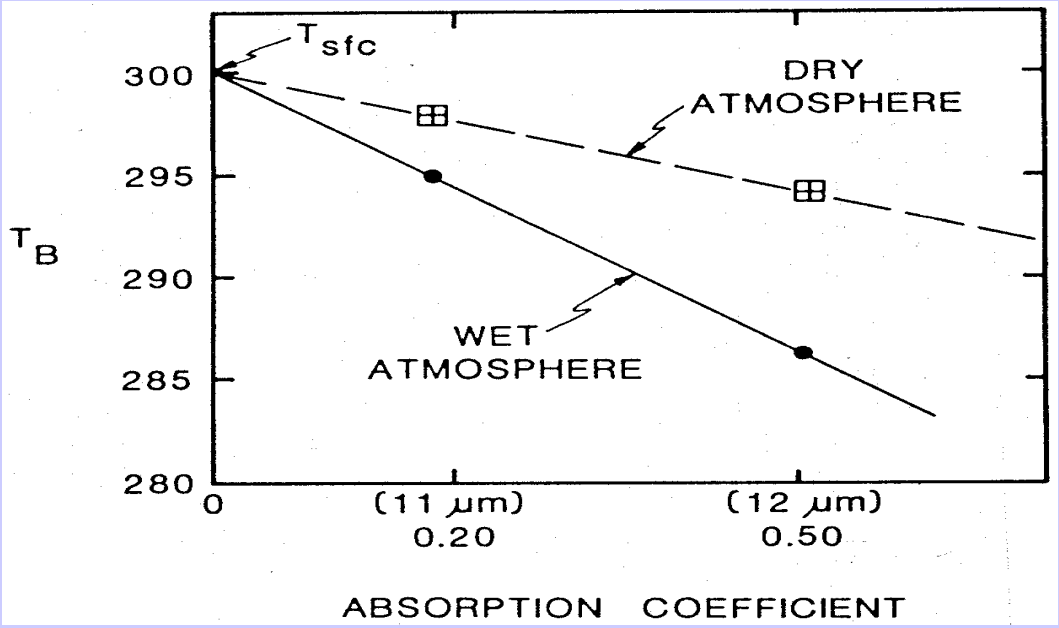

MODIS SEA SURFACE TEMPERATURE

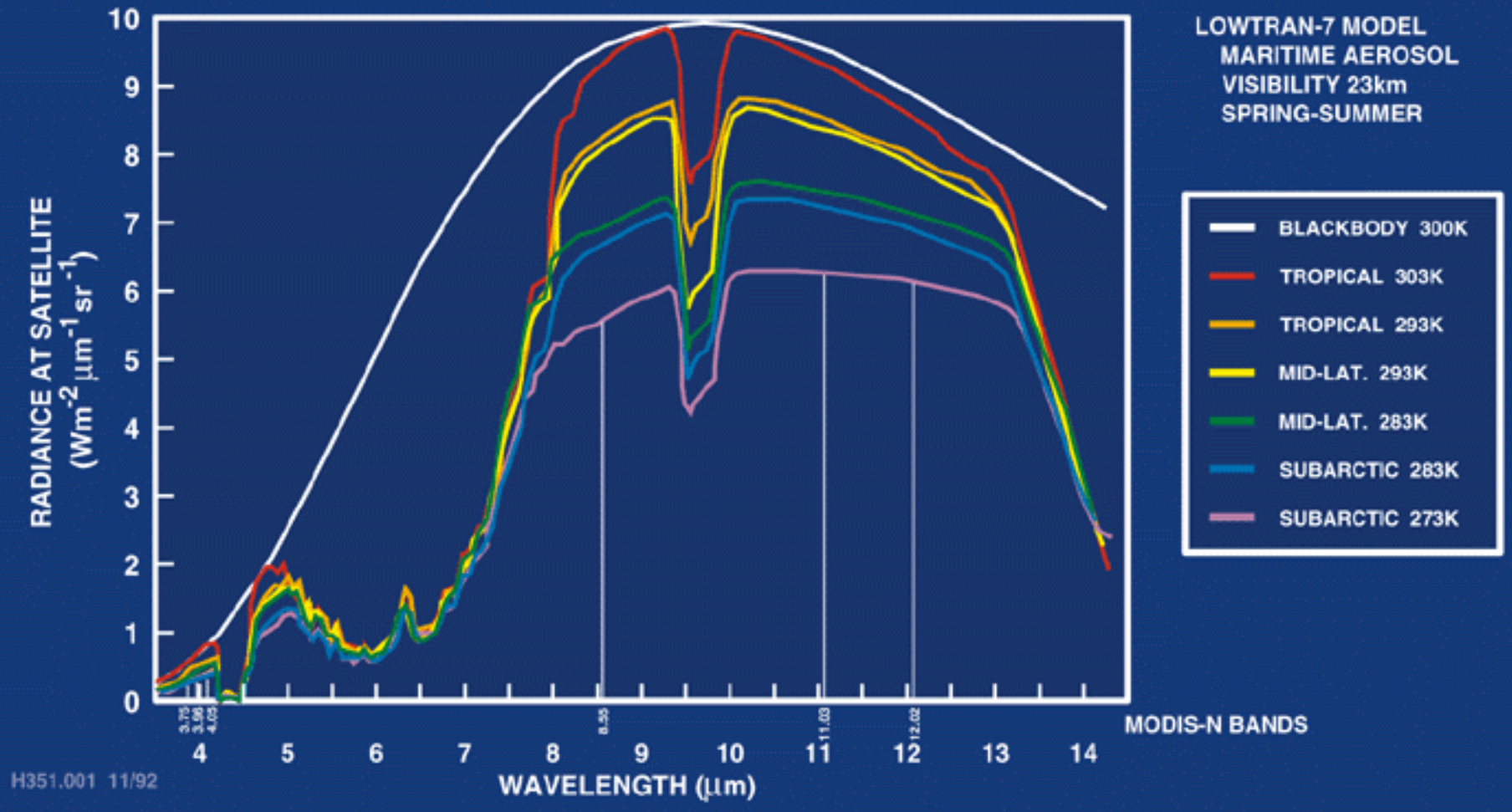

SST - MODIS and AVHRR

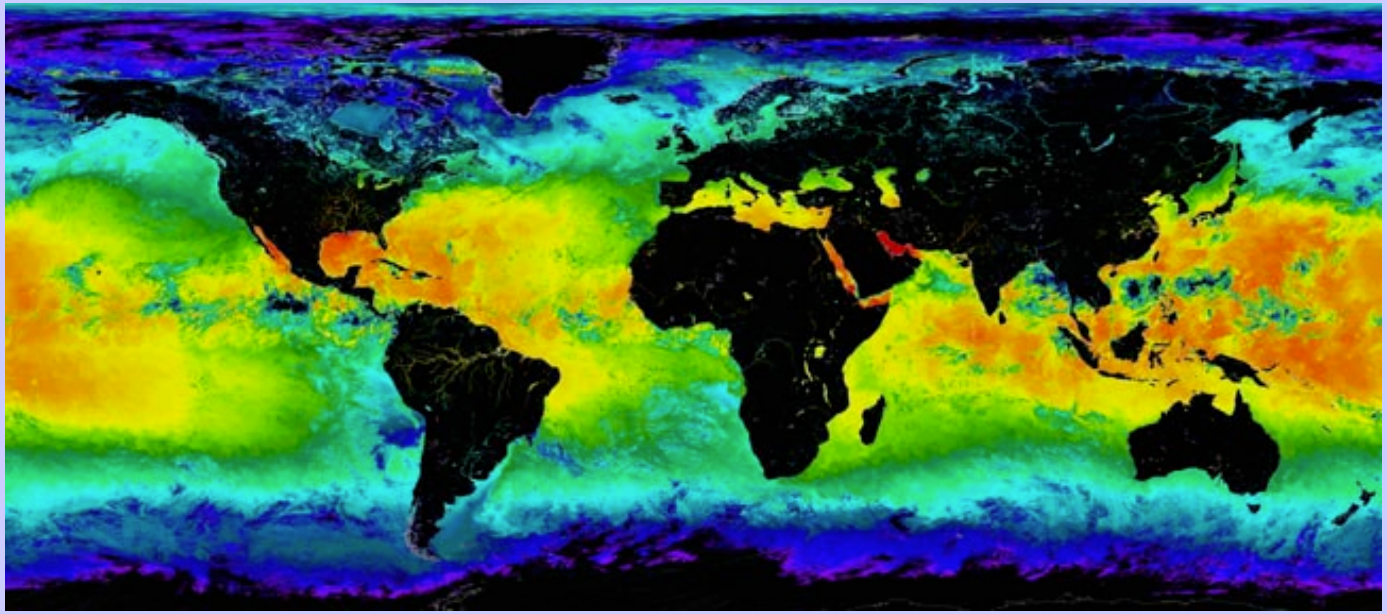

MODIS 4 µm Night SST

Improved coverage in tropical regions. Color scales are not identical, cloud mask is not applied.

AVHRR Night SST

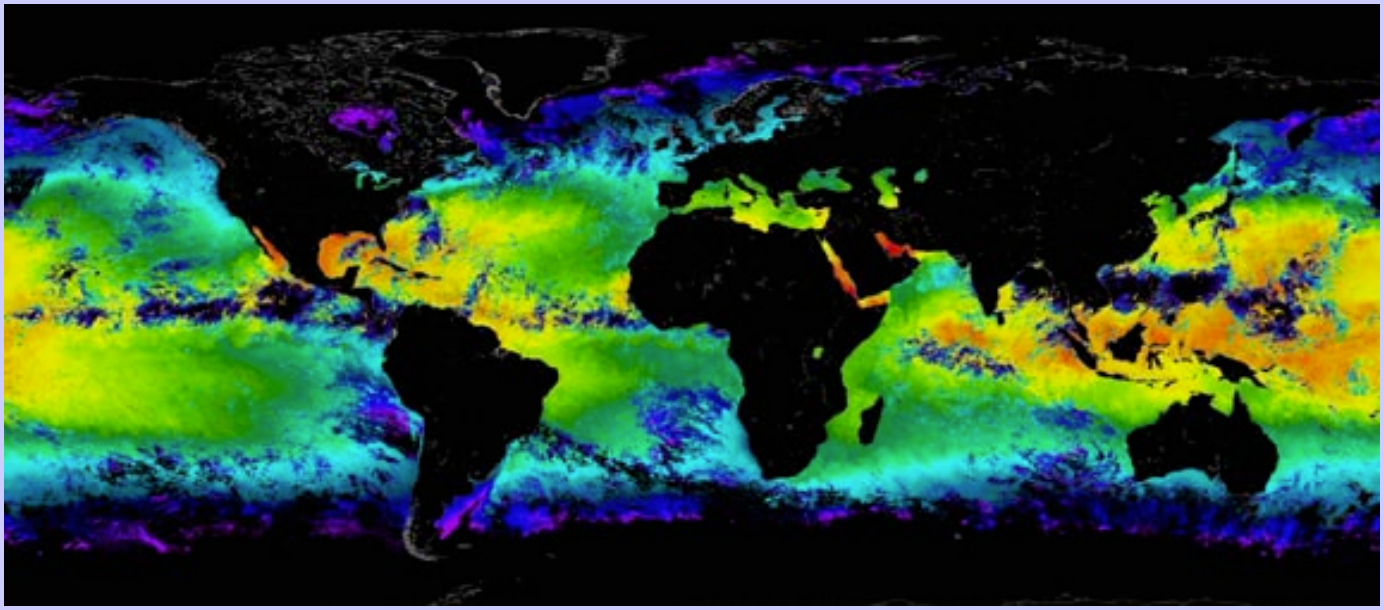

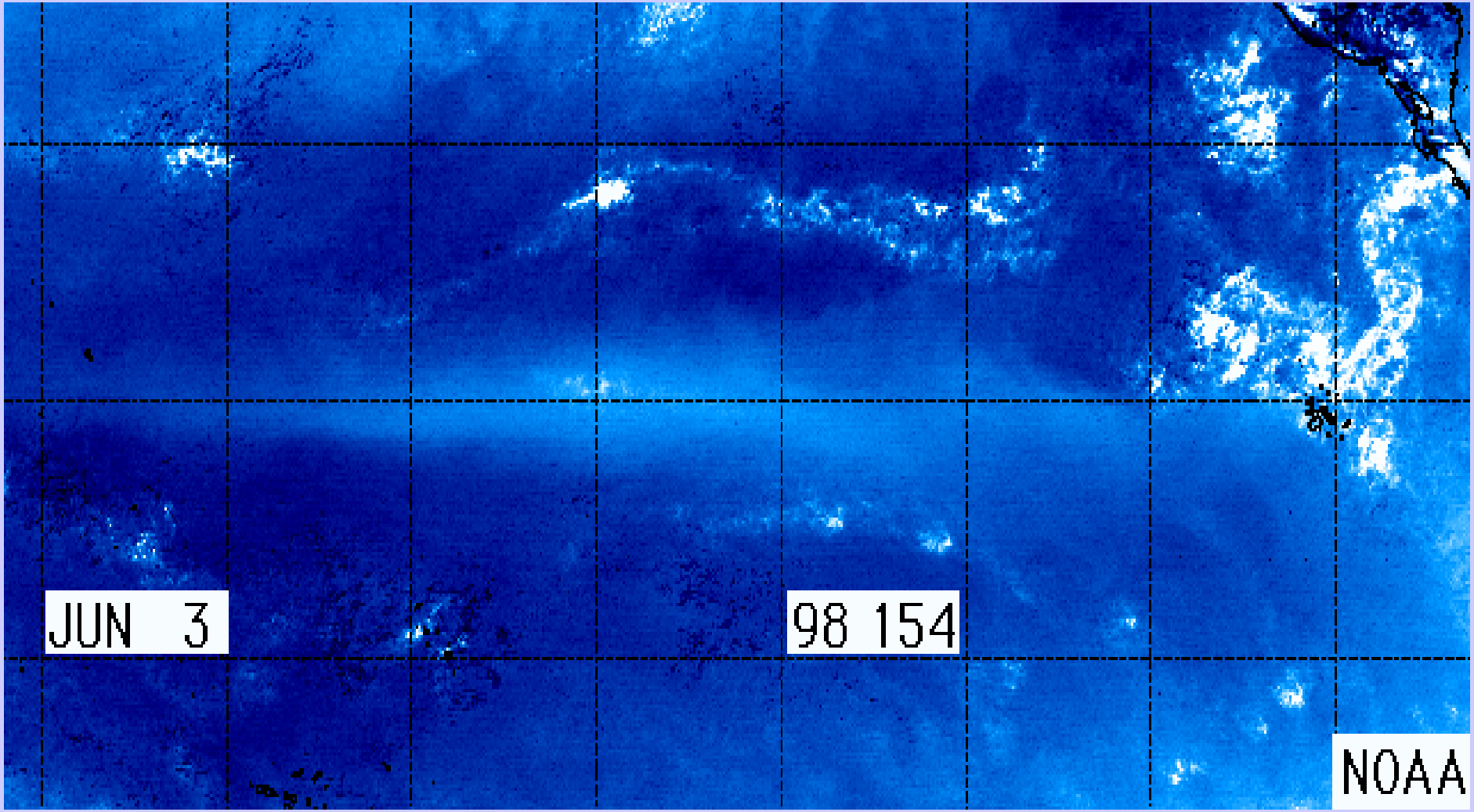

SST Waves from Legeckis

Applications with Multispectral Remote Sensing Data

Satellite Remote Sensing

Energy Balance

VIS, IR, and MW Radiative Transfer

EOS Terra & Aqua MODIS

Multispectral Signatures

*(Ocean Color, SST, **Snow/Ice, Vegetation**, Aerosols, Clouds, Moisture, Fires, Volcanic Ash)*

Detecting Climate Trends

LAND-SOLAR RADIATION

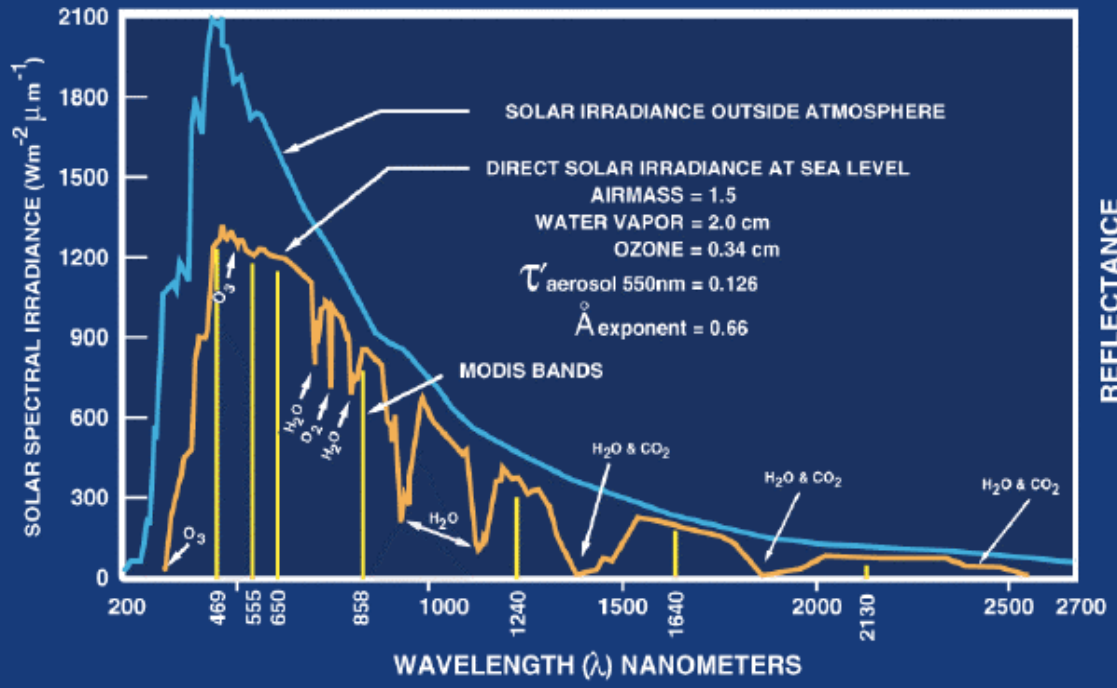

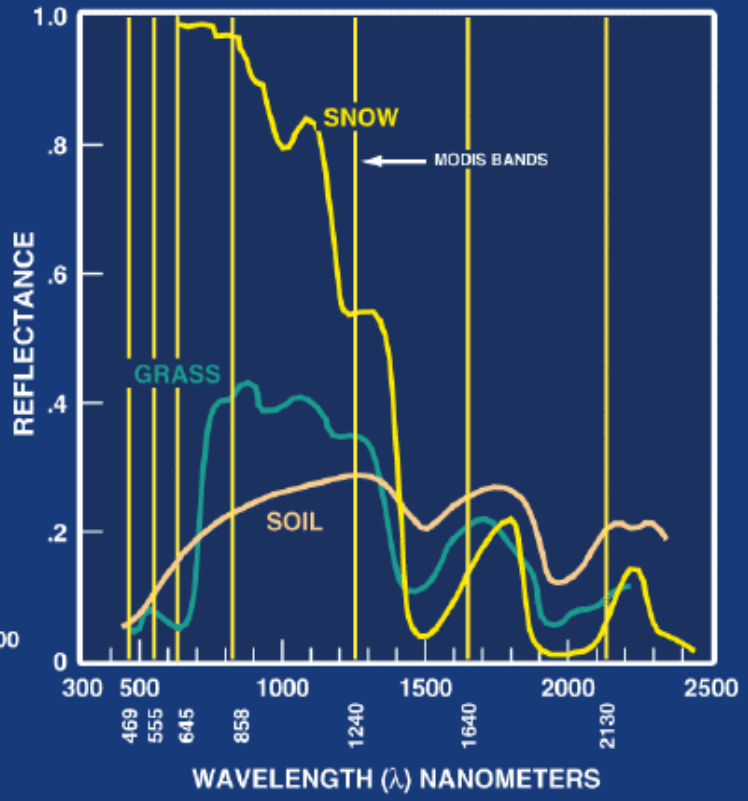

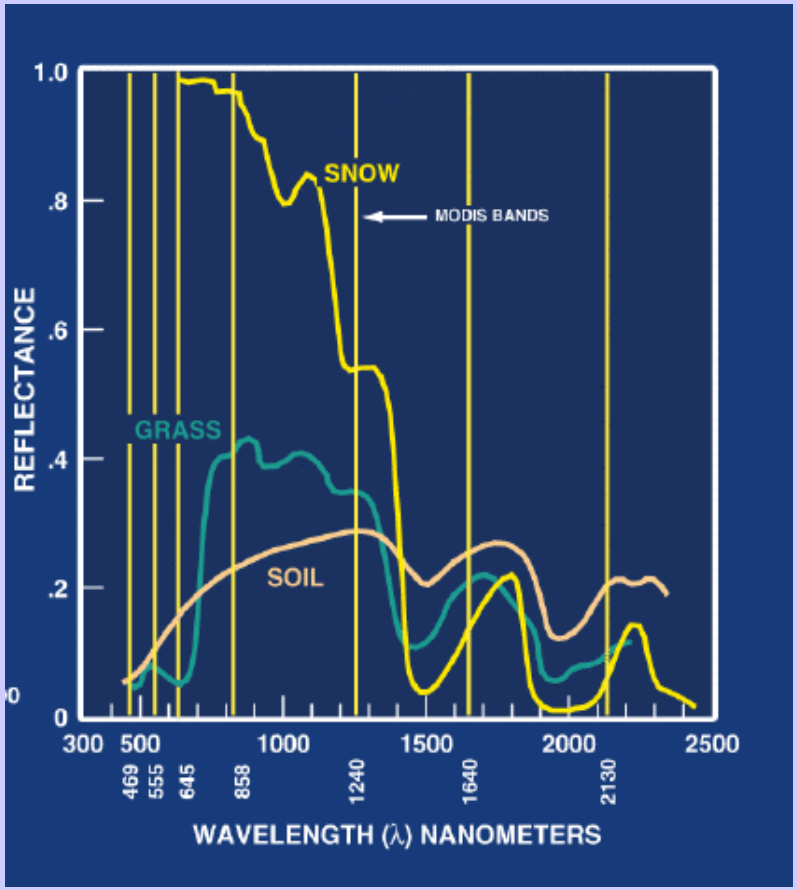

Investigating with Multi-spectral Combinations

Given the spectral response of a surface or atmospheric feature

Select a part of the spectrum where the reflectance or absorption changes with wavelength

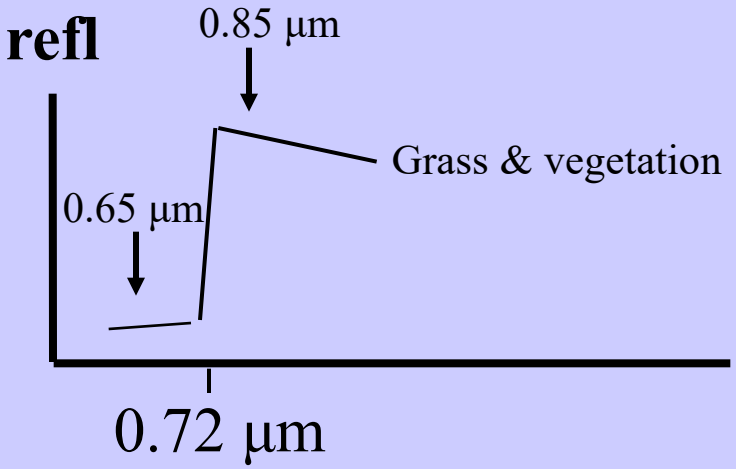

e.g. reflection from grass

If 0.65 μm and 0.85 μm channels see the same reflectance than surface viewed is not grass;
if 0.85 μm sees considerably higher reflectance than 0.65 μm then surface might be grass

LAND - THERMAL RADIATION

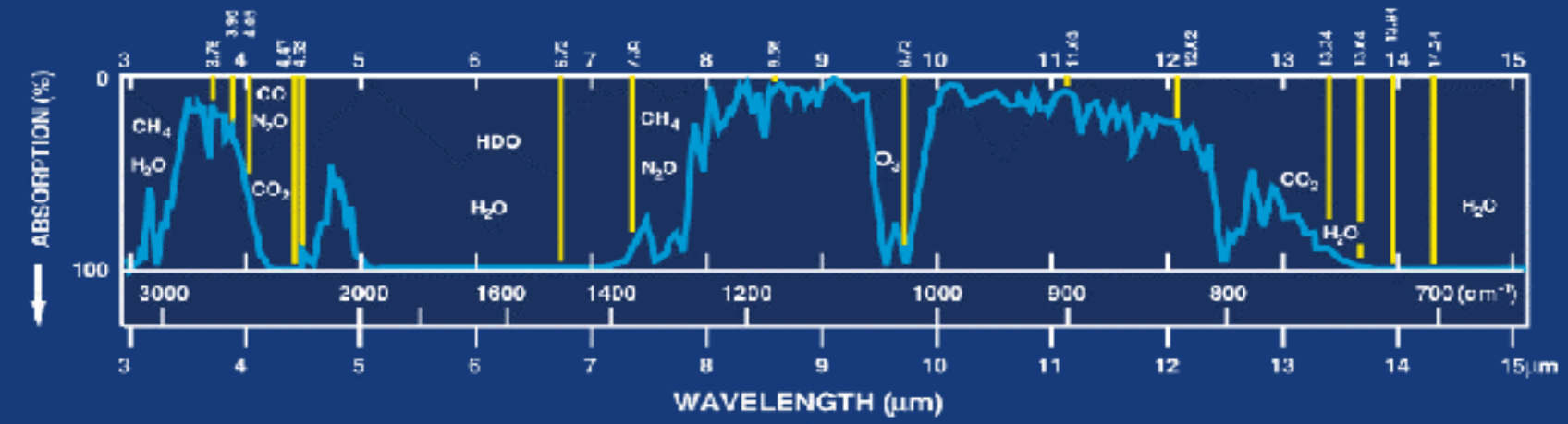

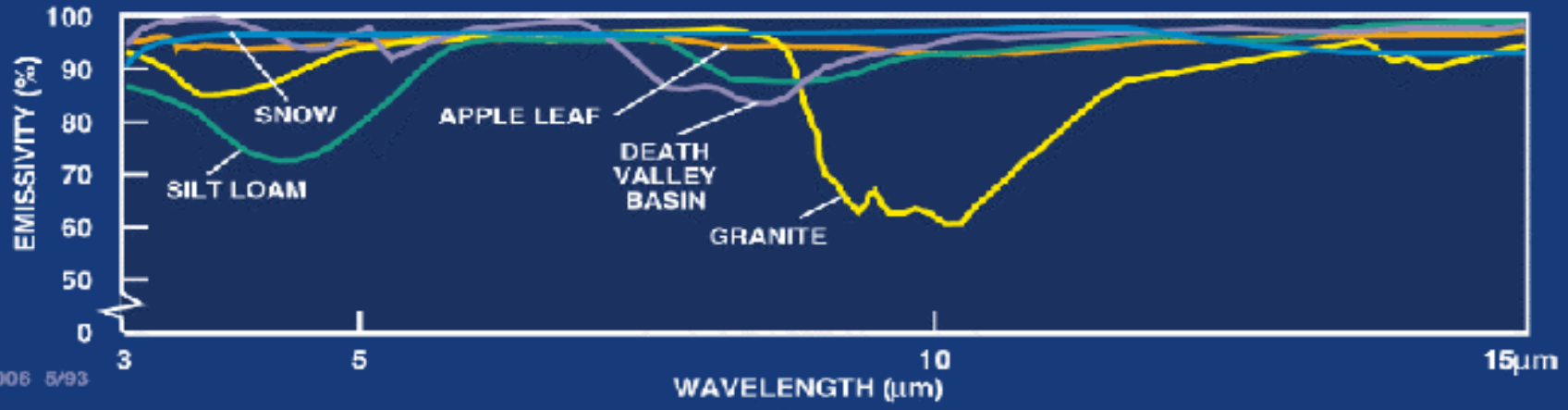

C351.006 5/93

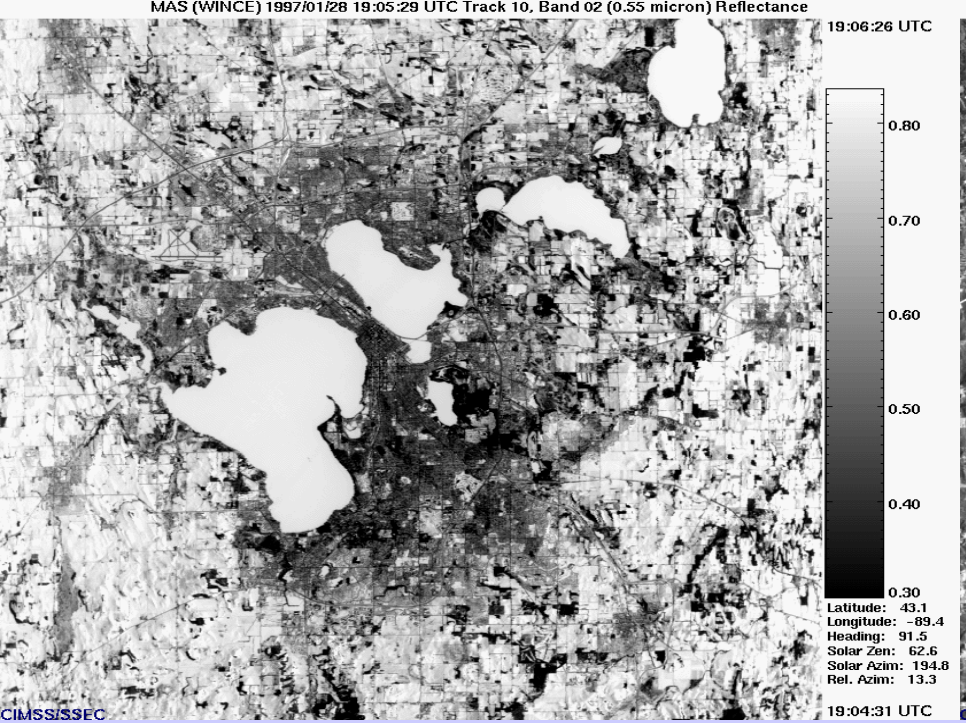

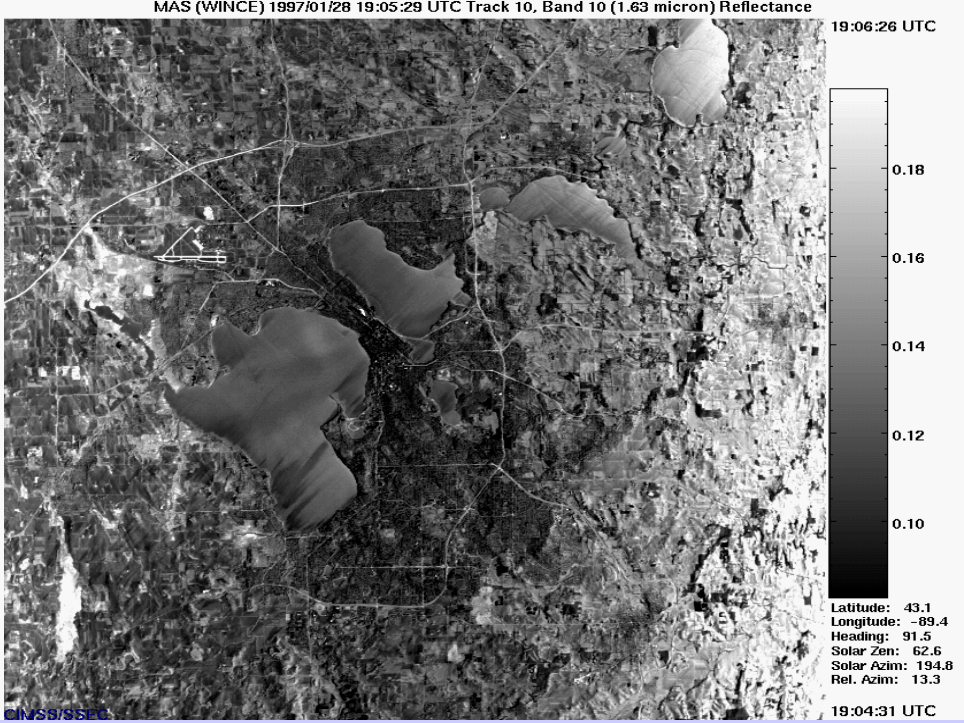

MODIS Airborne Simulator (MAS)
0.6, 1.6, & 11.0 um data over Madison in Jan 97

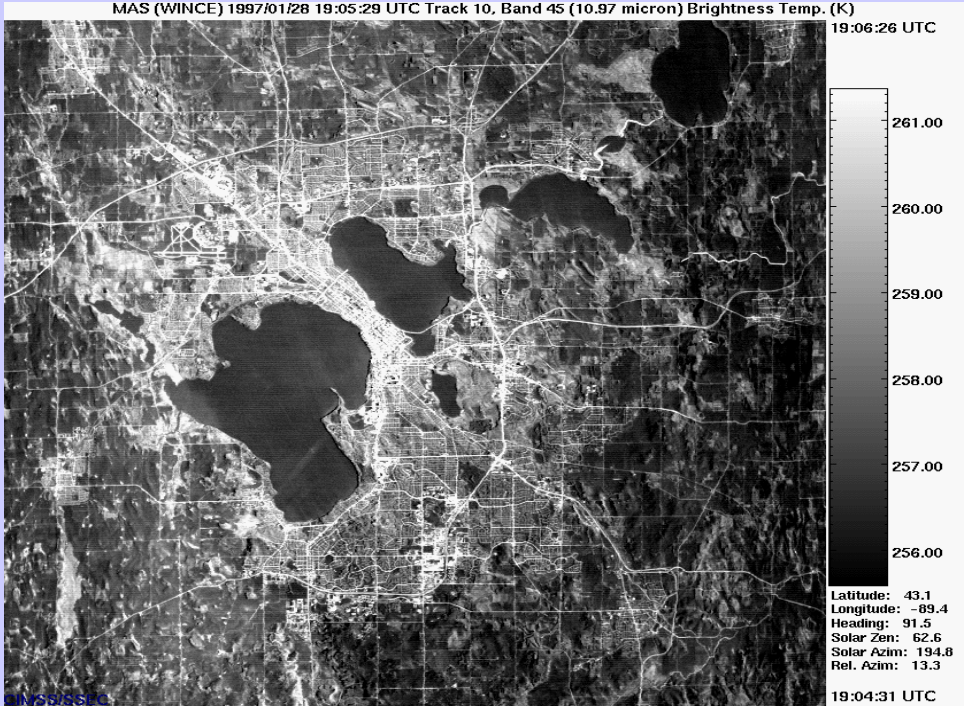

Example with MODIS

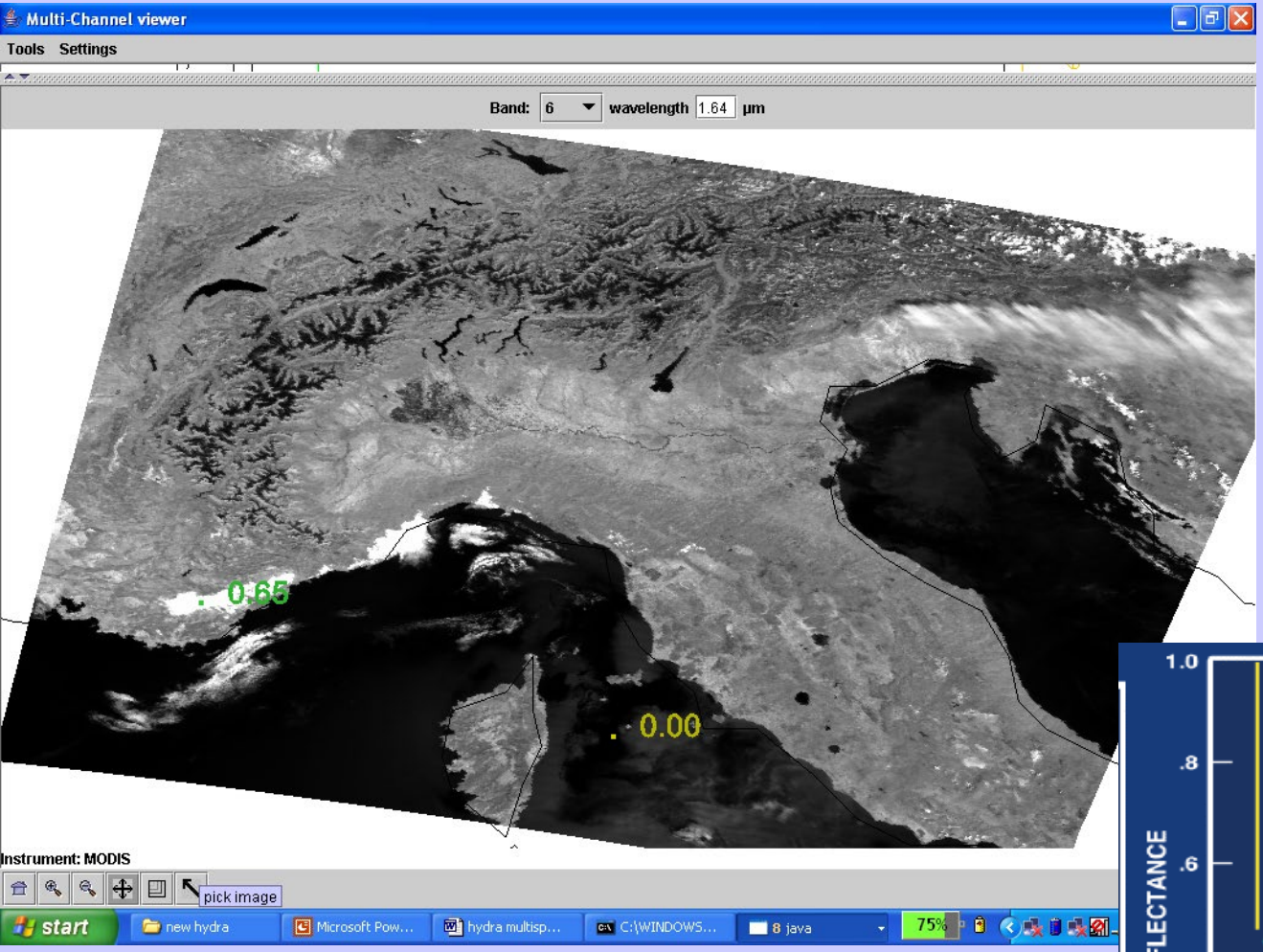

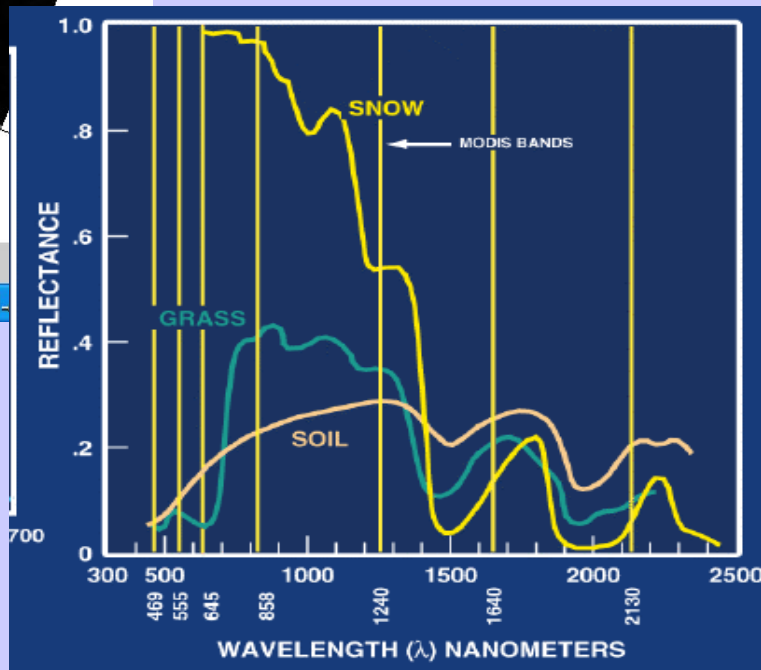

low refl at 1.6 um from snow in mountains

NDVI versus EVI

EVI is a useful proxy for 'greenness' or photosynthetically active vegetation in optically dense canopies, as found throughout the Amazon (LAI= 4 -7), by relying on the more sensitive NIR canopy reflectance which is less prone to saturate

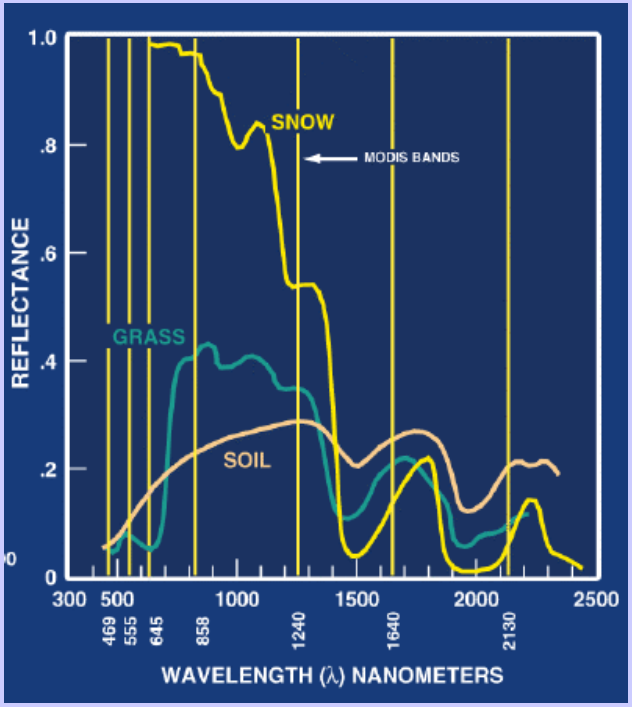

$$NDVI = (\rho 0.8 - \rho 0.6) / (\rho 0.8 + \rho 0.6)$$

$$EVI = 2.5 \times \frac{\rho_{NIR} - \rho_{red}}{1 + \rho_{NIR} + (6 \times \rho_{red} - 7.5 \times \rho_{blue})}$$

Basin-wide greening in dry season

October EVI (dry) minus June EVI (wet season) CMG

from Huete et al

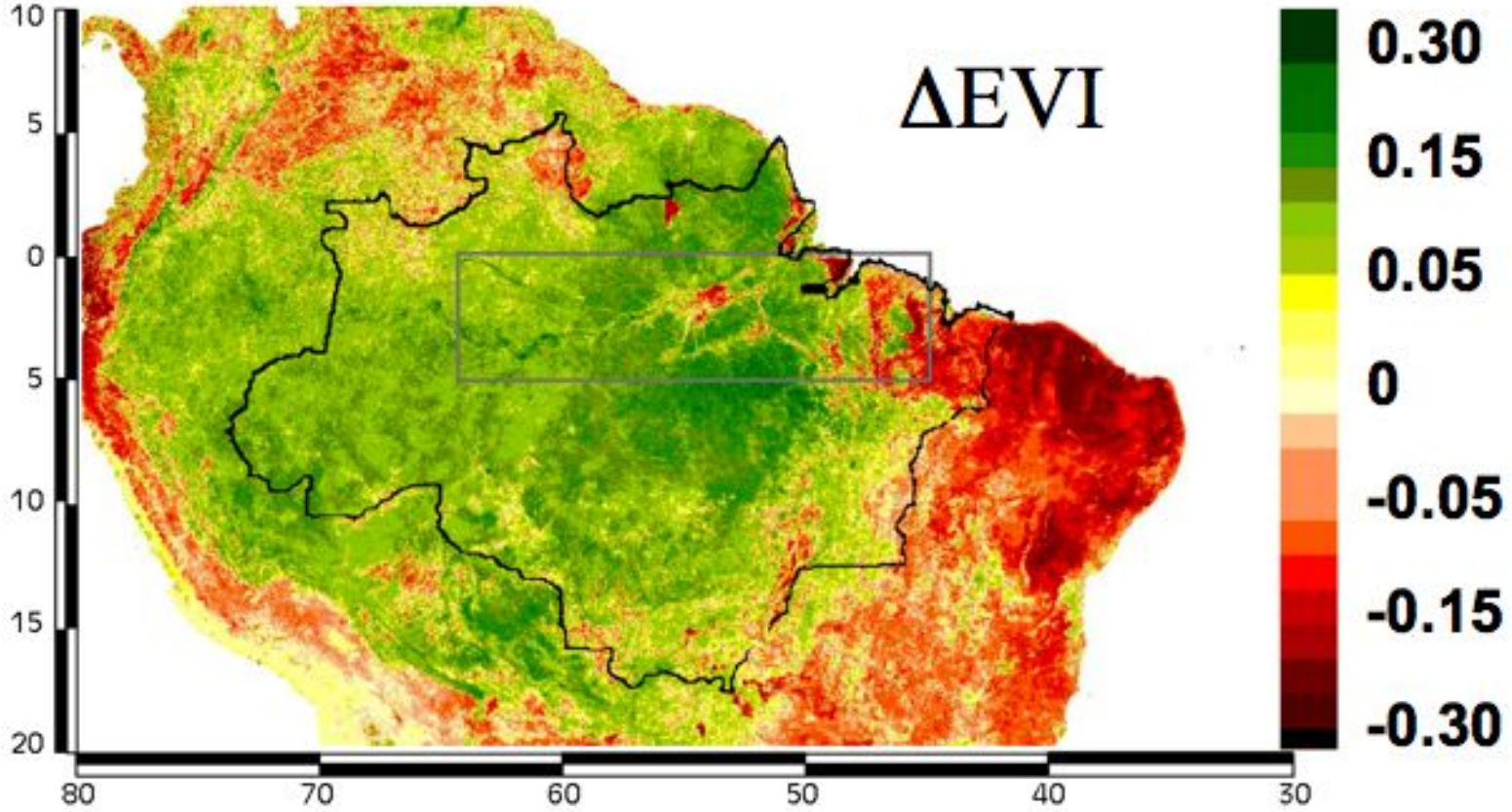

- green colors depict 'greening' and red colors depict 'browning' in the dry season

Applications with Multispectral Remote Sensing Data

Satellite Remote Sensing

Energy Balance

VIS, IR, and MW Radiative Transfer

EOS Terra & Aqua MODIS

Multispectral Signatures

*(Ocean Color, SST, Snow/Ice, Vegetation, **Aerosols**, Clouds, Moisture, Fires, Volcanic Ash)*

Detecting Climate Trends

Aerosol Types and Origin

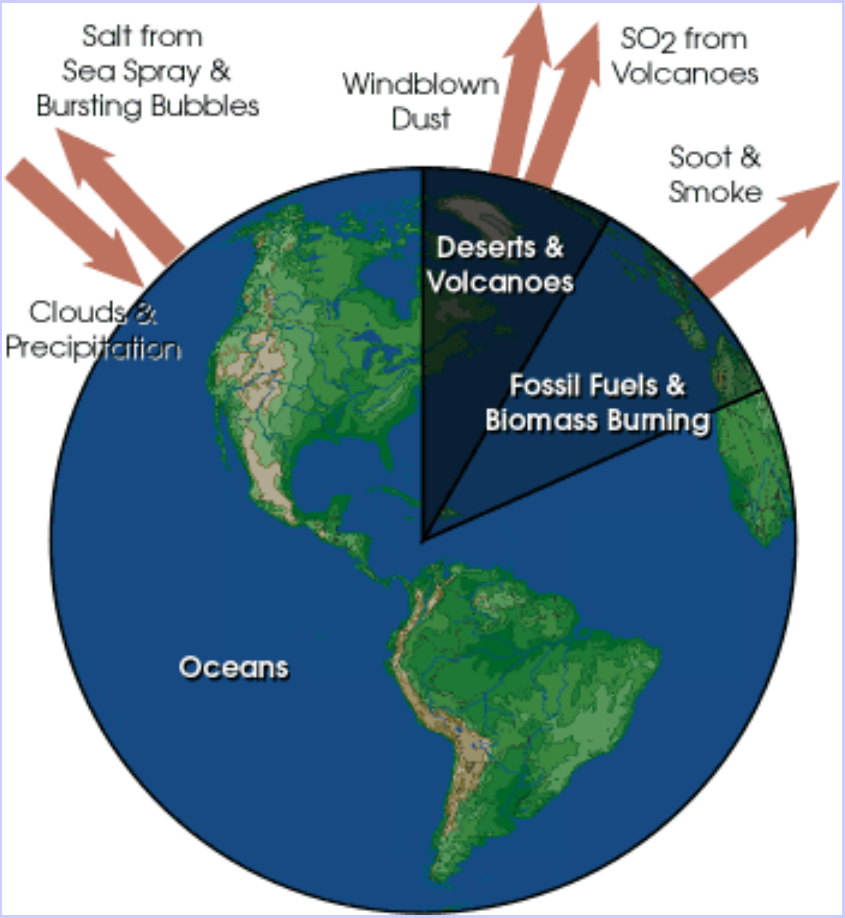

- Aerosol particles larger than about 1 μm in size are produced by windblown dust and sea salt from sea spray and bursting bubbles
- Aerosols smaller than 1 μm are mostly formed by condensation processes such as conversion of sulfur dioxide (SO2) gas (released from volcanic eruptions) to sulfate particles and by formation of soot and smoke during burning processes.
- After formation, aerosols are mixed and transported by atmospheric motions and are primarily removed by clouds and precipitation.

Aerosol Size Distribution

There are 3 modes :

- « **nucleation** »: radius is between 0.002 and 0.05 µm. They result from combustion processes, photo-chemical reactions, etc.

- « **accumulation** »: radius is between 0.05 µm and 0.5 µm. Coagulation processes.

- « **coarse** »: larger than 1 µm. From mechanical processes like aeolian erosion.

« fine » particles (nucleation and accumulation) result from anthropogenic activities, coarse particles come from natural processes.

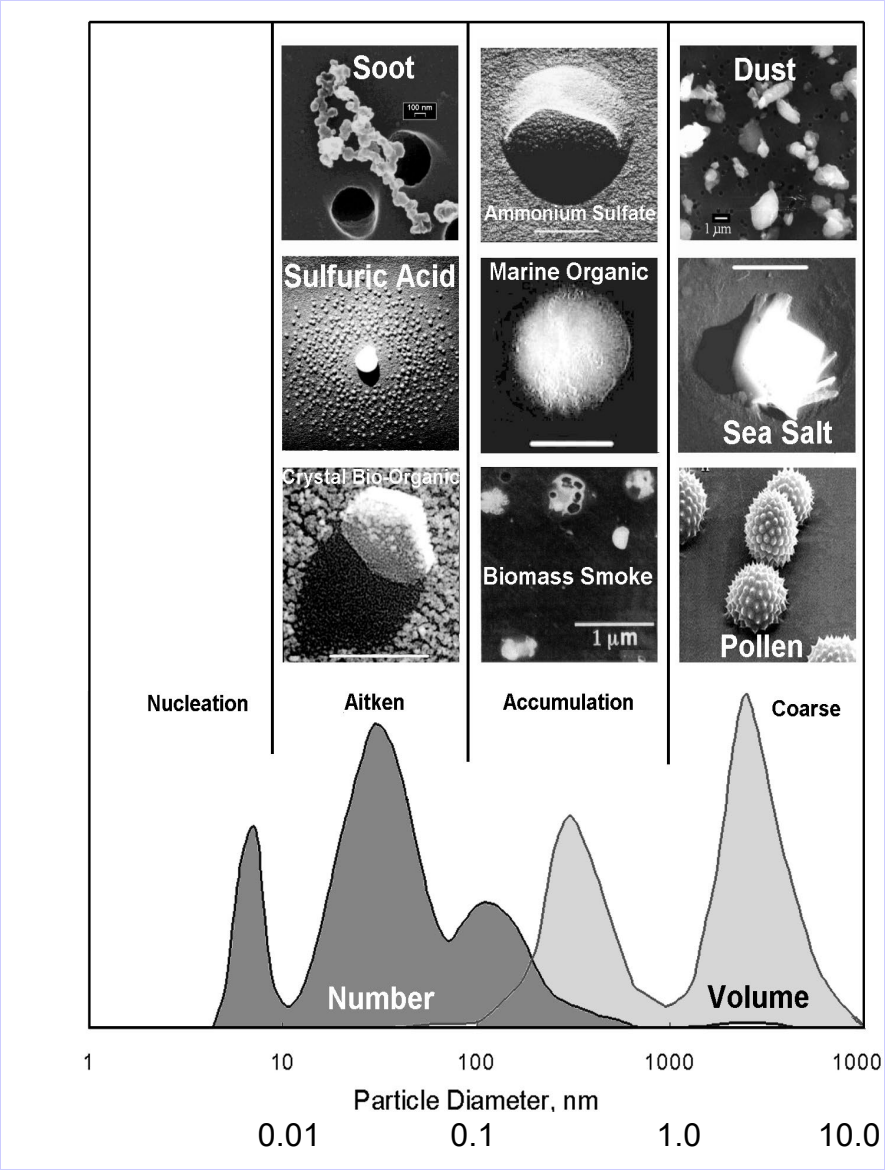

Aerosols over Ocean

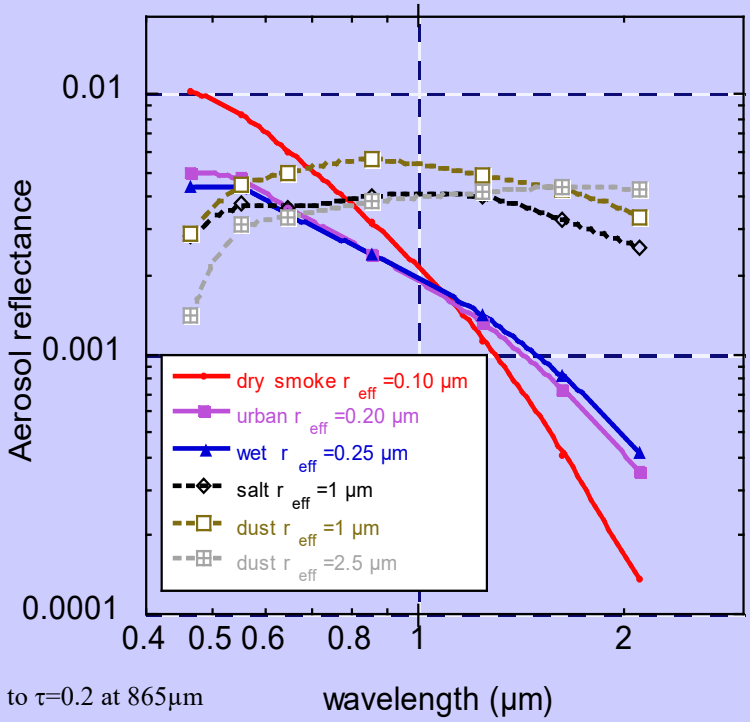

Normalized to τ=0.2 at 865μm

- Radiance data in 6 bands (550-2130nm).
- Spectral radiances (LUT) to derive the aerosol size distribution
- Two modes (accumulation 0.10-0.25μm; coarse1.0-2.5μm); ratio is a free parameter
- Radiance at 865μm to derive τ

Ocean products :

- The total Spectral Optical thickness
- The effective radius
- The optical thickness of small & large modes/ratio between the 2 modes

Global aerosol AOT trends

Remer et al 2005

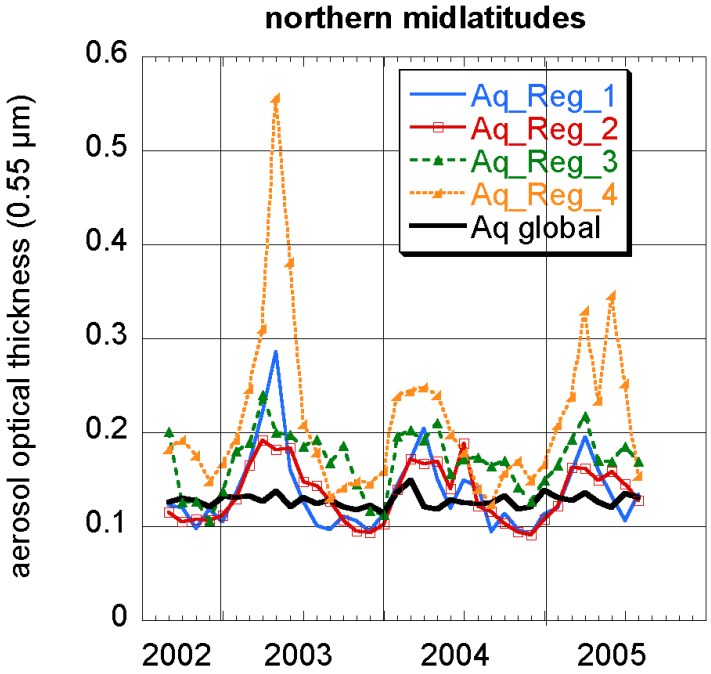

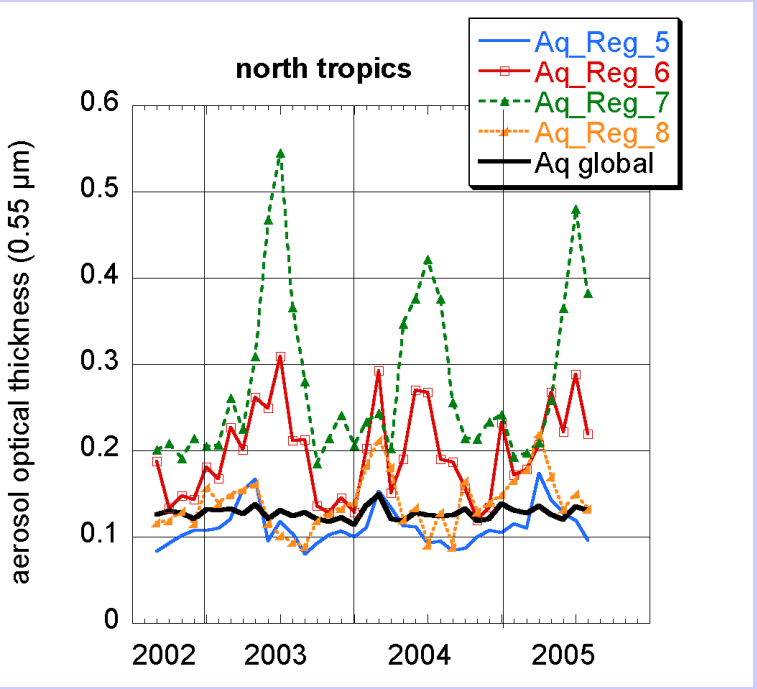

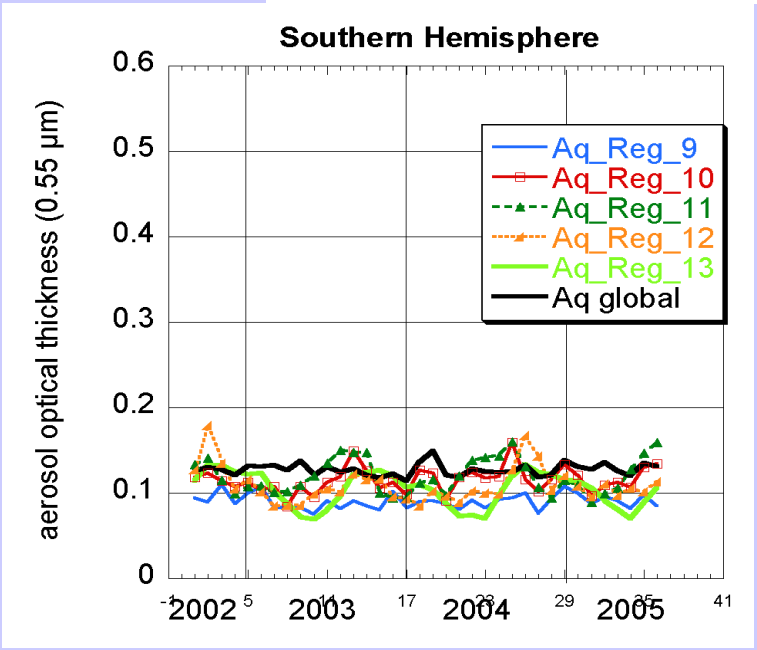

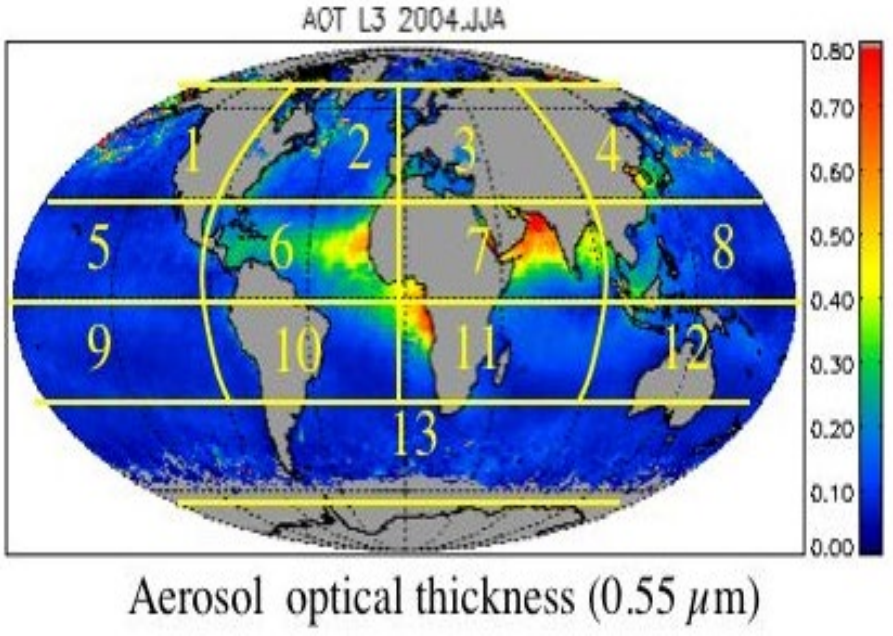

Aerosol effects on cloud cover over the Atlantic Ocean - several aerosol types interact with clouds

June-Aug 2002

Pollution zone

Dust zone

Smoke zone

Marine aerosol

aerosol forcing increased cloud cover 5% (~ 6 W/m2) and height 40 hPa (~ 400 m) in June-Aug 02 over Atlantic Ocean

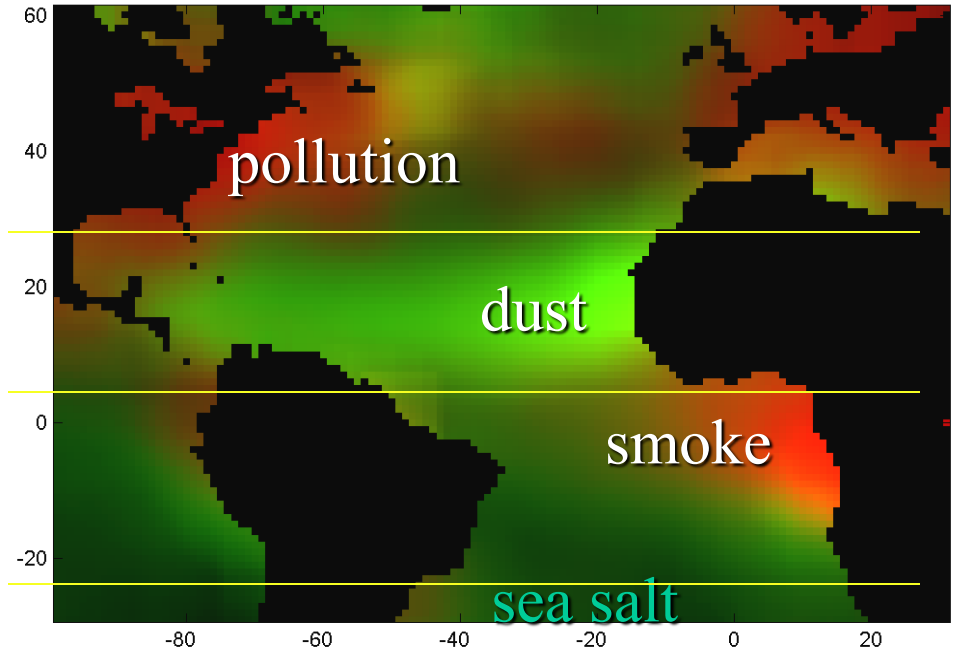

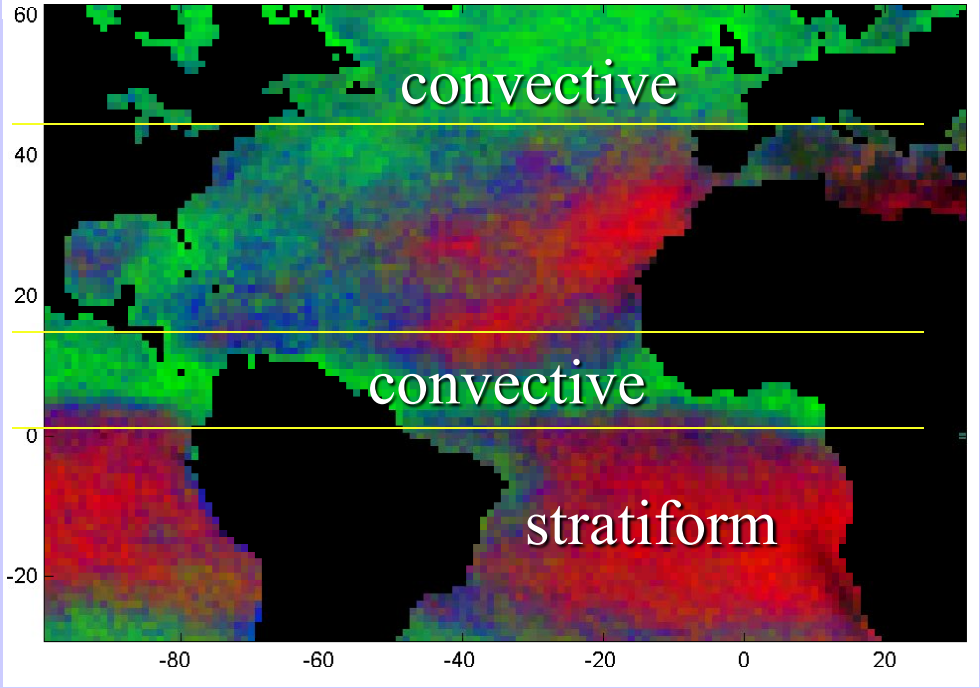

clean

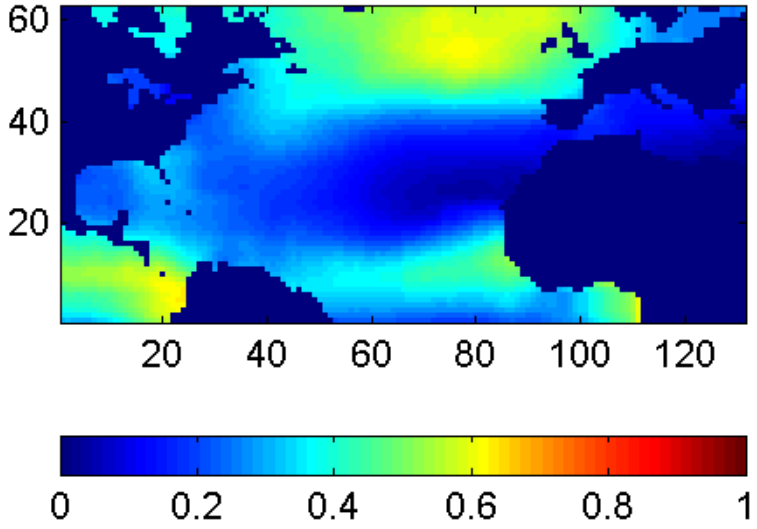

Cloud fraction

hazy

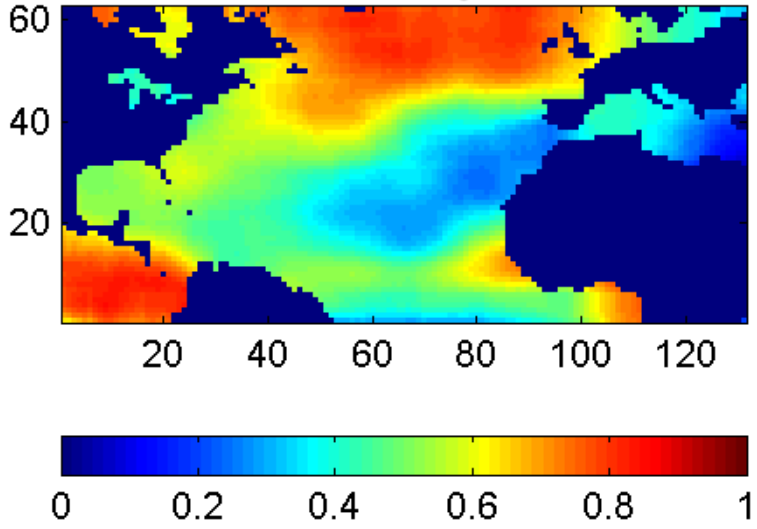

Cloud fraction

clean

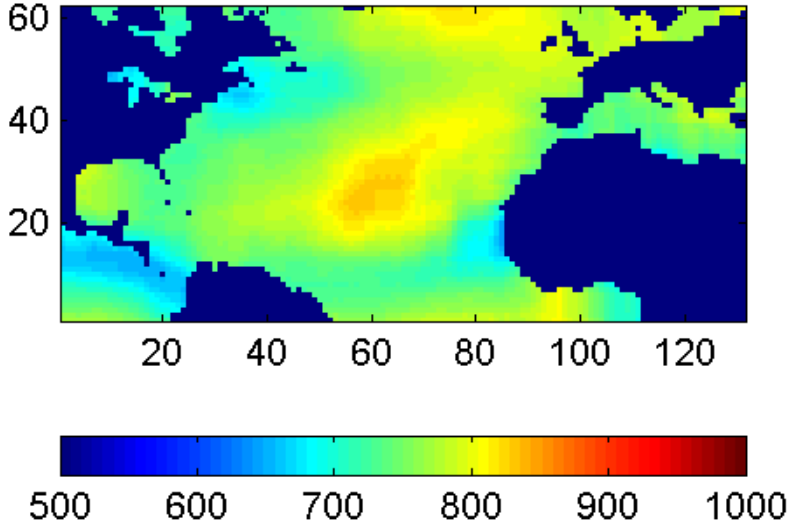

Cloud top pressure

hazy

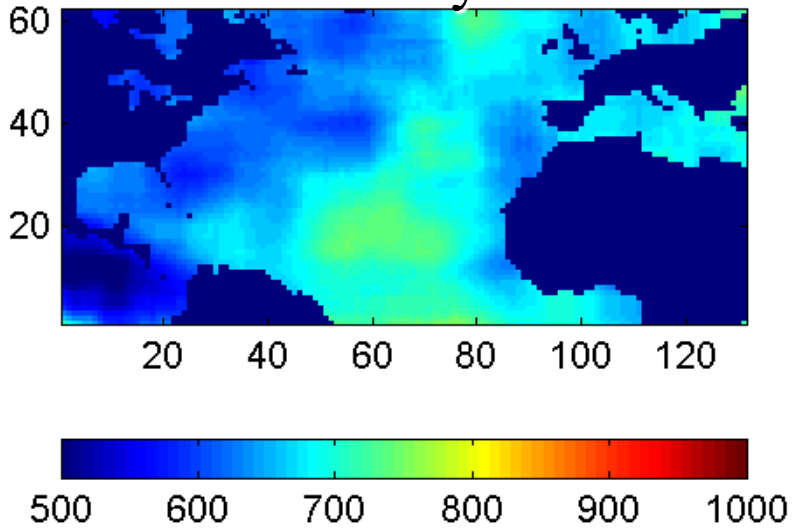

Cloud top pressure

Applications with Multispectral Remote Sensing Data

Satellite Remote Sensing

Energy Balance

VIS, IR, and MW Radiative Transfer

EOS Terra & Aqua MODIS

Multispectral Signatures

(Ocean Color, SST, Snow/Ice, Vegetation, Aerosols,

***Clouds**, Moisture, Fires, Volcanic Ash)*

Detecting Climate Trends

ATMOSPHERE-SOLAR RADIATION

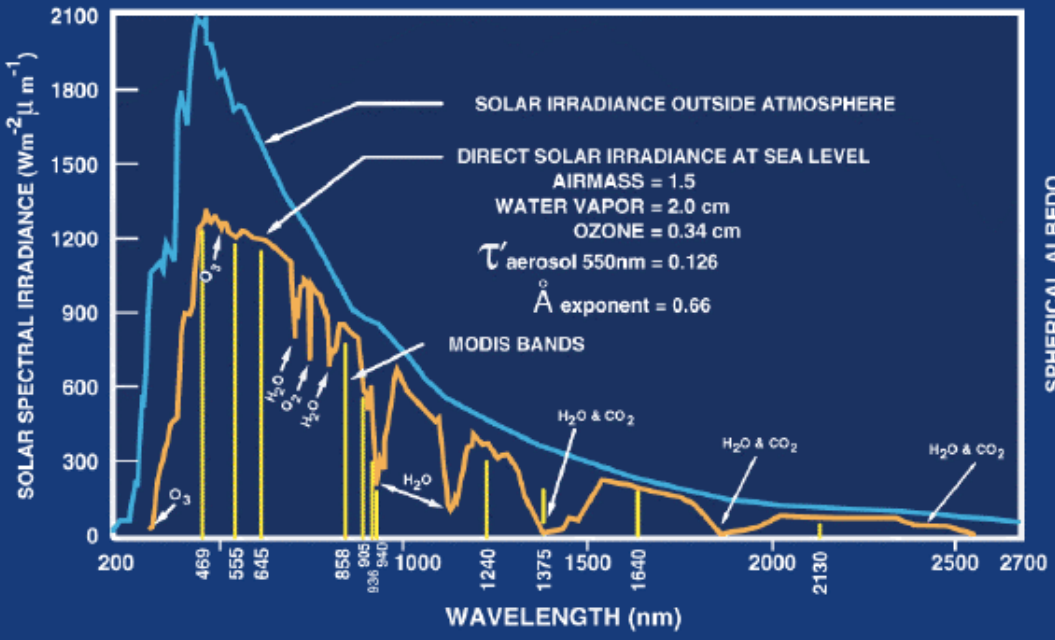

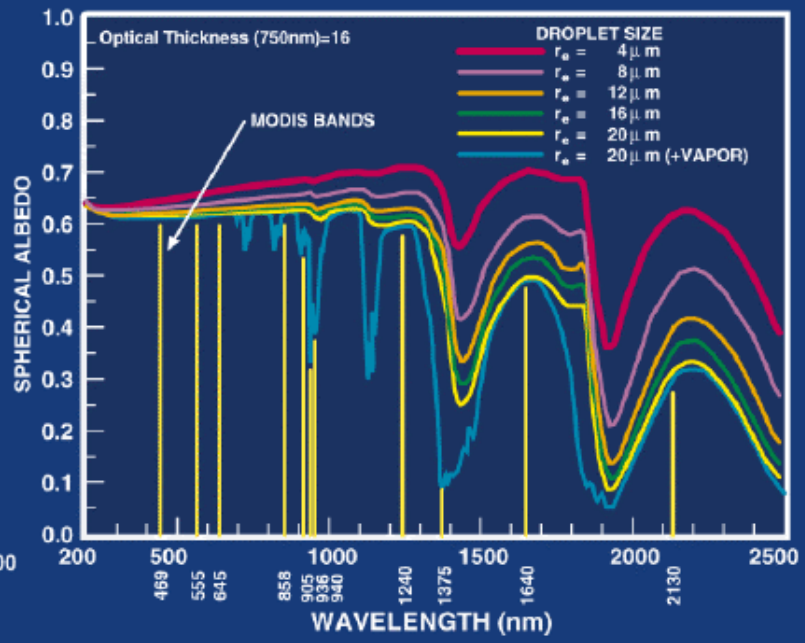

ATMOSPHERE - CLEAR SKY
THERMAL EMISSION

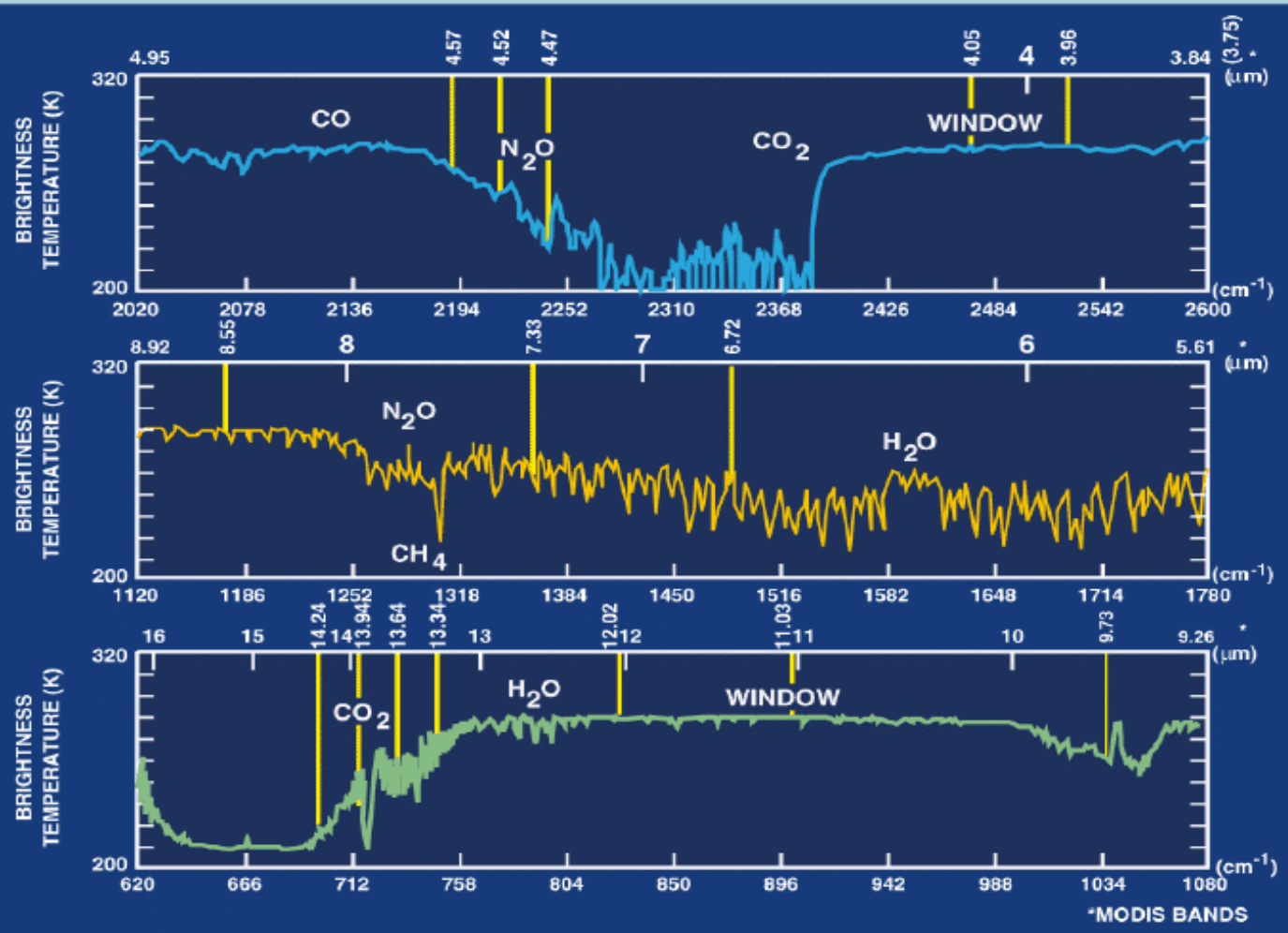

002 11/92

ATMOSPHERE - THERMAL RADIATION

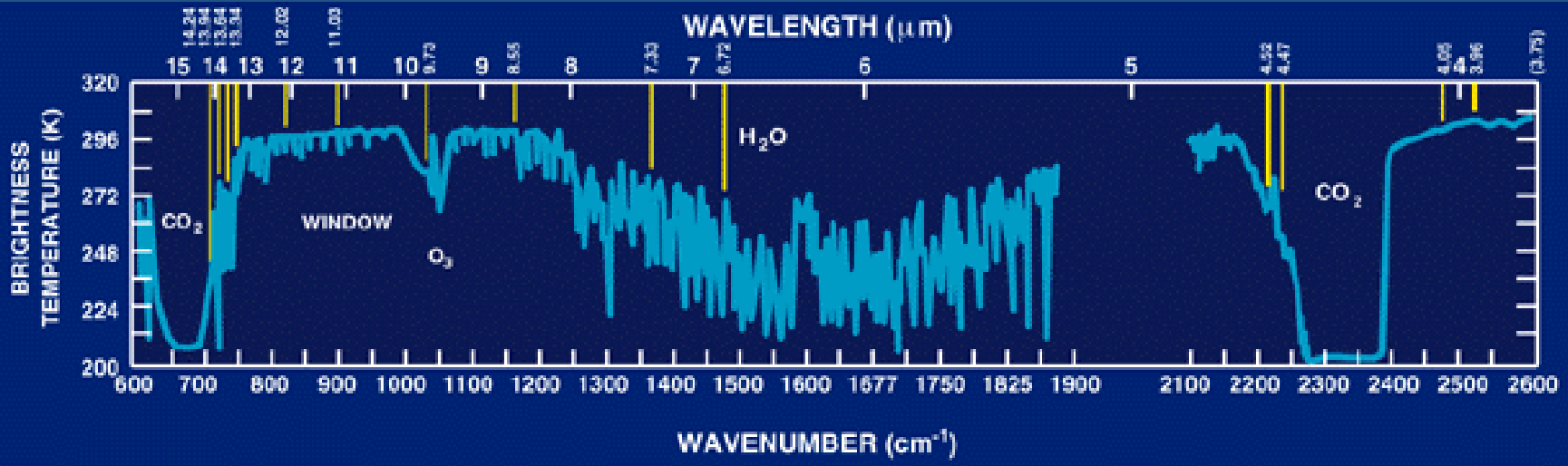

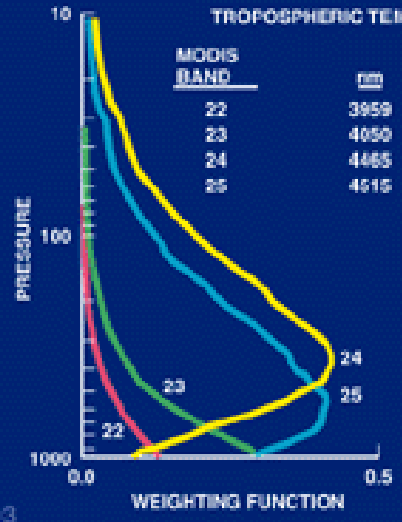

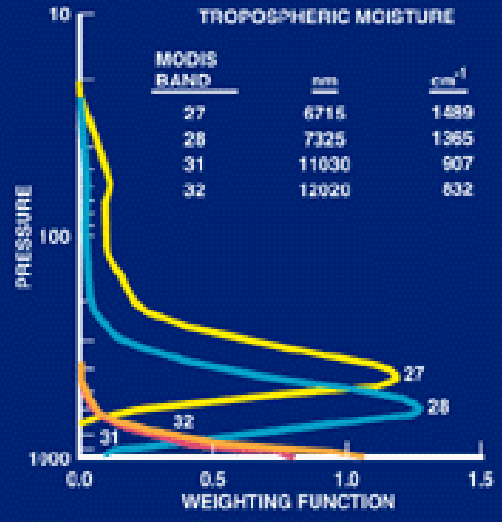

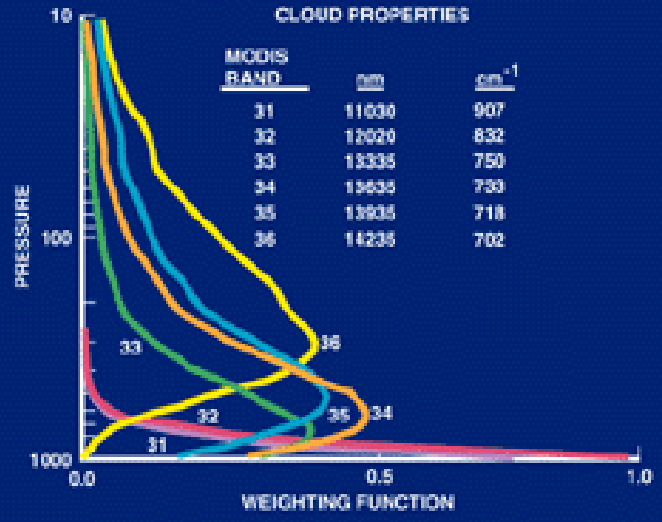

E351.002 5/93

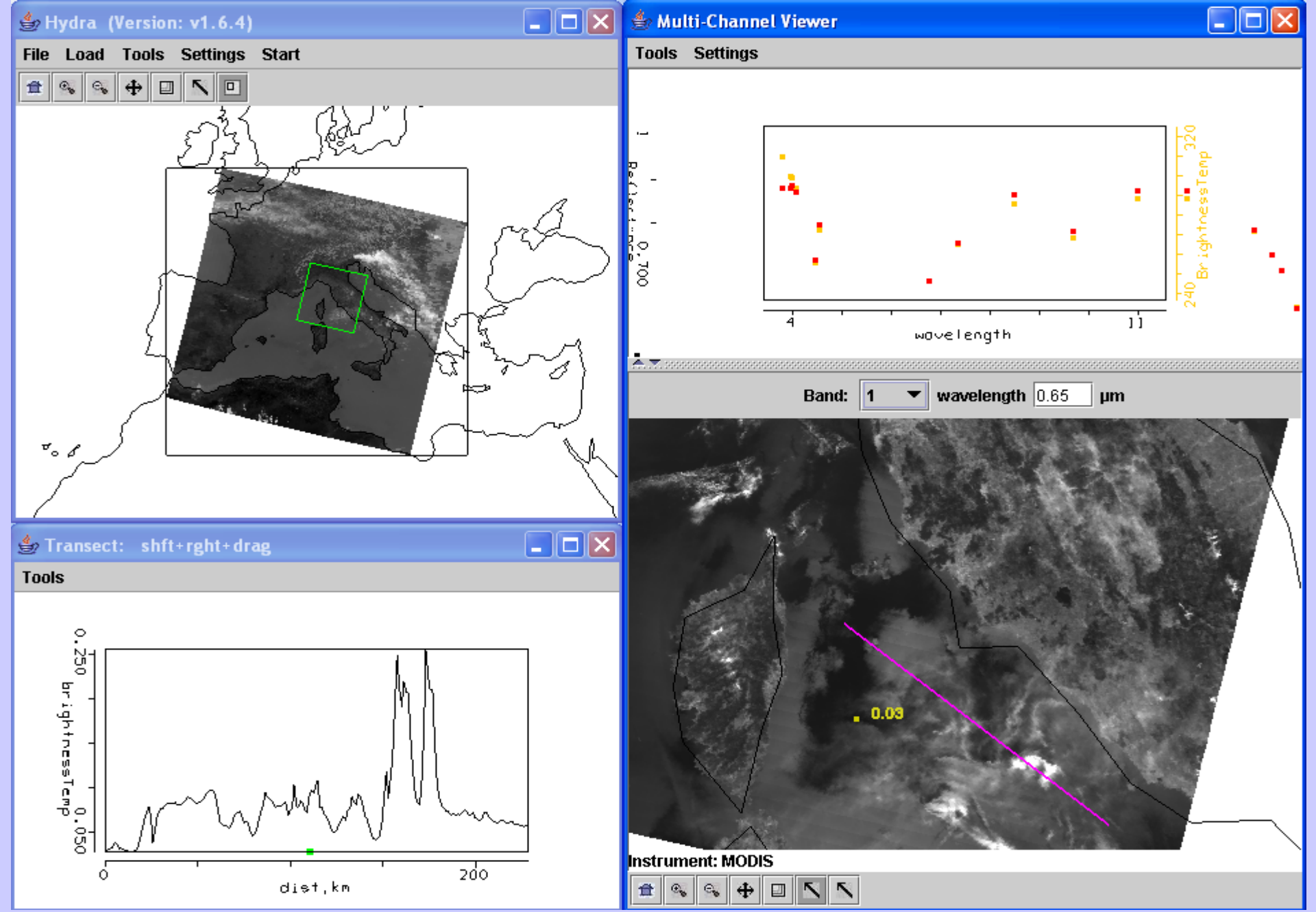

High clouds reflect more than surface at 0.65 µm

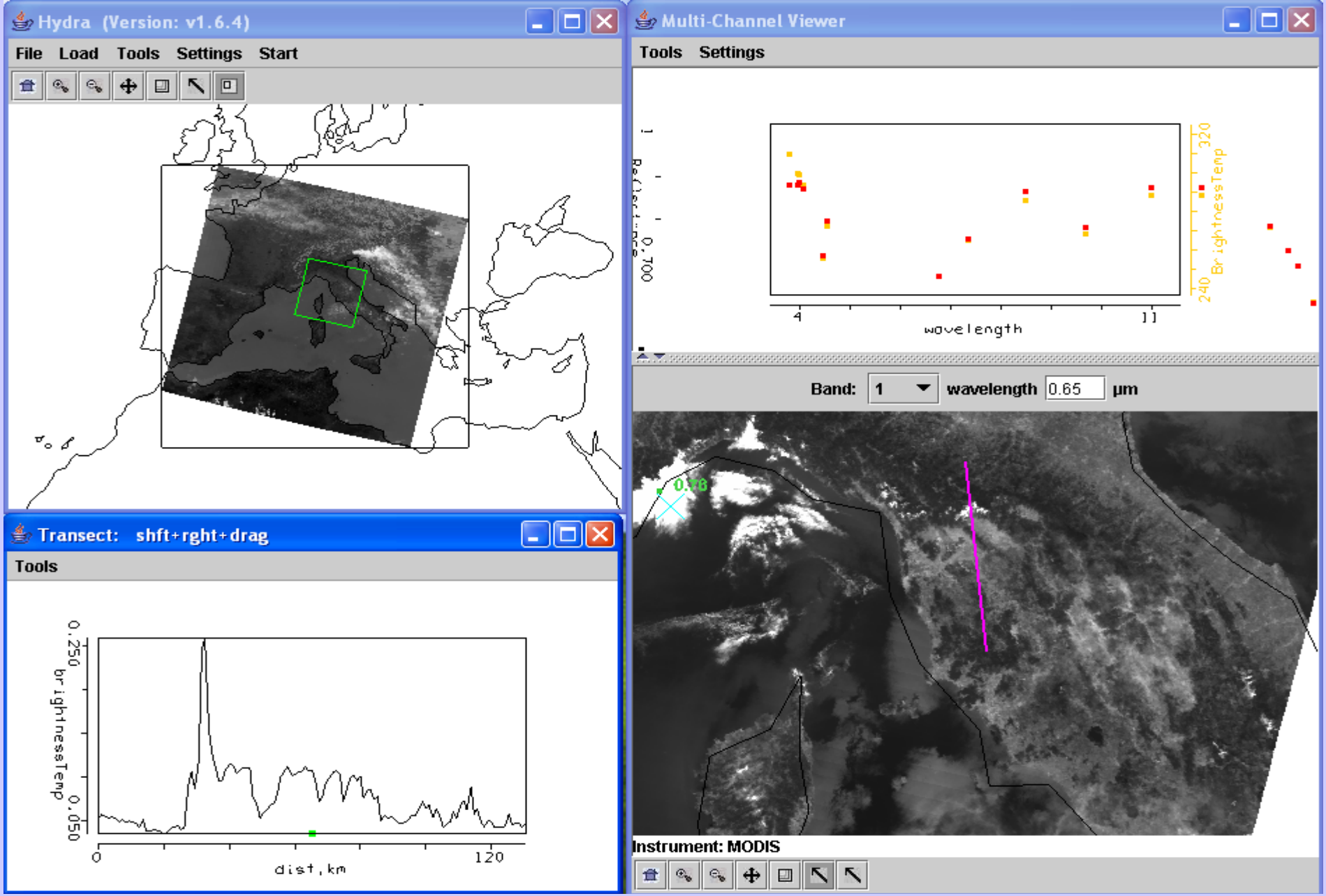

High clouds reflect more than surface at 0.65 µm, even over vegetation

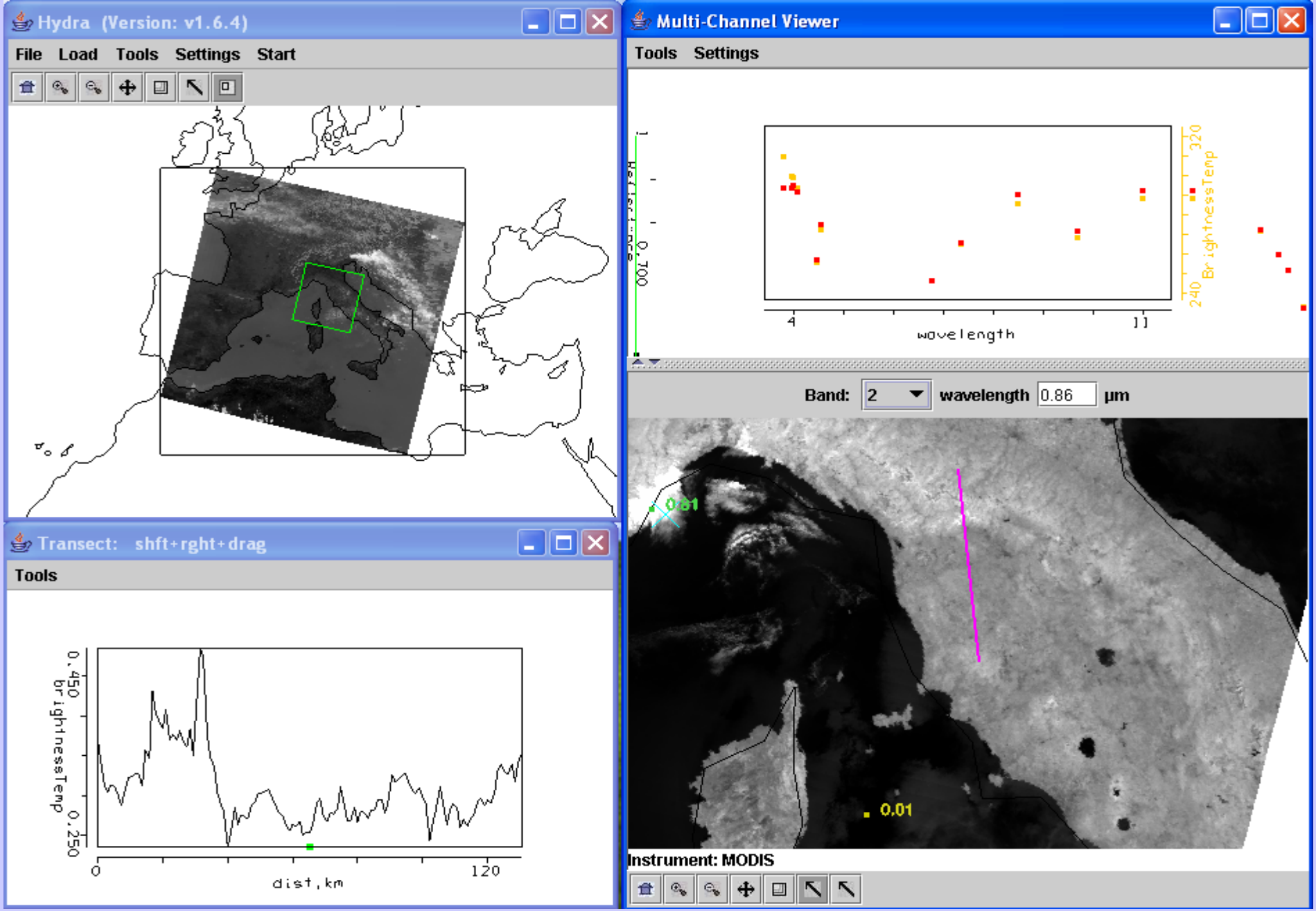

High clouds are more difficult to detect at 0.86 µm over vegetation

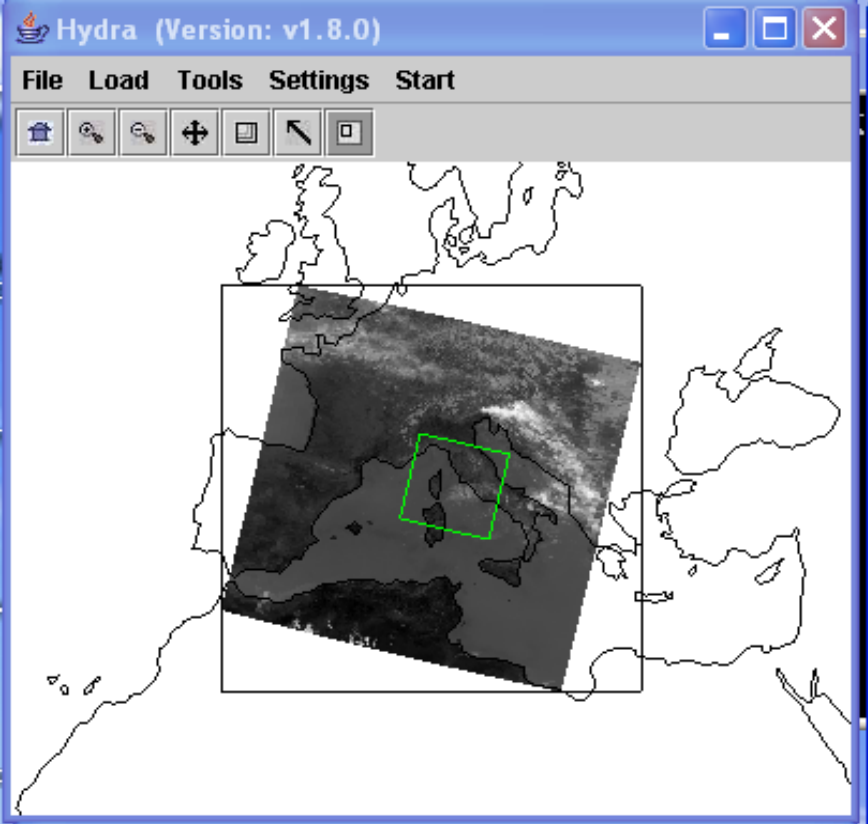
Hydra (Version: v1.8.0)
File Load Tools Settings Start

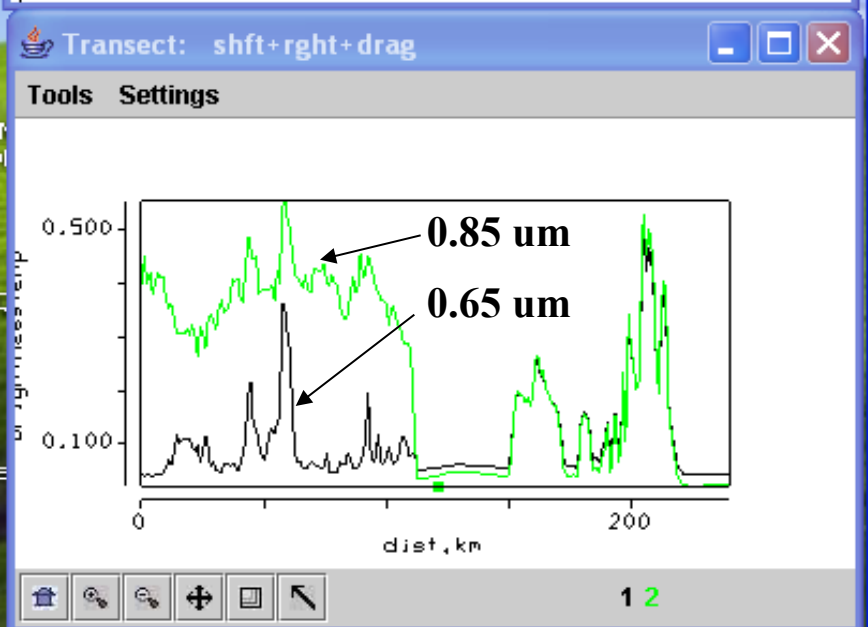
Transect: shft+rght+drag
Tools Settings
0.500
0.100
0.85 um
0.65 um
0
200
dist,km
1 2

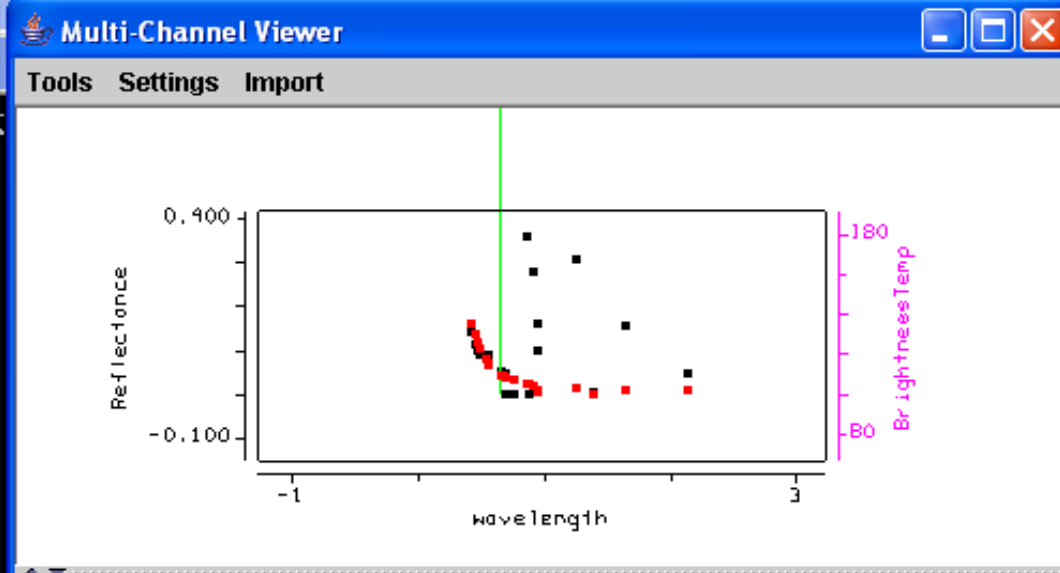
Multi-Channel Viewer
Tools Settings Import
0.400
-0.100
Reflectance
180
80
BrightneesTemp
-1
3
wavelength

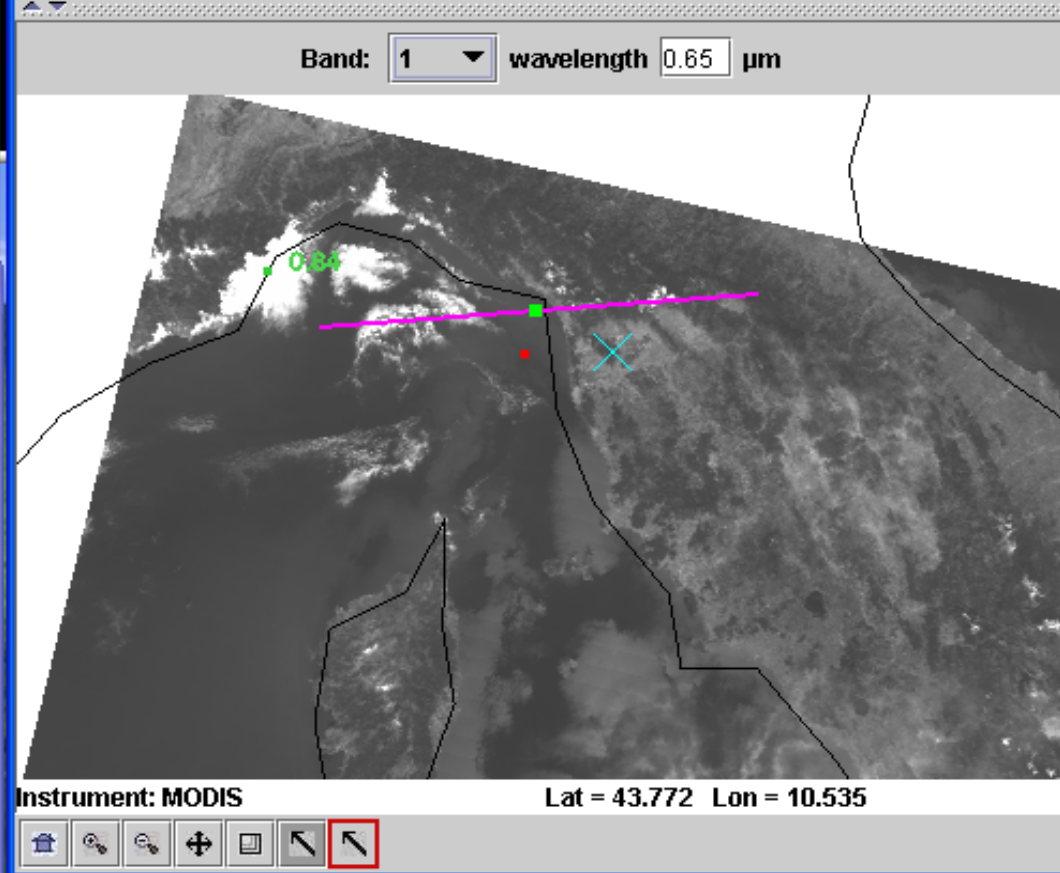
Band: 1 wavelength 0.65 µm
0.84
Instrument: MODIS
Lat = 43.772 Lon = 10.535

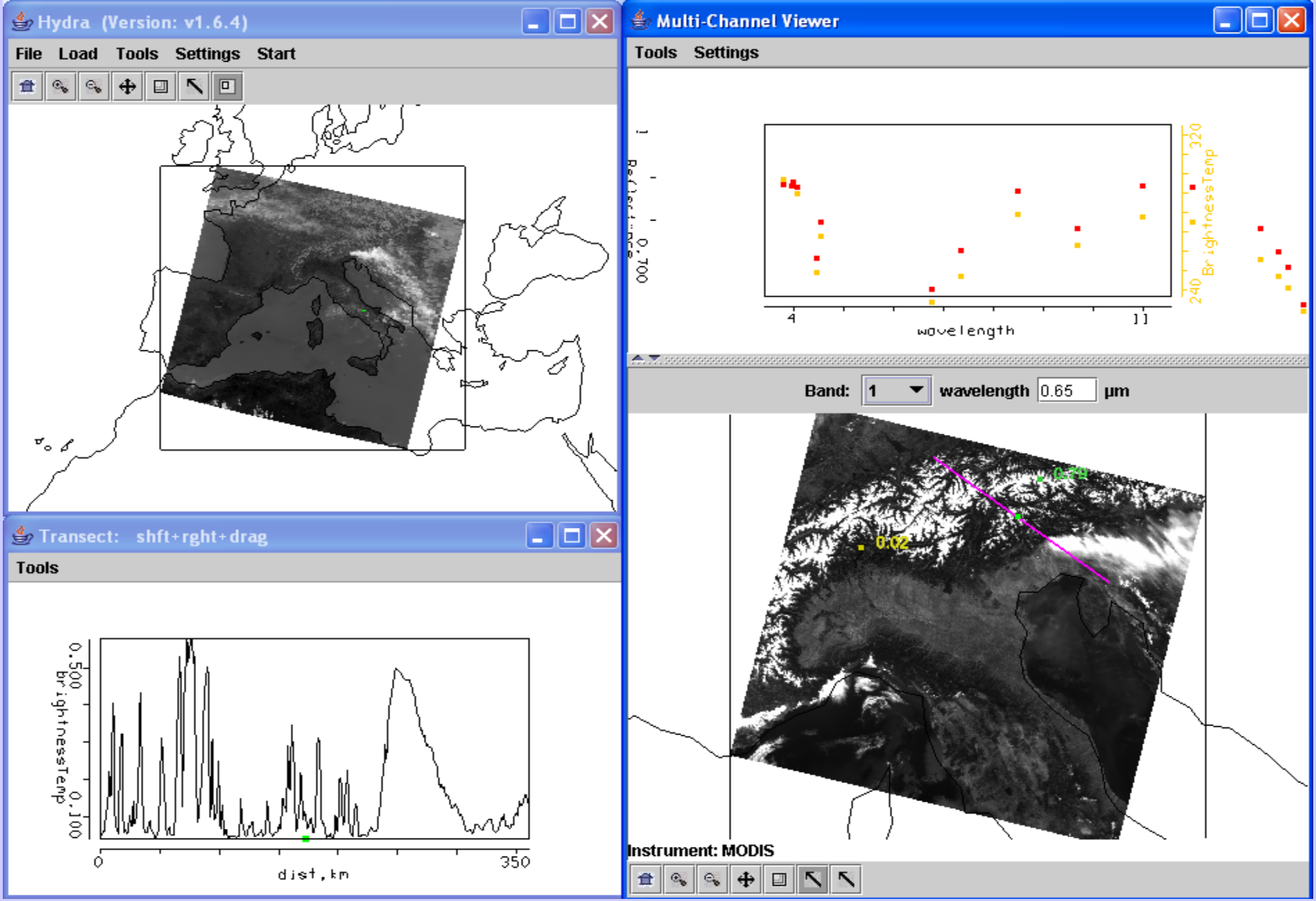

High clouds and snow both reflect a lot at 0.65 µm

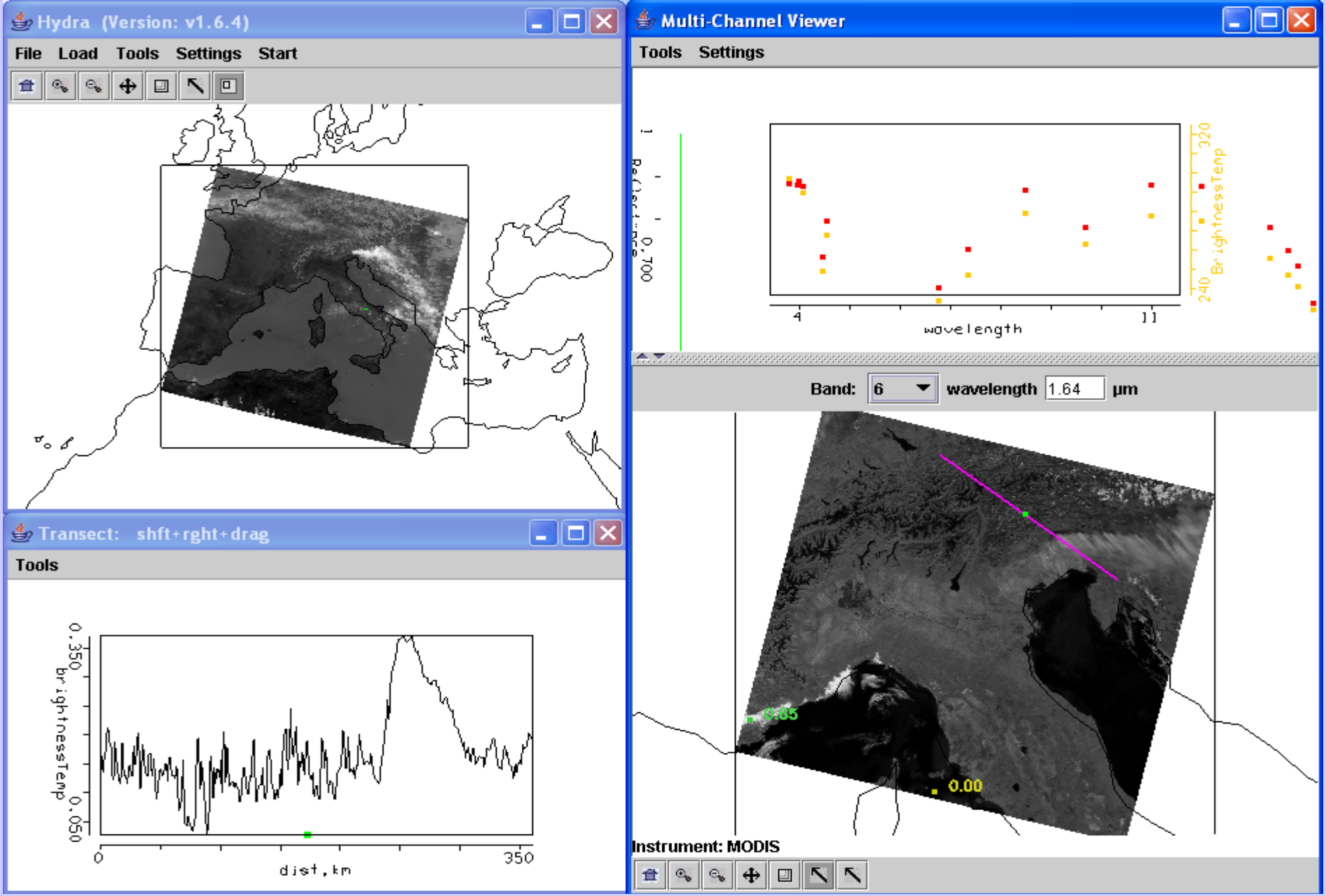

High clouds reflect but snow doesn't at 1.64 µm

Hydra (Version: v1.8.0)

File Load Tools Settings Start

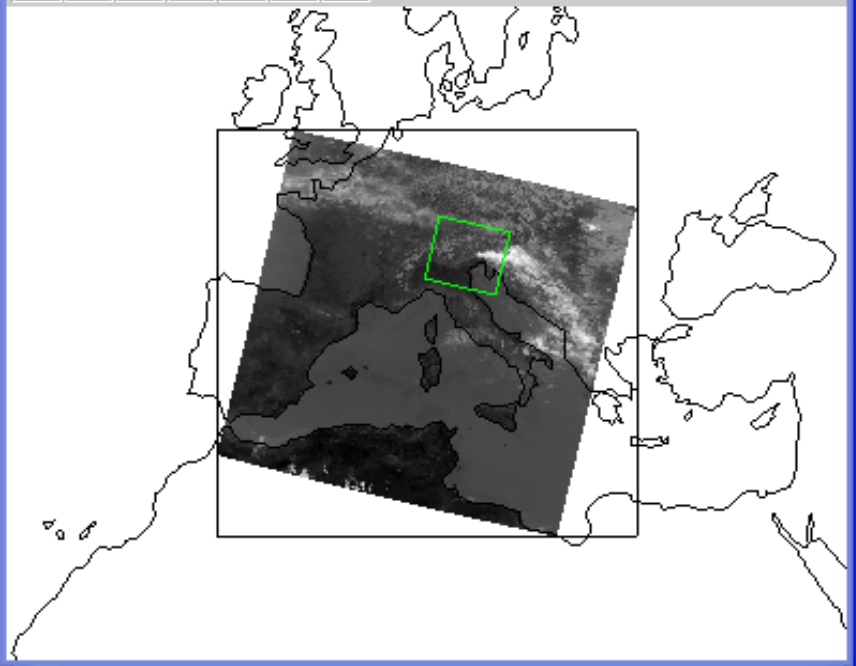

Transect: shft+rght+drag

Tools Settings

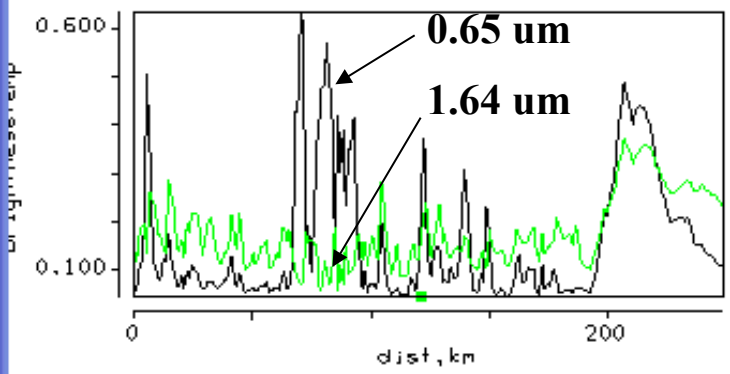

1 6

Multi-Channel Viewer

Tools Settings Import

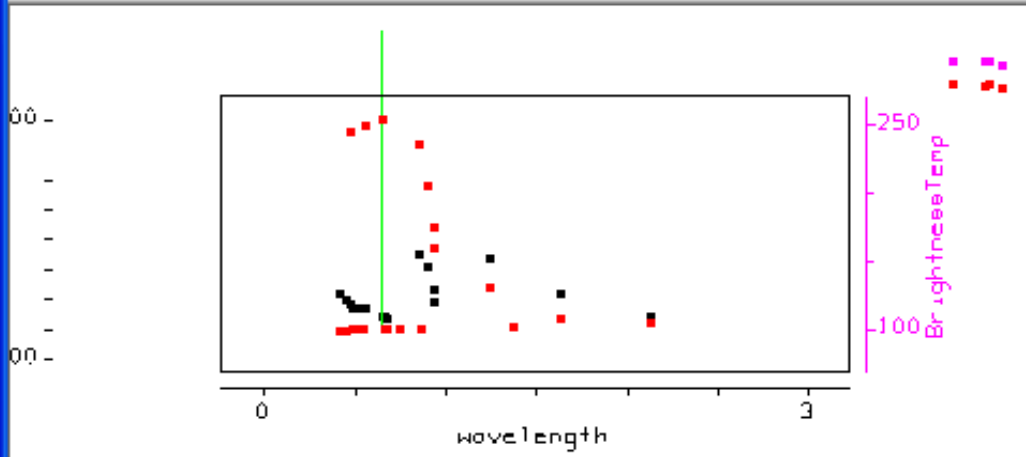

Band: 1 wavelength 0.65 µm

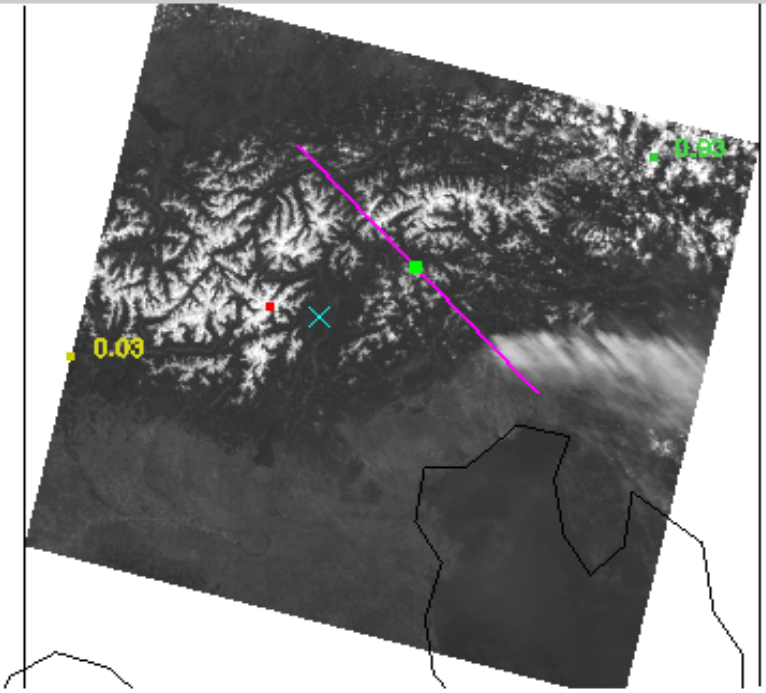

Instrument: MODIS Lat = 46.418 Lon = 11.127

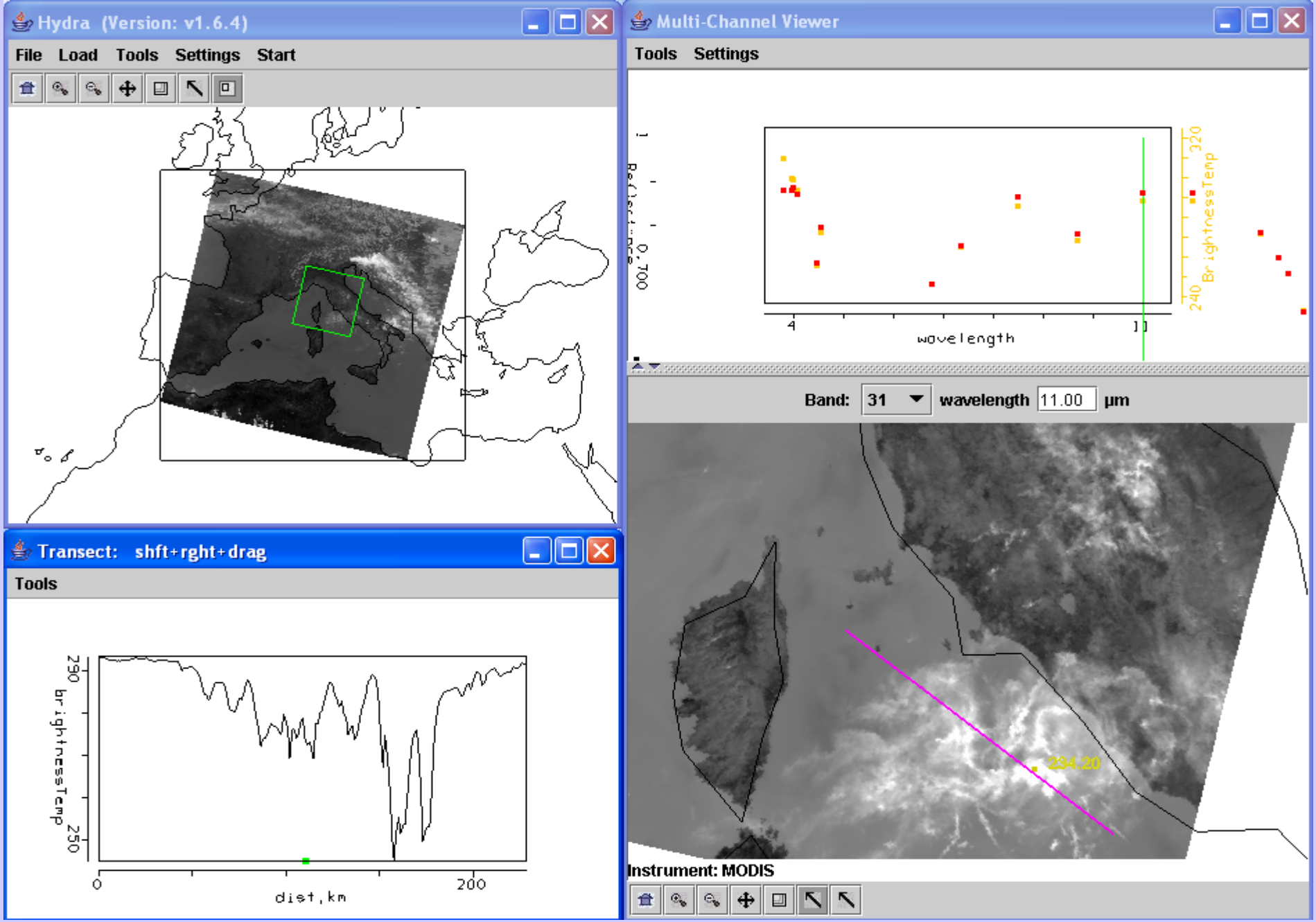

High clouds, cooler than surface, create lower 11 µm BTs

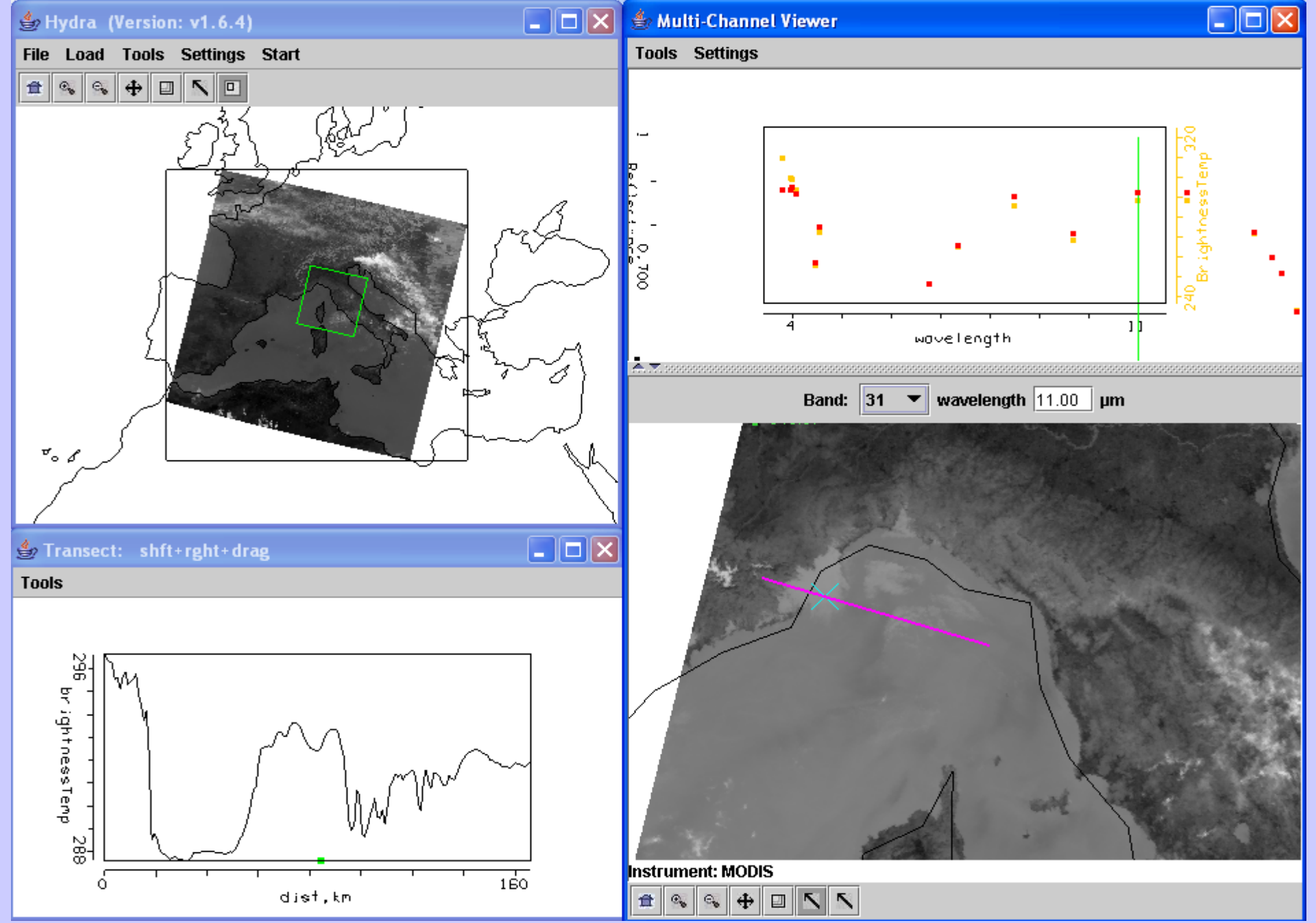

Low clouds, cooler than surface, create lower 11 µm BTs

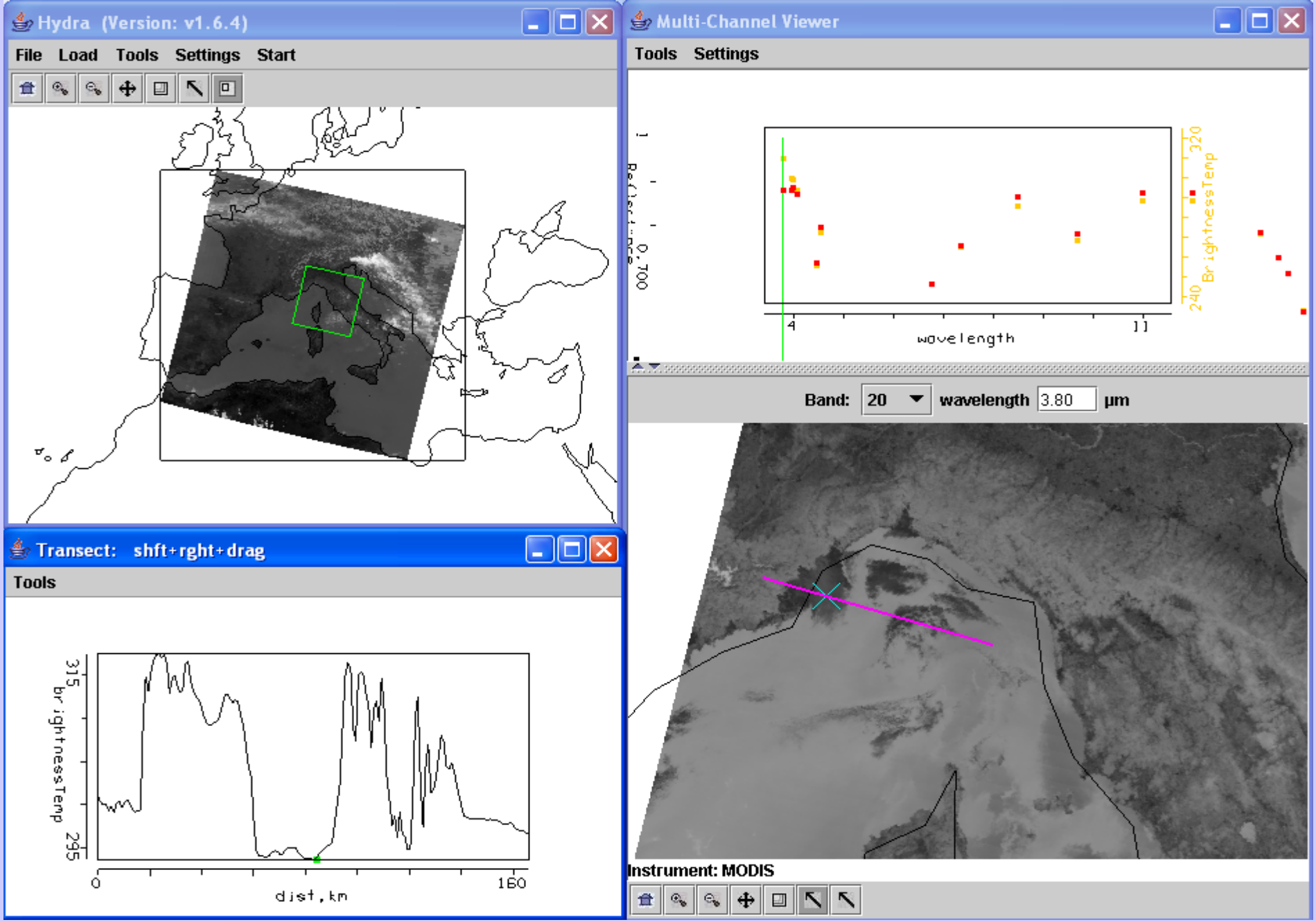

Low clouds reflecting create larger 4 µm brightness temperatures

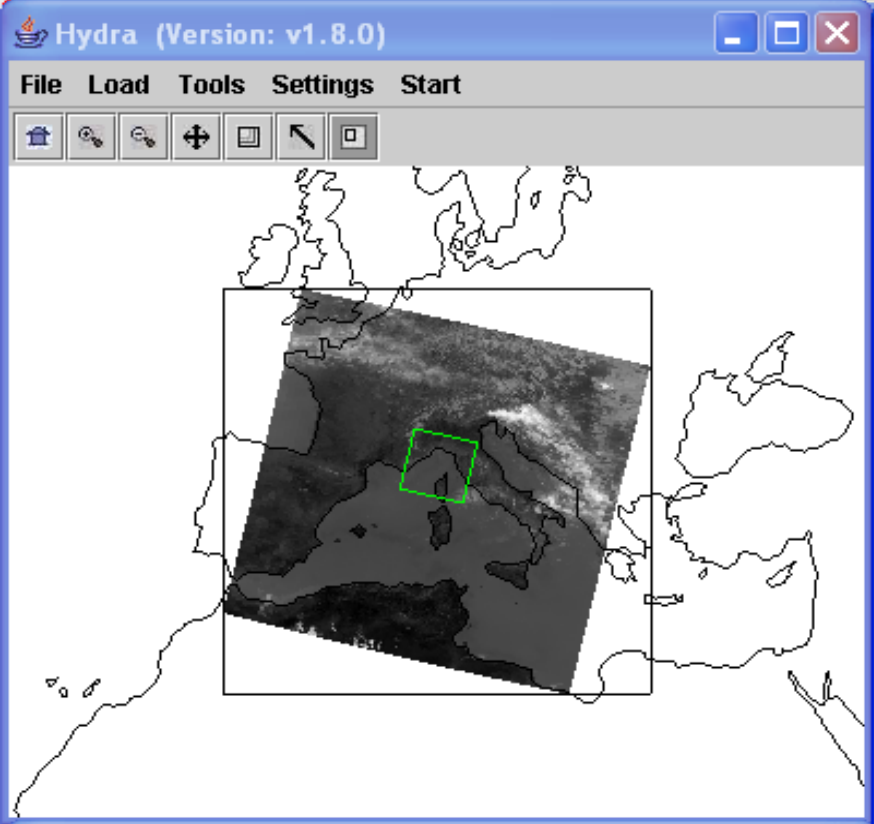
Hydra (Version: v1.8.0)
File Load Tools Settings Start

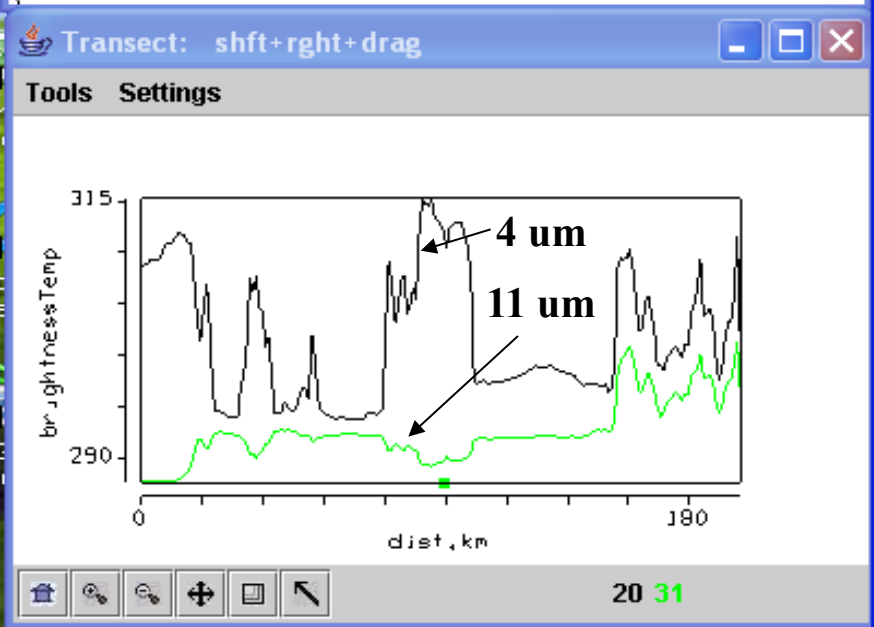
Transect: shft+rght+drag
Tools Settings
315
290
brightnessTemp
4 um
11 um
0
180
dist,km
20 31

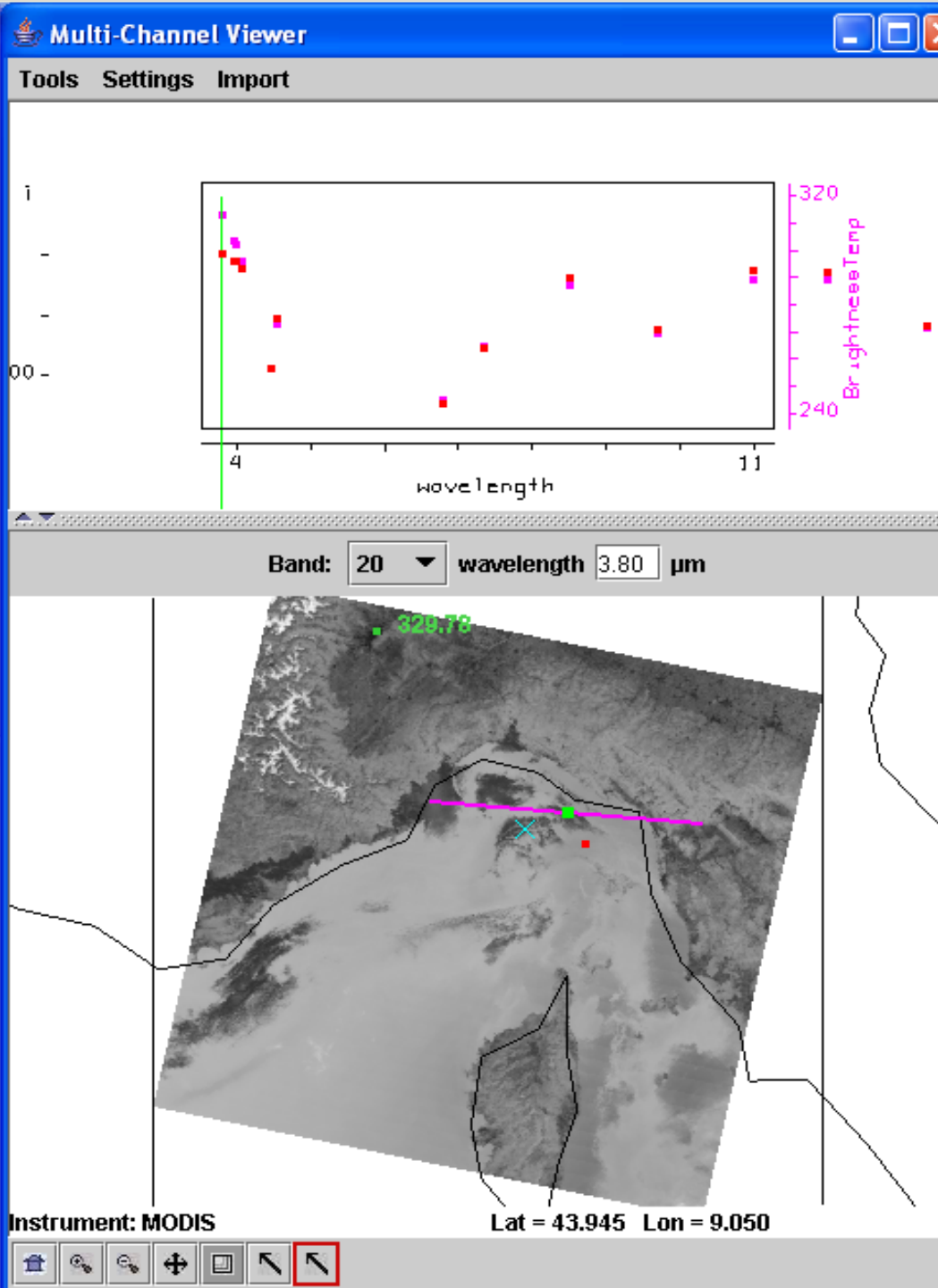
Multi-Channel Viewer
Tools Settings Import
320
240
BrightnessTemp
4
11
wavelength
Band: 20 wavelength 3.80 µm
329.78
Instrument: MODIS
Lat = 43.945 Lon = 9.050

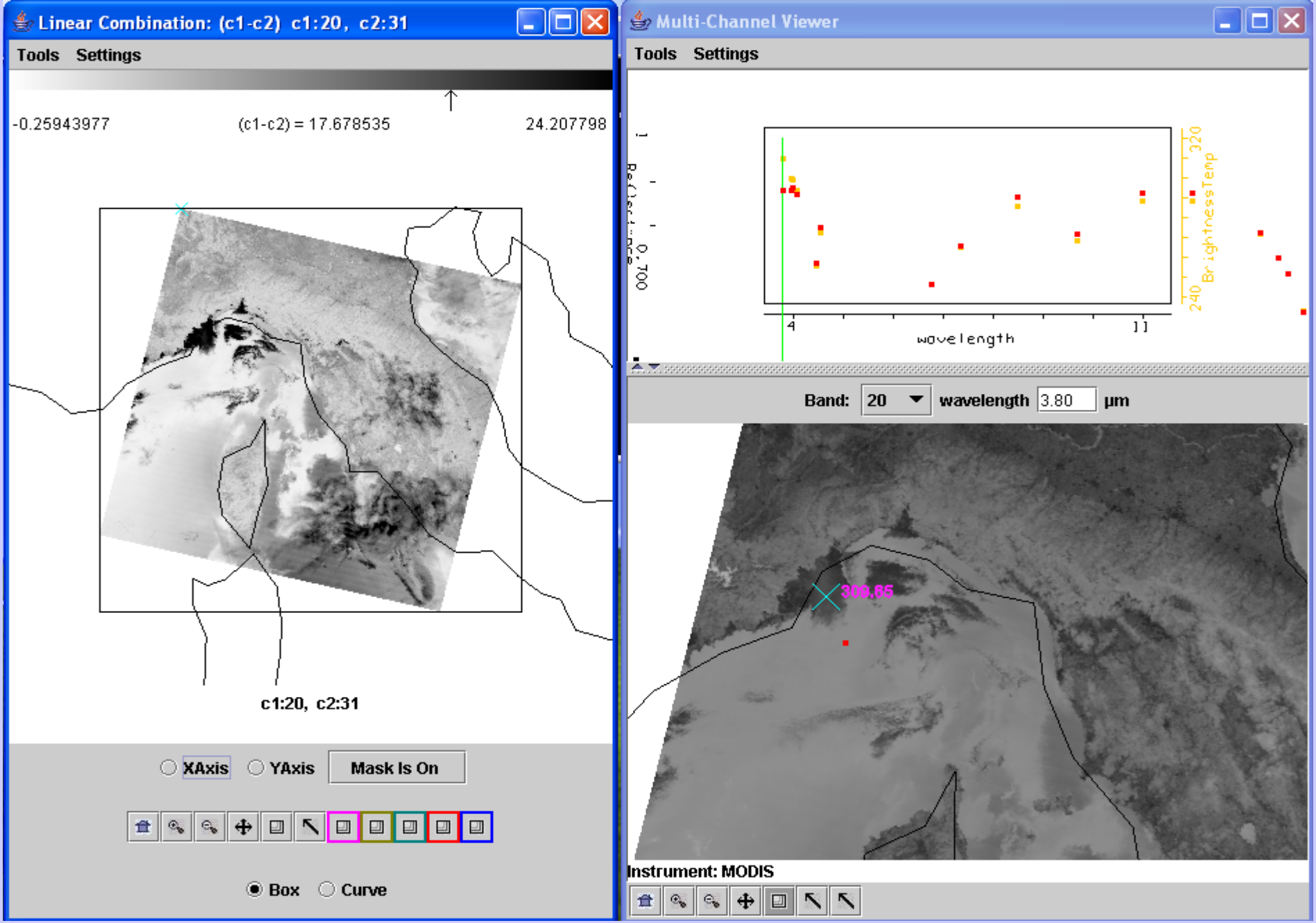

Detecting low clouds in 4-11 µm brightness temperature differences

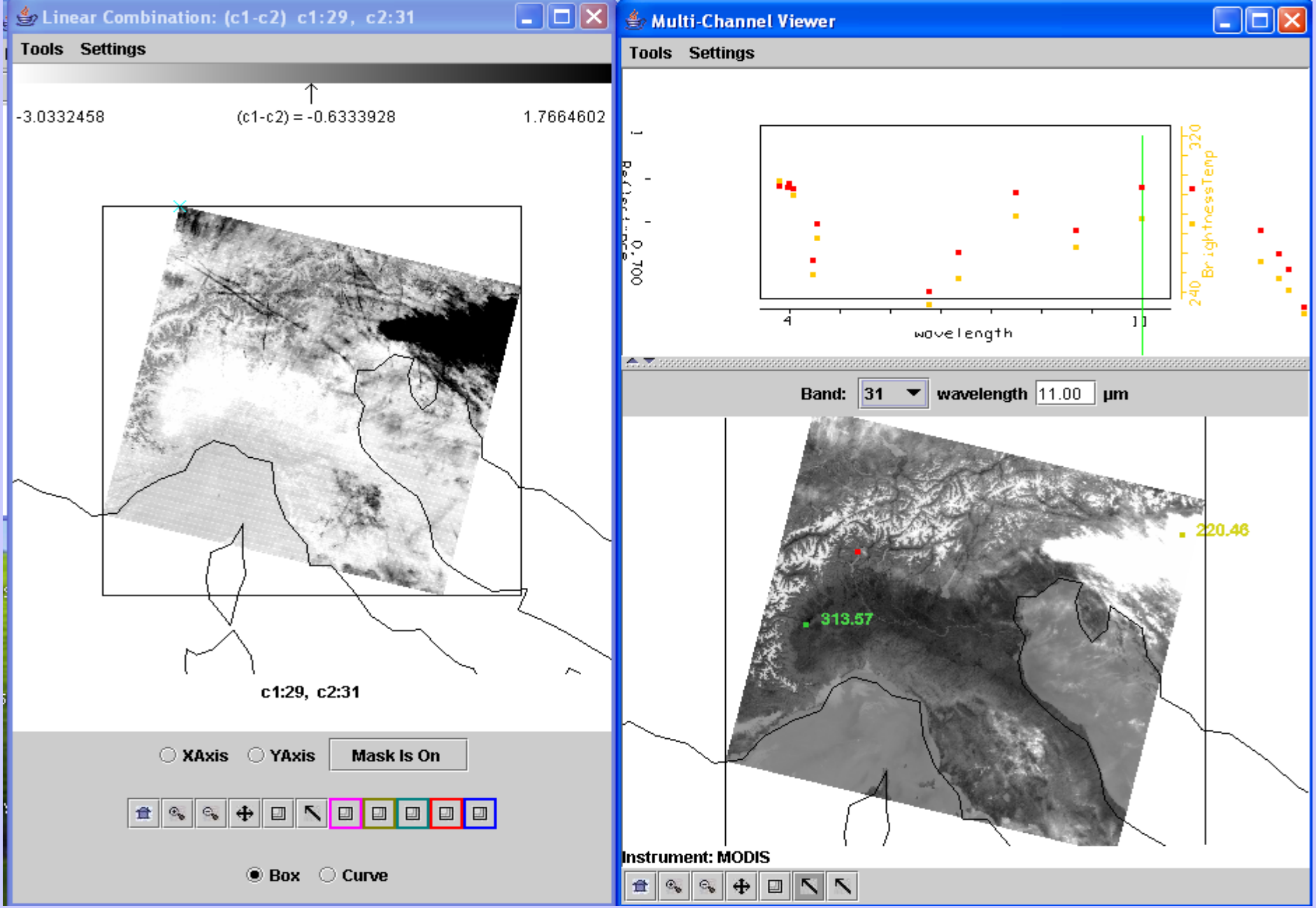

Detecting ice clouds in 8.6-11 μm brightness temperature differences

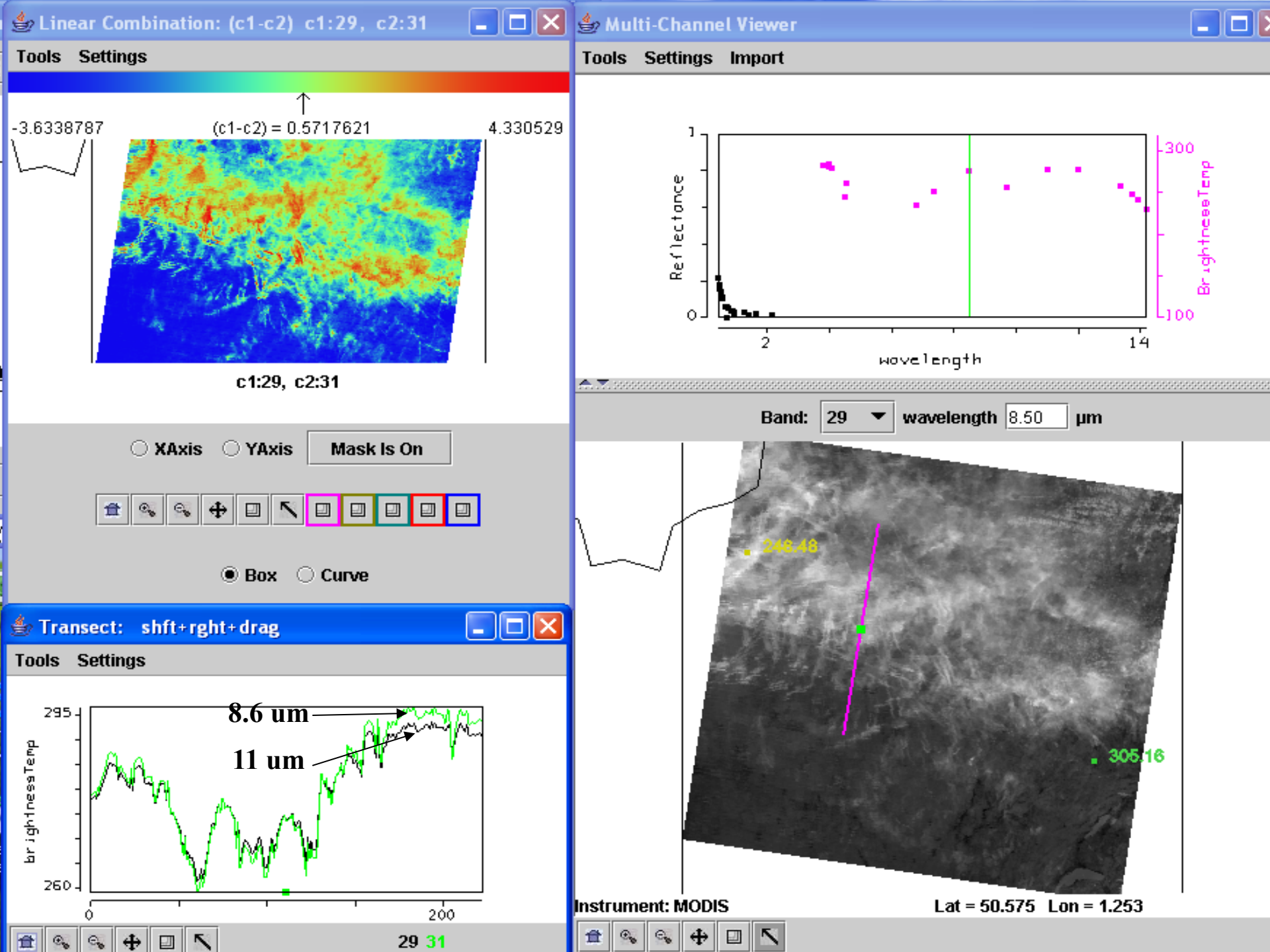
Linear Combination: (c1-c2) c1:29, c2:31
Tools Settings
-3.6338787
(c1-c2) = 0.5717621
4.330529
c1:29, c2:31
XAxis YAxis
Mask Is On
Box Curve
Transect: shft+rght+drag
Tools Settings
295
260
brightnessTemp
0
200
8.6 um
11 um
29 31
Multi-Channel Viewer
Tools Settings Import
1
0
Reflectance
2
14
wavelength
300
100
BrightnessTemp
Band: 29 wavelength 8.50 µm
248.48
305.16
Instrument: MODIS
Lat = 50.575 Lon = 1.253

Optical properties of cloud particles: imaginary part of refraction index

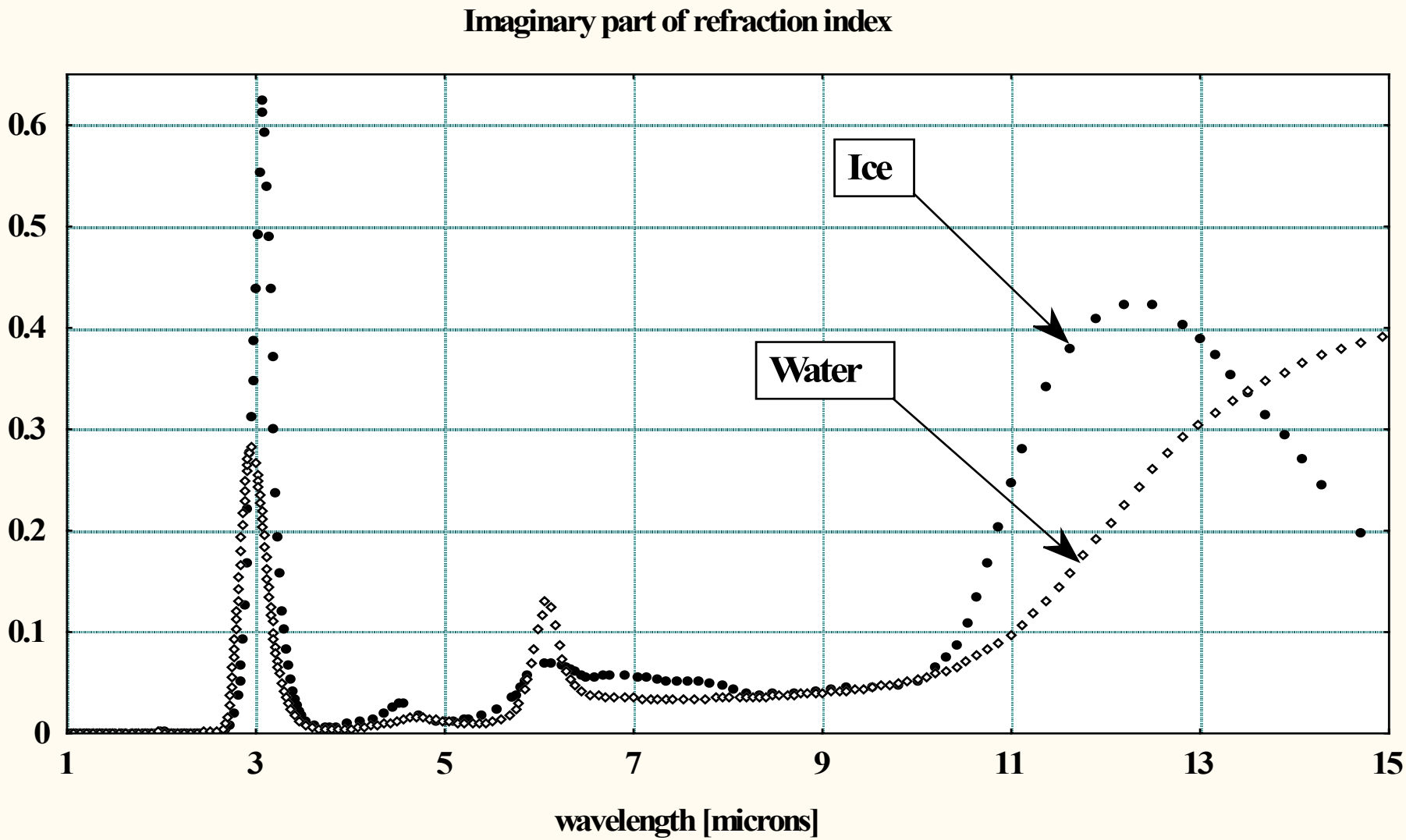

BT[8.6] – BT[11] will be positive for ice clouds

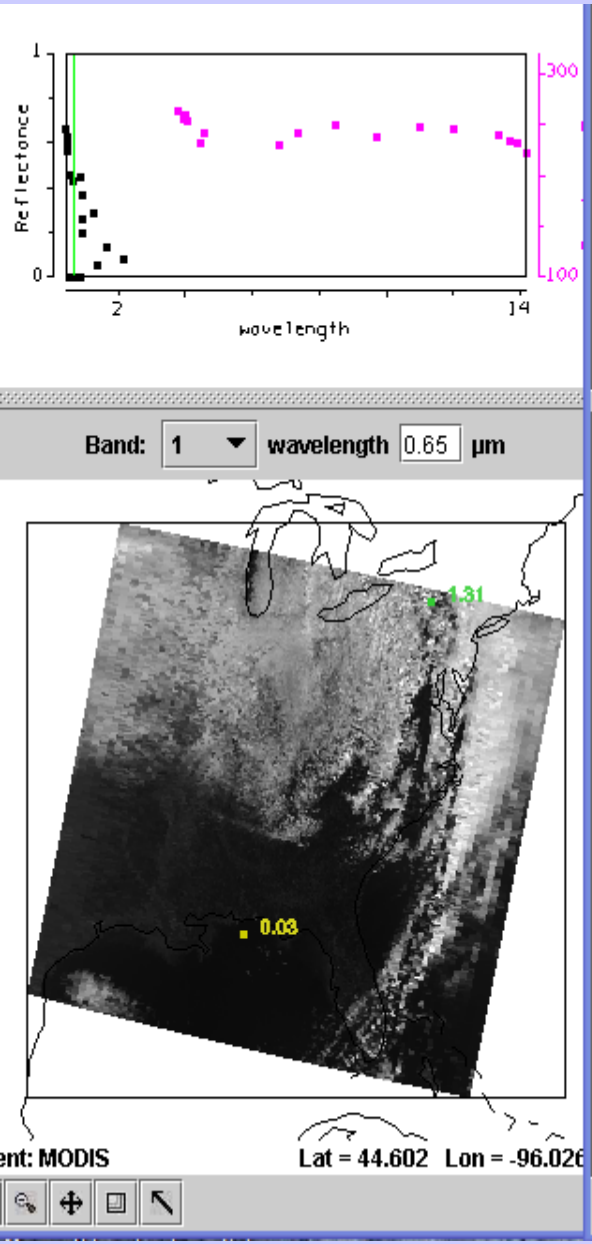
Reflectance
1
0
300
100
2
14
wavelength
Band: 1
wavelength 0.65 µm
1.31
0.03
Lat = 44.602 Lon = -96.026

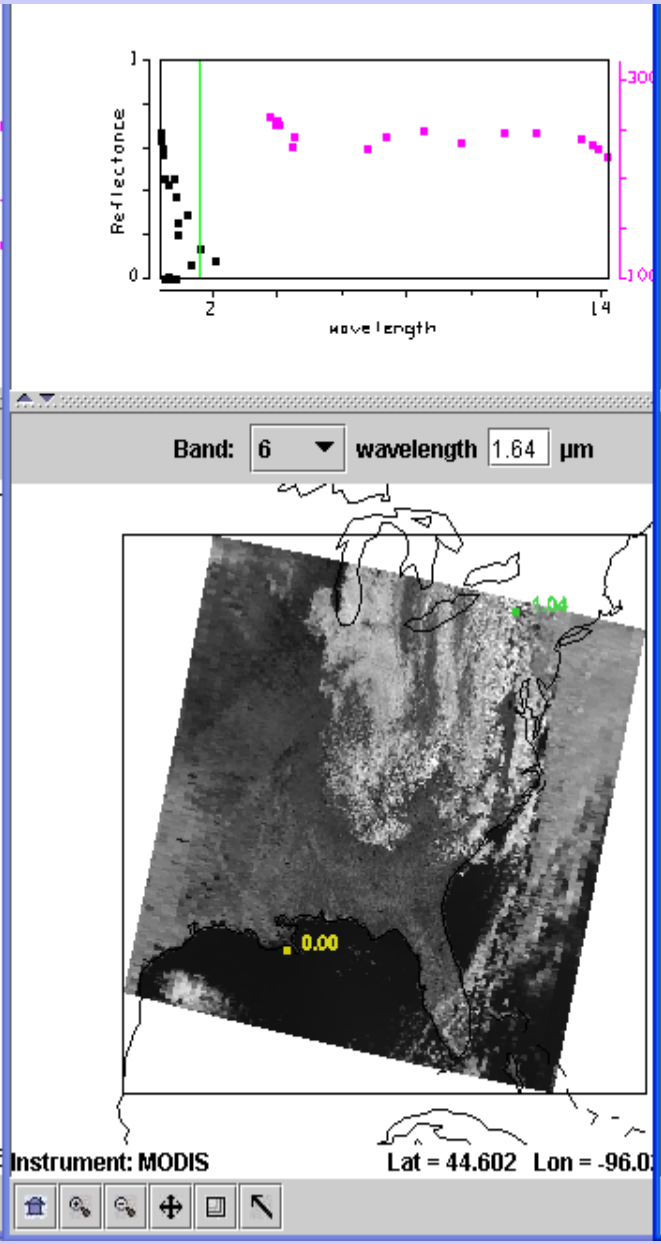
Reflectance
1
0
300
100
2
14
wavelength
Band: 6
wavelength 1.64 µm
1.04
0.00
Instrument: MODIS
Lat = 44.602 Lon = -96.0

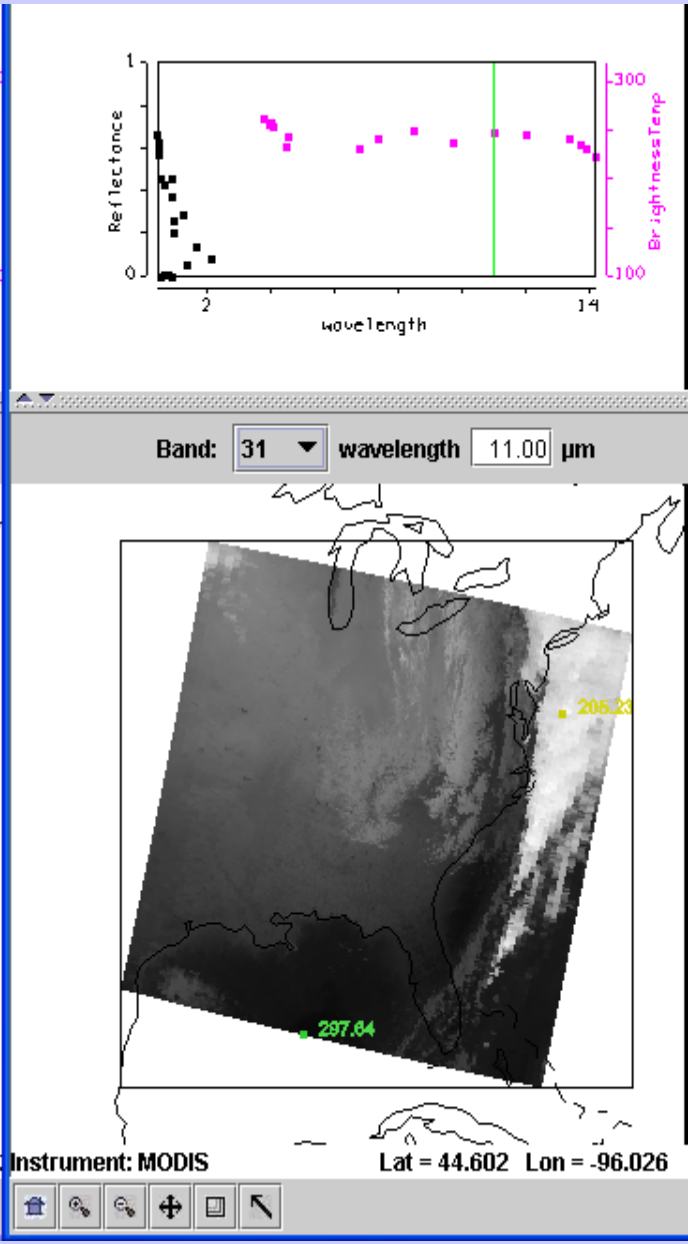
Reflectance
BrightnessTemp
1
0
300
100
2
14
wavelength
Band: 31
wavelength 11.00 µm
297.64
Instrument: MODIS
Lat = 44.602 Lon = -96.026

MODIS identifies cloud classes

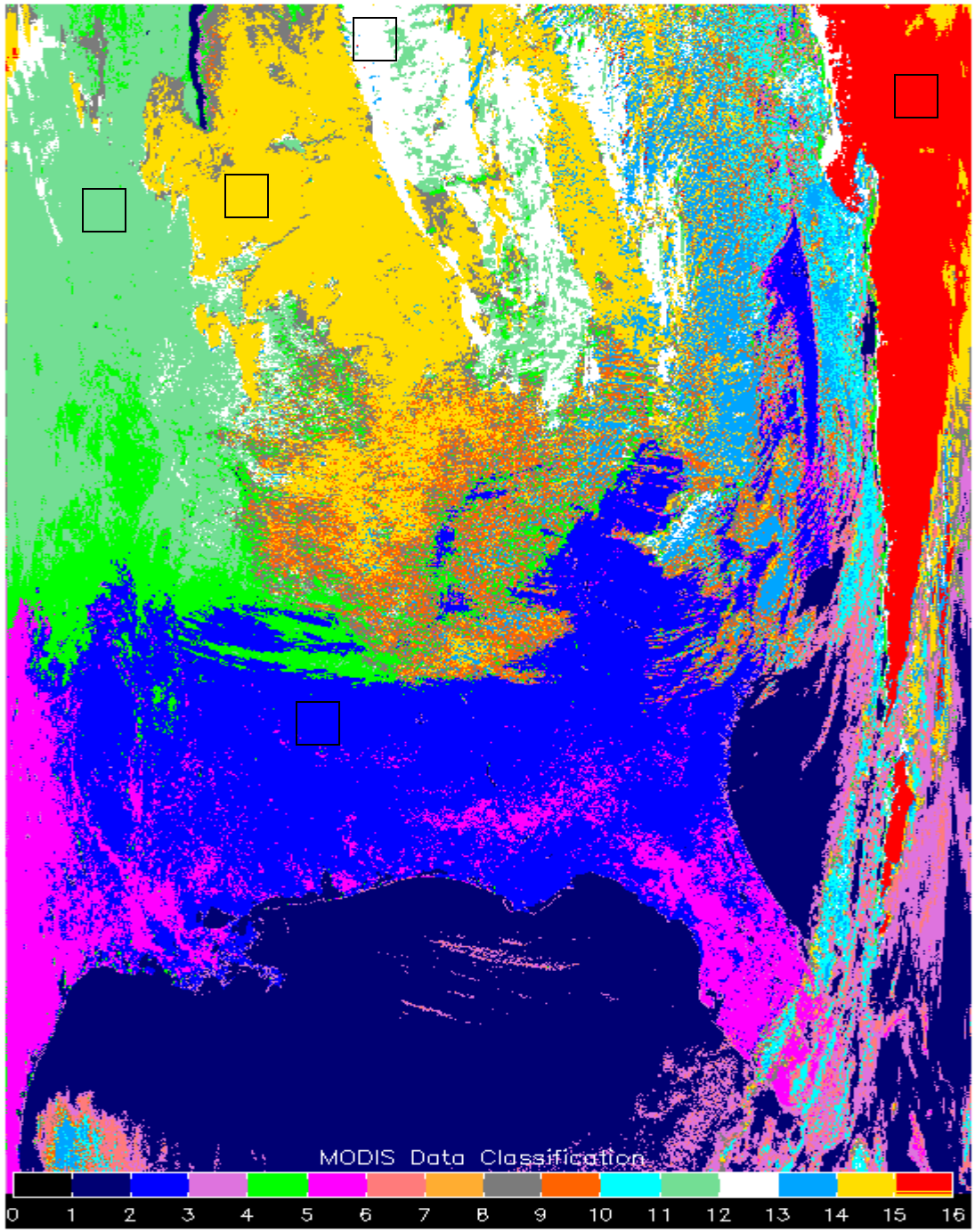

Hi cld

Mid cld

Lo cld

Snow

clr

Clouds separate into classes when multispectral radiance information is viewed

vis

LSD 1.6 um

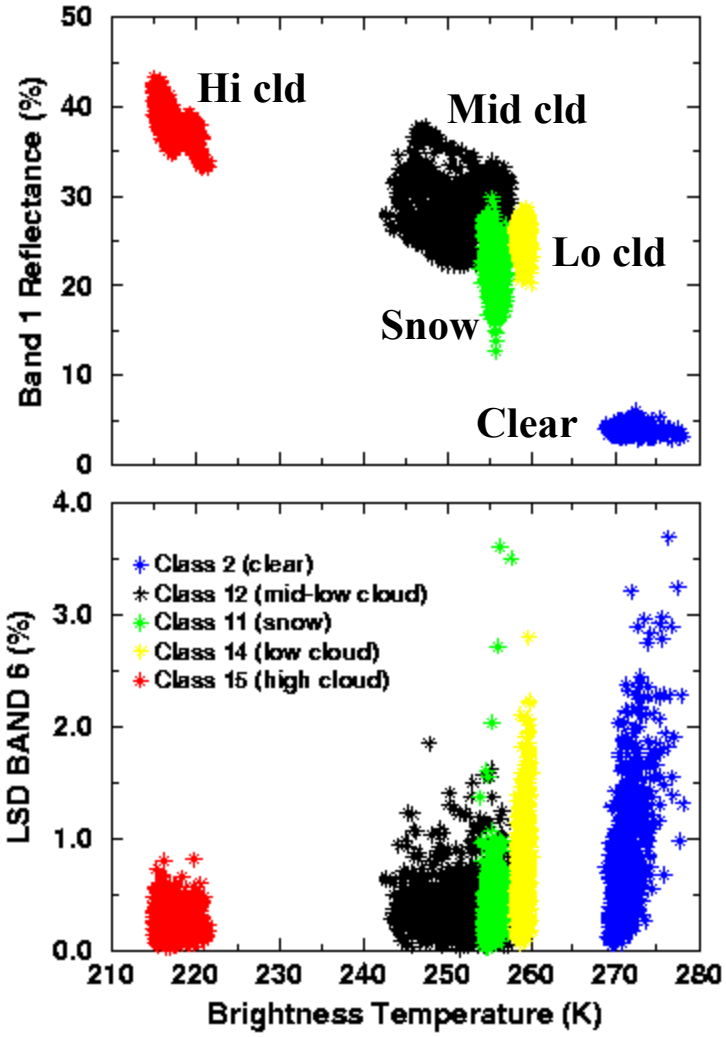

11 um

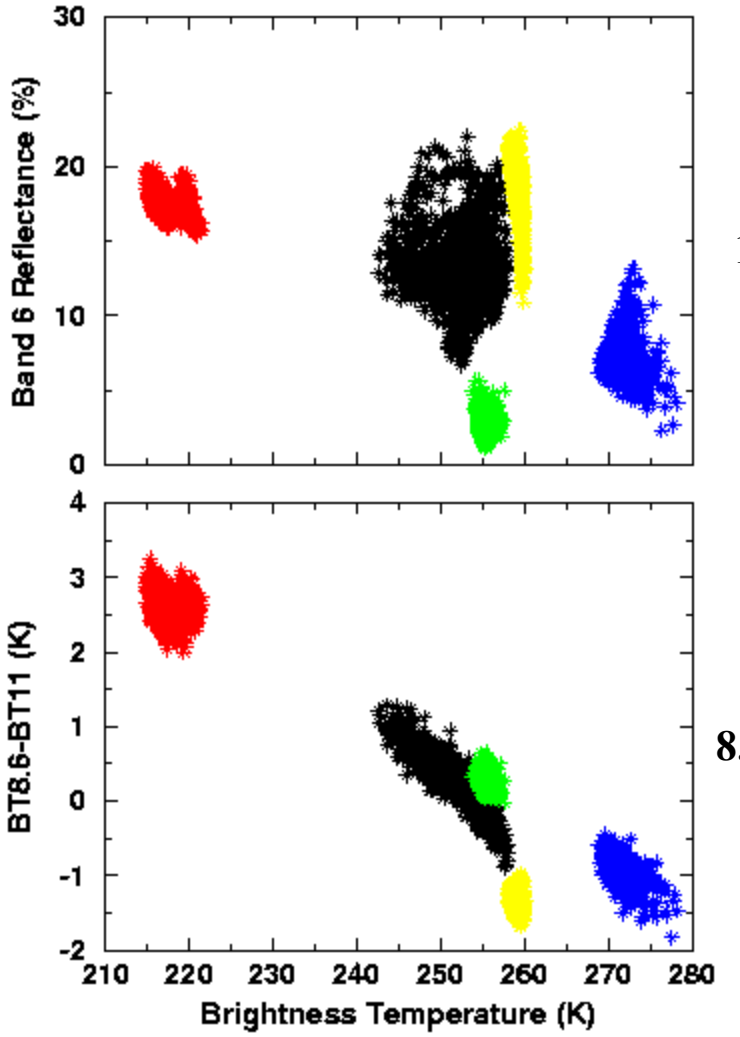

1.6 um

8.6-11 um

11 um

Cloud Properties

True Color Image
Cloud Mask
Land Classification
Cloud Opt Thickness
Cloud Eff Radius
Cloud Top Temp
Bispectral Phase

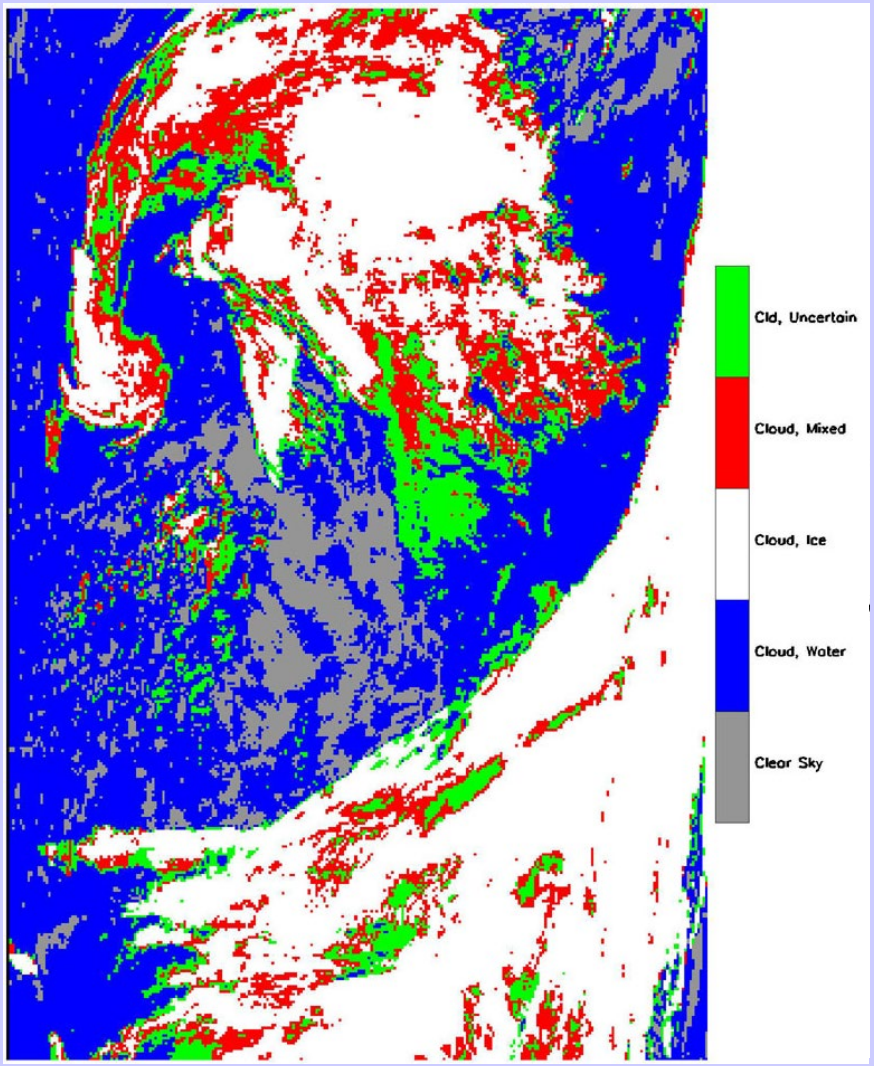

October 1, 2001

Cloud optical, microphysical properties

retrieval space example

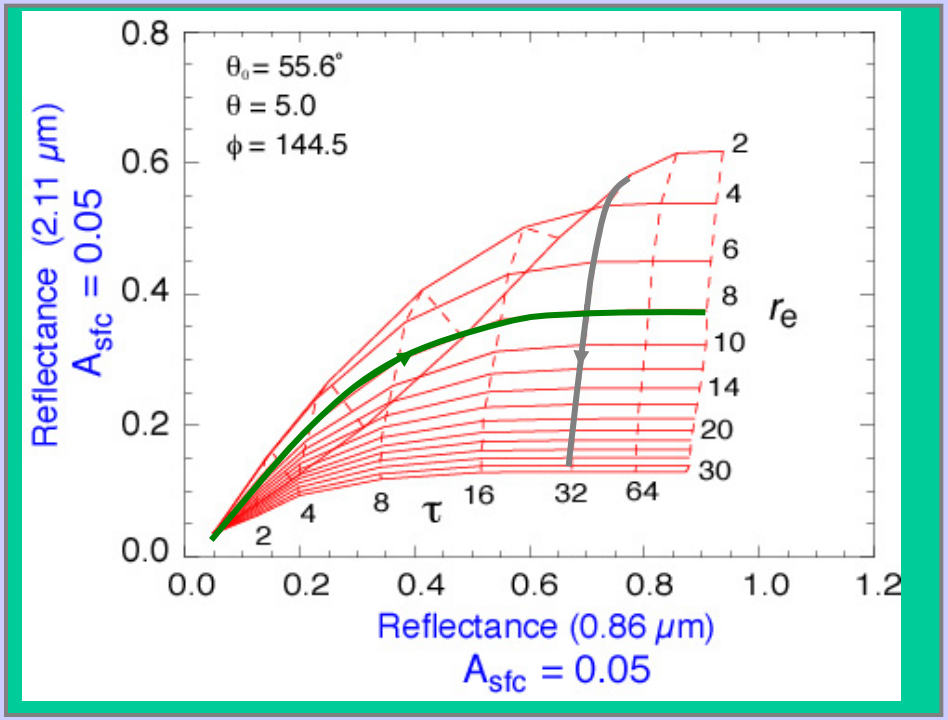

2.1 μm absorption increases with particle size, little effect at 0.86 μm

2.1 μm reflectance reaches limiting values with optical thickness

Liquid water cloud
ocean surface

Radiance from a partly cloudy FOV

Cloud Parameter Determinations from Satellite Measured Radiances
for a given field of view (FOV) partly clear and partly cloudy

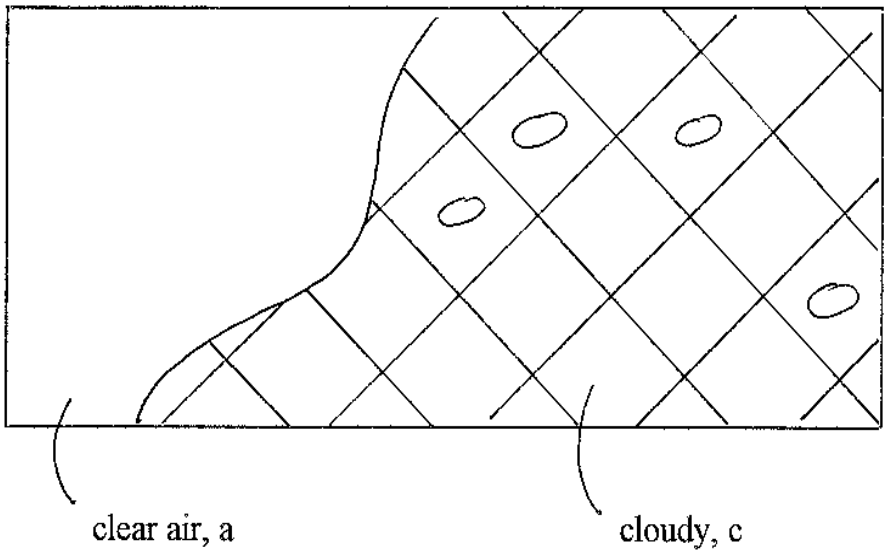

$$R = [1 - N] R_a + N R_c$$

but if b indicates opaque "black" cloud

$$R_c = [1 - \varepsilon] R_a + \varepsilon R_b(p_c)$$

so together

$$R = [1 - N\varepsilon] R_a + N\varepsilon R_b(p_c)$$

Two unknowns, ε and Pc, require two measurements

RTE in Cloudy Conditions

$$I_\lambda = \eta\, I_\lambda^{cd} + (1 - \eta)\, I_\lambda^{clr}$$ where cd = cloud, clr = clear, η = cloud fraction

$$I_\lambda^{clr} = B_\lambda(T_s)\, \tau_\lambda(p_s) + \int_{p_s}^{o} B_\lambda(T(p))\, d\tau_\lambda \,.$$

$$I_\lambda^{cd} = (1-\varepsilon_\lambda)\, B_\lambda(T_s)\, \tau_\lambda(p_s) + (1-\varepsilon_\lambda) \int_{p_s}^{p_c} B_\lambda(T(p))\, d\tau_\lambda$$

$$+ \varepsilon_\lambda\, B_\lambda(T(p_c))\, \tau_\lambda(p_c) + \int_{p_c}^{o} B_\lambda(T(p))\, d\tau_\lambda$$

ε_λ is emittance of cloud. First two terms are from below cloud, third term is cloud contribution, and fourth term is from above cloud. After rearranging

$$I_\lambda - I_\lambda^{clr} = \eta\varepsilon_\lambda \int_{p_s}^{p_c} \tau(p)\, \frac{dB_\lambda}{dp}\, dp \,.$$

CO2 channels see to different levels in the atmosphere

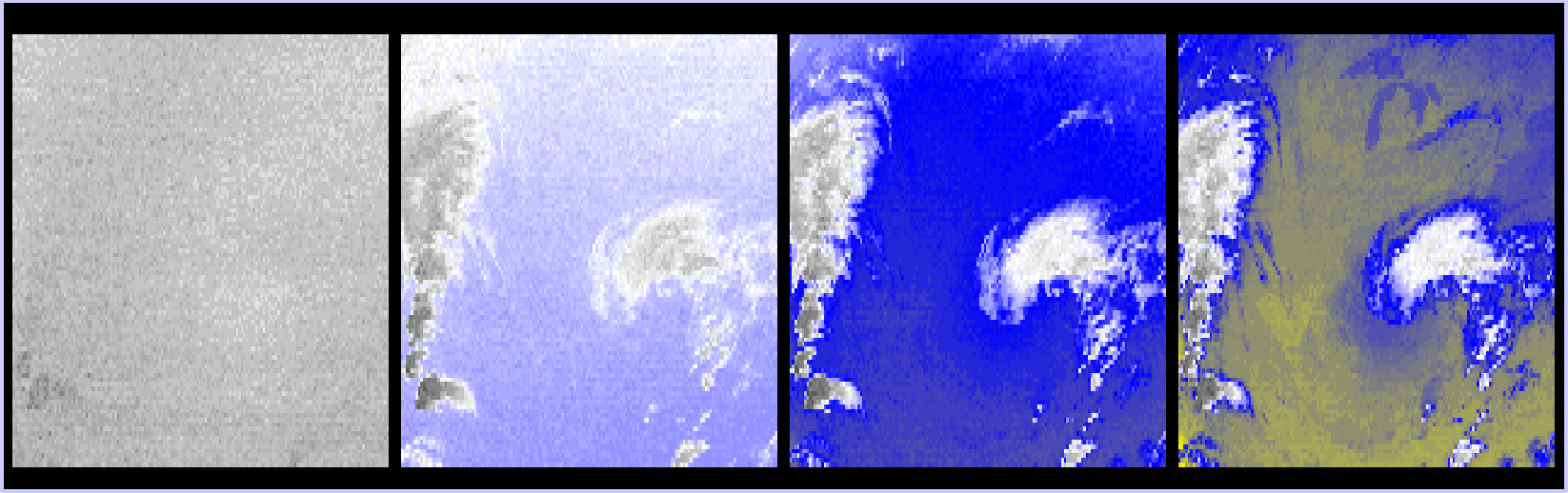

14.2 um 13.9 um 13.6 um 13.3 um

Cloud Properties from CO2 Slicing

RTE for cloudy conditions indicates dependence of cloud forcing (observed minus clear sky radiance) on cloud amount ($\eta\varepsilon_\lambda$) and cloud top pressure (p_c)

$$(I_\lambda - I_\lambda^{clr}) = \eta\varepsilon_\lambda \int_{p_s}^{p_c} \tau_\lambda \, dB_\lambda \, .$$

Higher colder cloud or greater cloud amount produces greater cloud forcing; dense low cloud can be confused for high thin cloud. Two unknowns require two equations.

p_c can be inferred from radiance measurements in two spectral bands where cloud emissivity is the same. $\eta\varepsilon_\lambda$ is derived from the infrared window, once p_c is known.

Different ratios reveal cloud properties at different levels

hi - 14.2/13.9
mid - 13.9/13.6
low - 13.6/13.3

Meas **Calc**

$$\frac{(I_{\lambda 1}-I_{\lambda 1}^{clr})}{(I_{\lambda 2}-I_{\lambda 2}^{clr})} = \frac{\eta\varepsilon_{\lambda 1}\int_{p_s}^{p_c}\tau_{\lambda 1}\,dB_{\lambda 1}}{\eta\varepsilon_{\lambda 2}\int_{p_s}^{p_c}\tau_{\lambda 2}\,dB_{\lambda 2}}$$

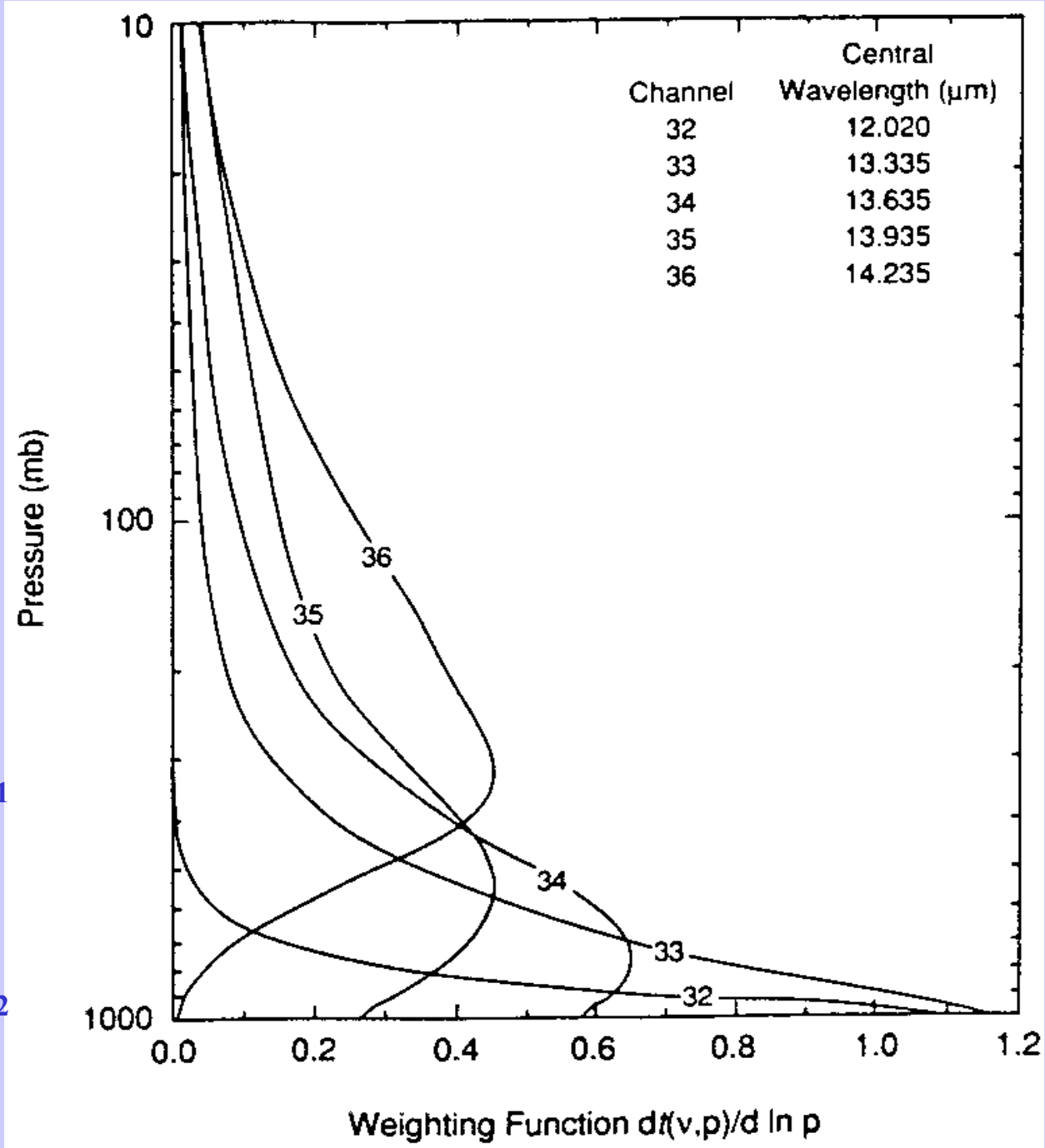

BTs in and out of clouds for MODIS CO_2 bands

demonstrate weighting functions and cloud top algorithm

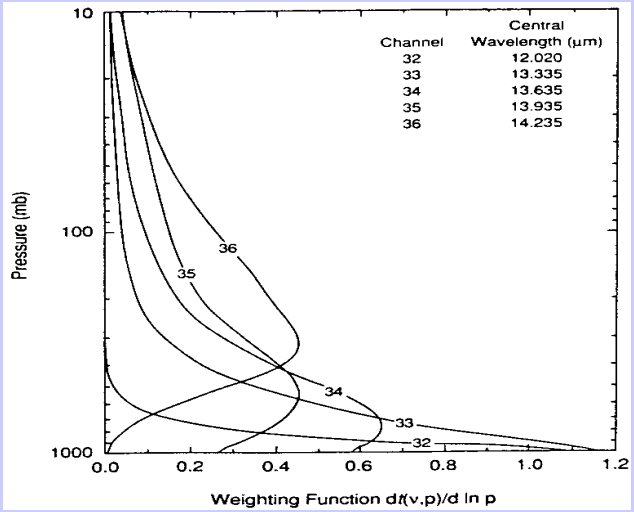

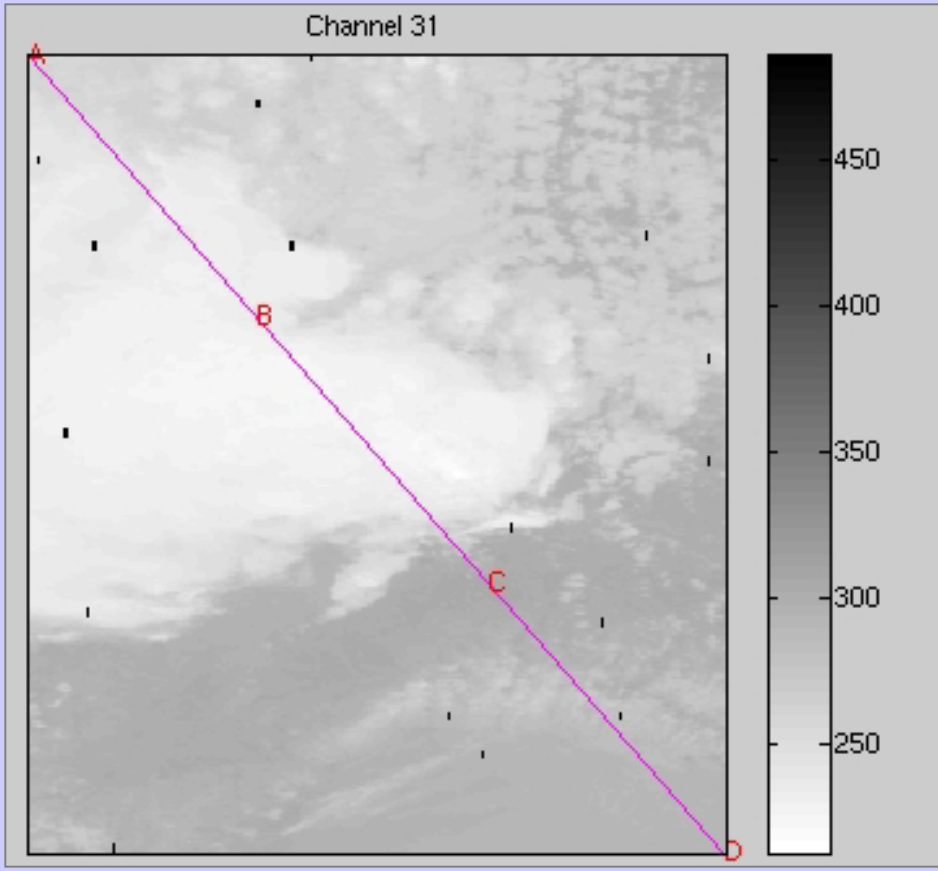

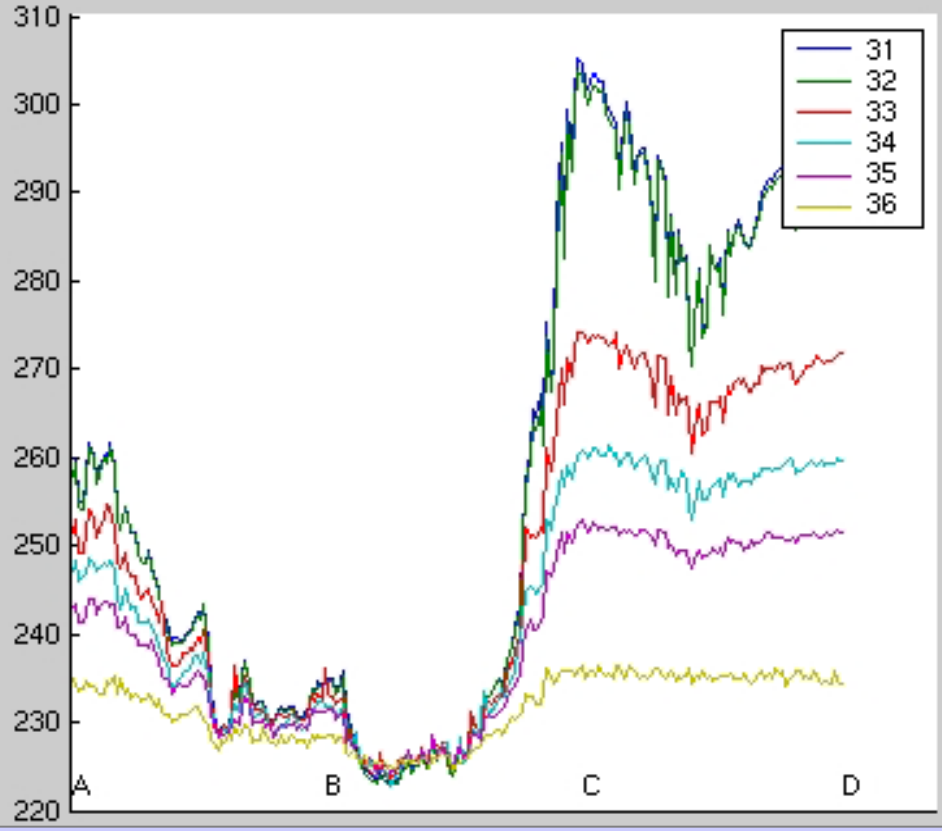

AQUA/MODIS BAND1 2300UTC 8/24/02

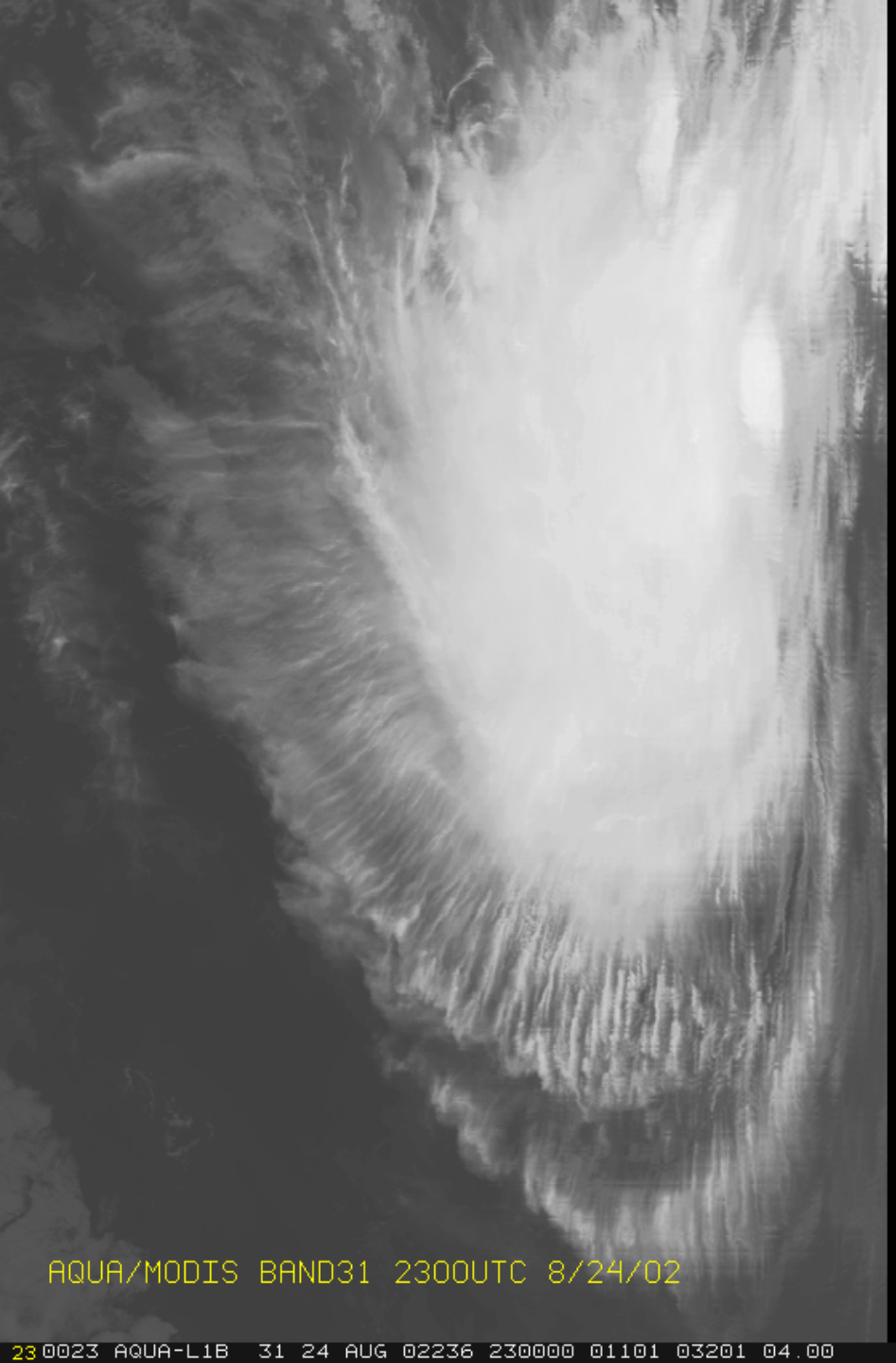

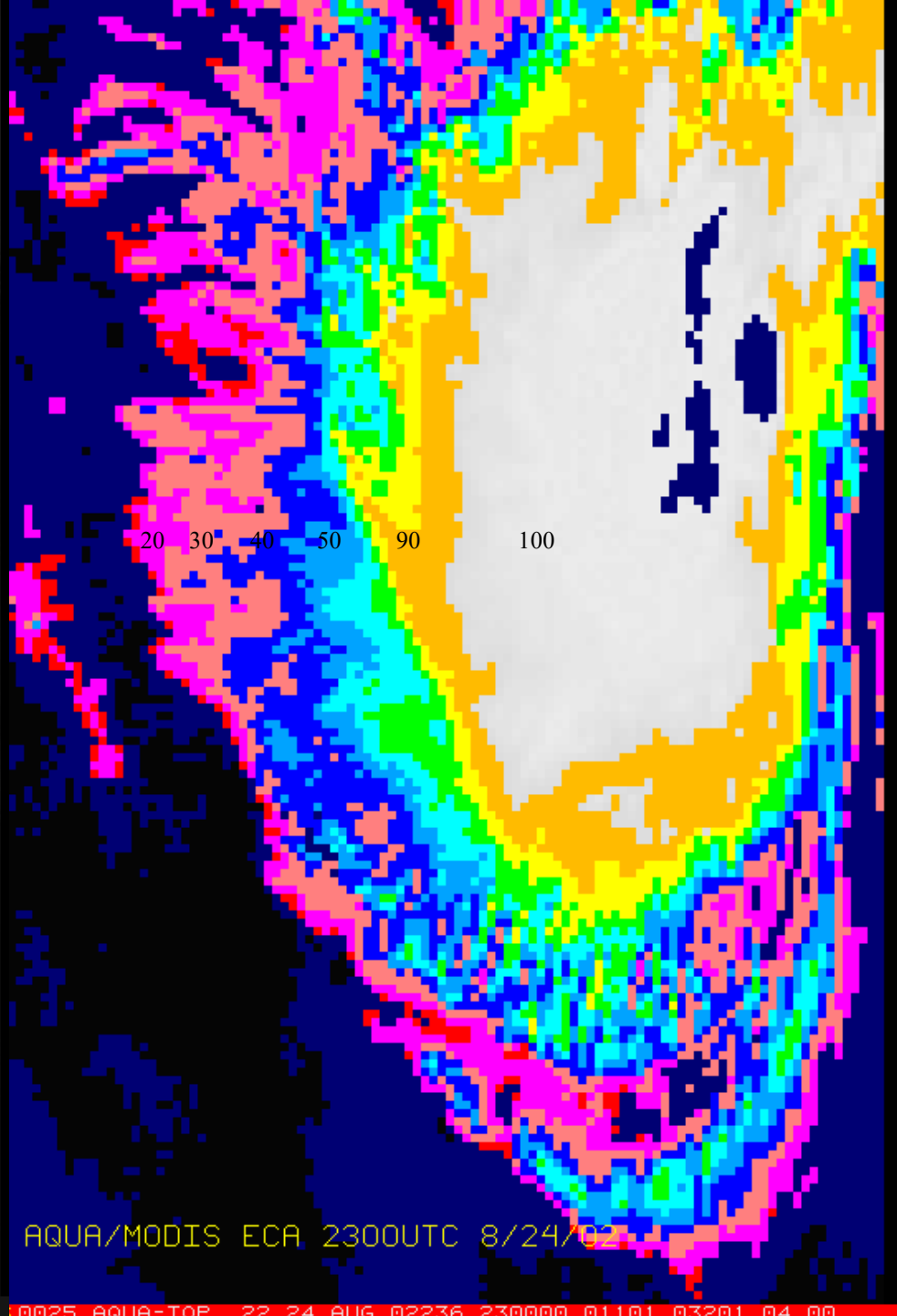

23 0023 AQUA-L1B 31 24 AUG 02236 230000 01101 03201 04.00
0025 AQUA-TOP 22 24 AUG 02236 230000 01101 03201 04.00

January 2001: MODIS High Clouds (0–400 mb)

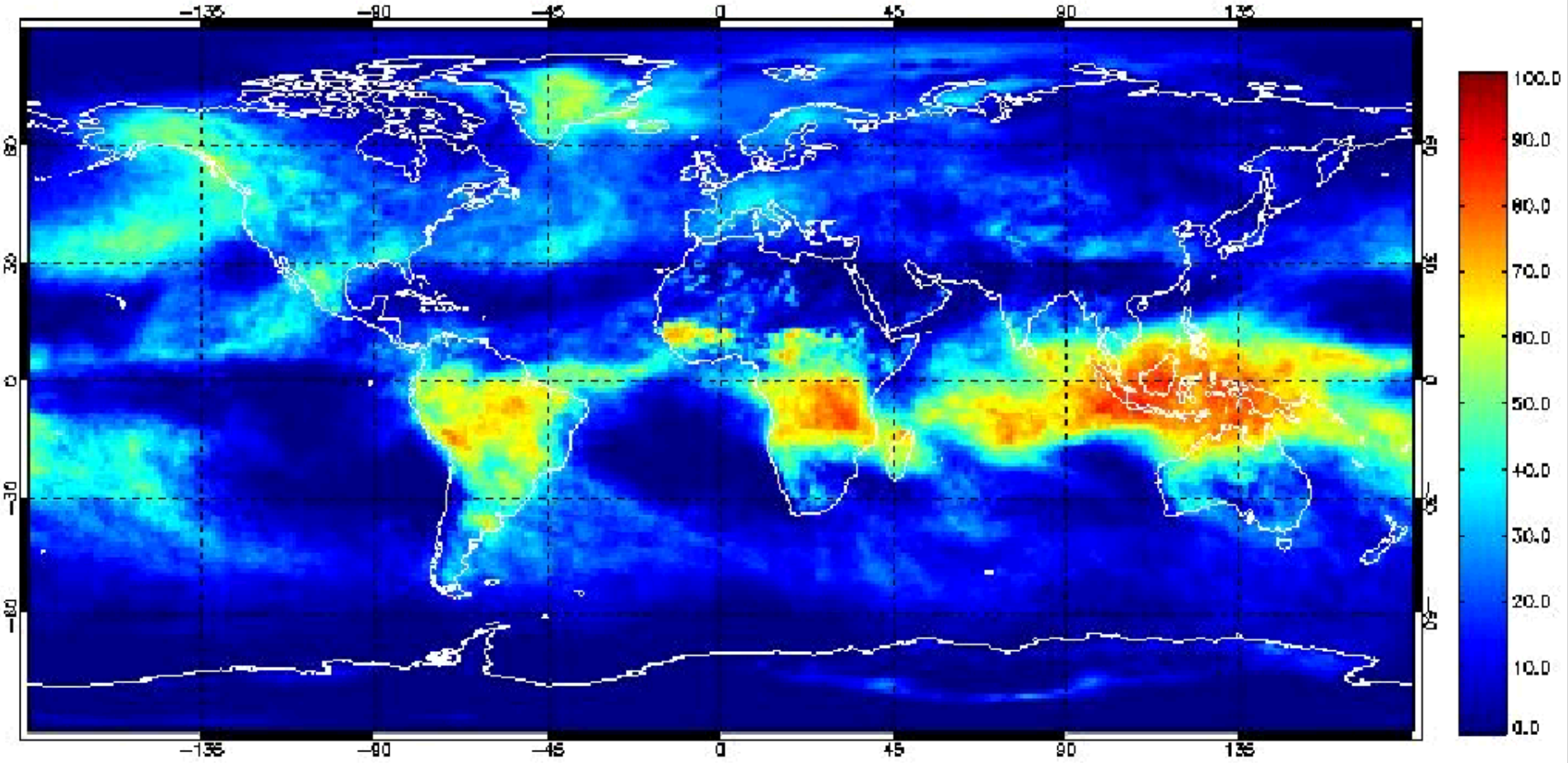

Simulations of Ice and Water Phase Clouds
8.5 - 11 μm BT Differences

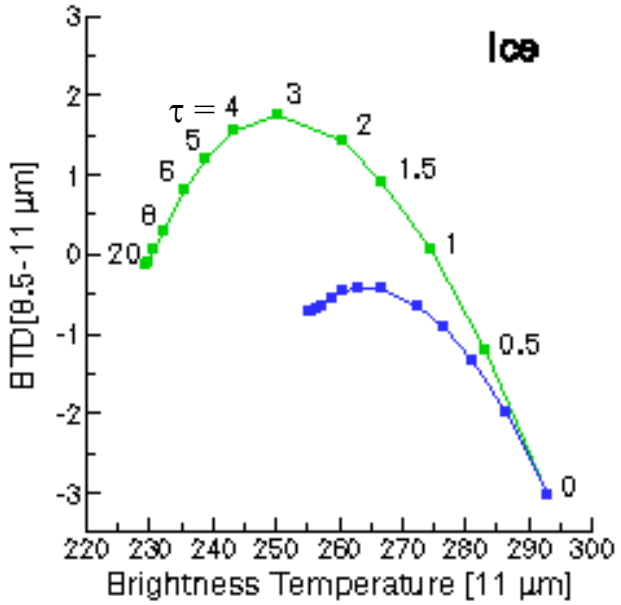

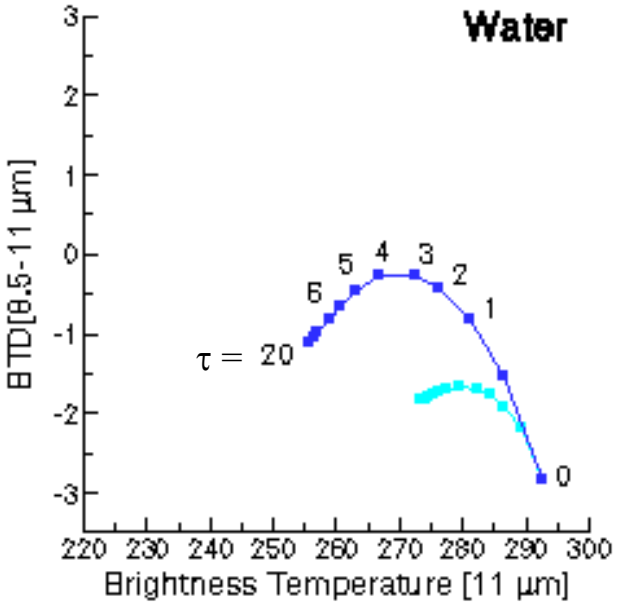

High Ice clouds

- BTD[8.5-11] > 0 over a large range of optical thicknesses τ
- T_{cld} = 228 K

Midlevel clouds

- BTD[8.5-11] values are similar (*i.e.*, negative) for both water and ice clouds
- T_{cld} = 253 K

Low-level, warm clouds

- BTD[8.5-11] values always negative
- T_{cld} = 273 K

Ice: Cirrus model derived from FIRE-I in-situ data (Nasiri et al, 2002)
Water: r_e=10 μm
Angles: θ_o = 45°, θ = 20°, and ϕ = 40°
Profile: midlatitude summer

MODIS Direct Broadcast

May 14, 2003 at 1458 UTC (Terra)
1-km resolution

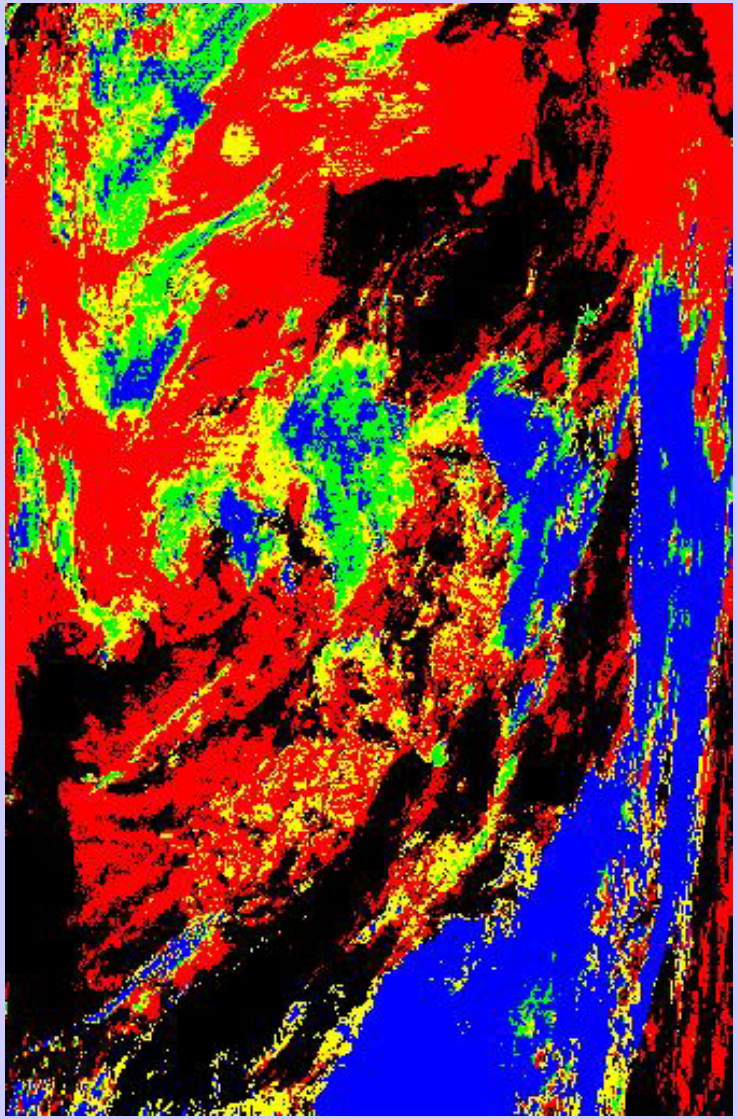

MODIS Frequency of Co-occurrence Water Phase with 253 K < T_{cld} < 268 K 05 Nov. 2000 - Daytime Only

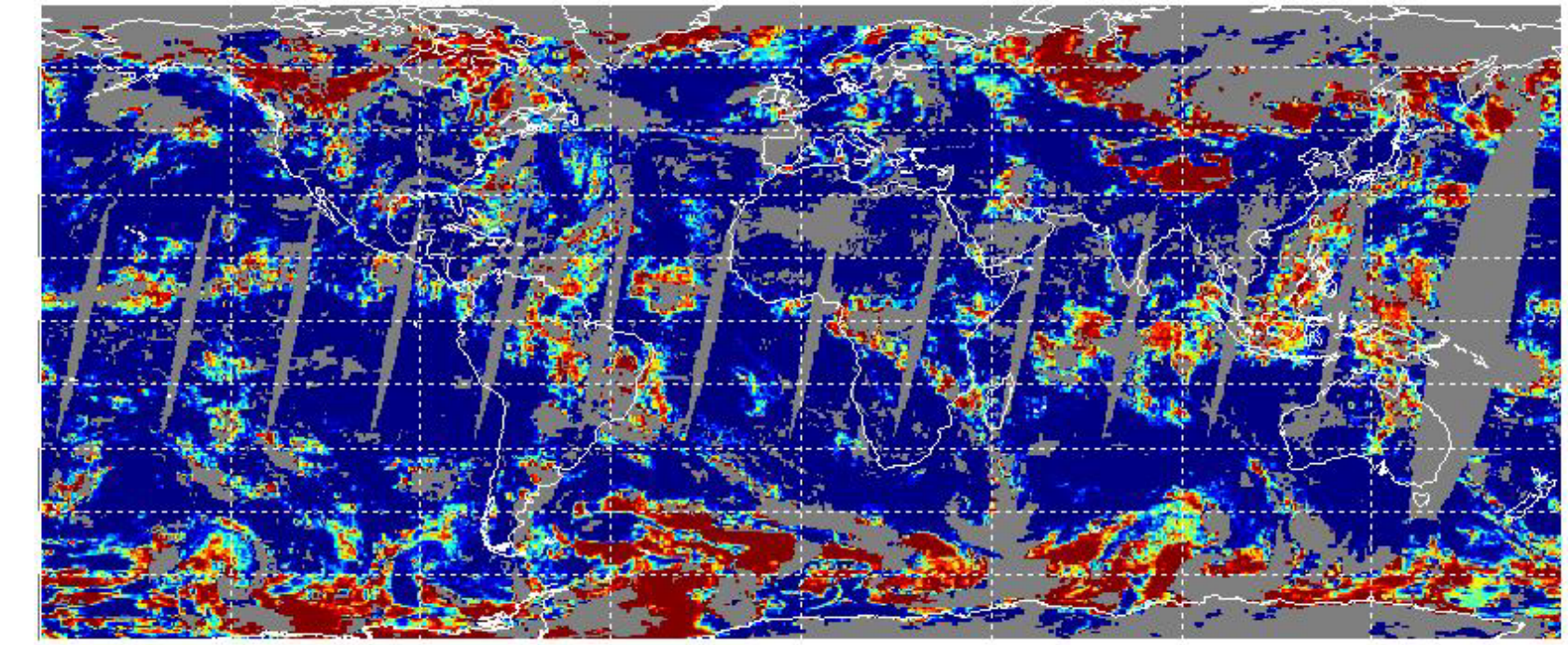

frequency of occurrence in percent (%)

MODIS Frequency of Co-occurrence
Water Phase with 253 K < T_{cld} < 268 K
05 Nov. 2000 - Nighttime Only

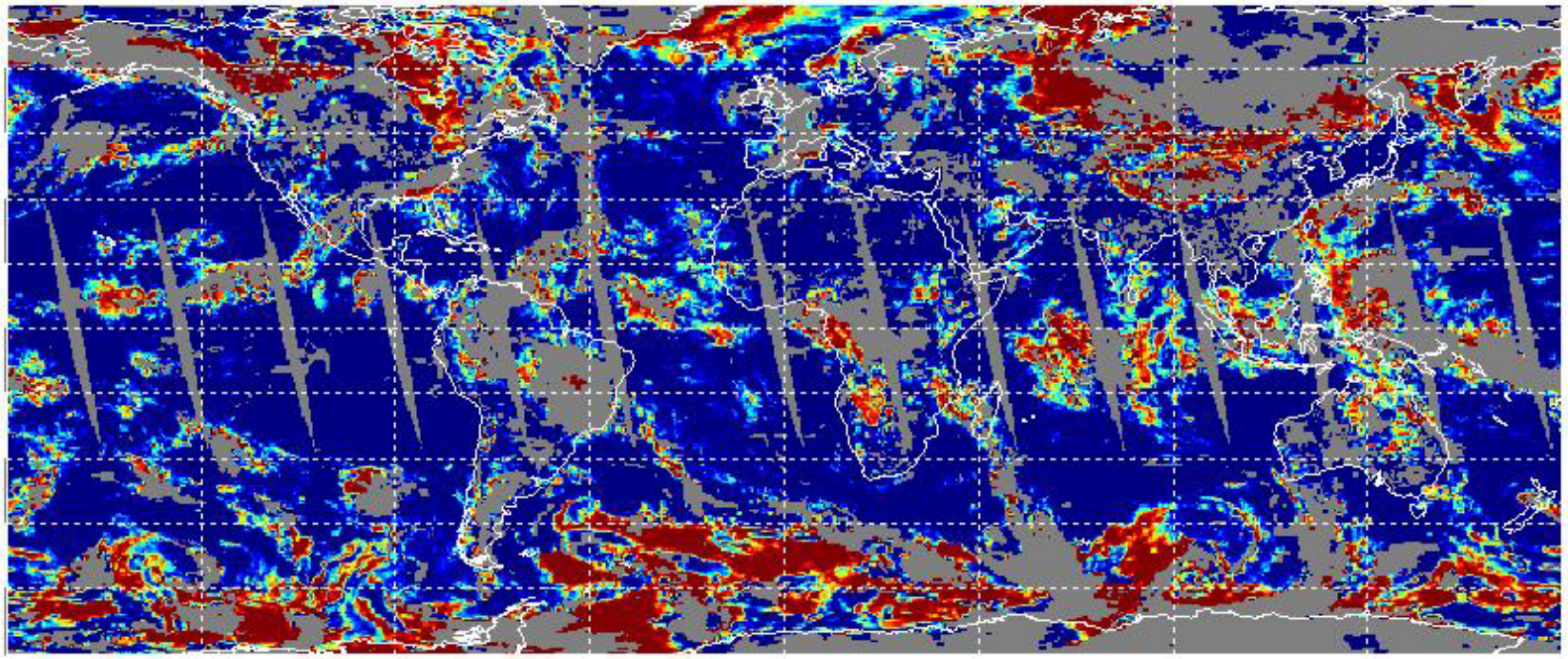

frequency of occurrence in percent (%)

CIRRUS FORMATION BY CONTRAILS OVER CENTRAL U.S. IN GOES-8 IR IMAGERY October 26, 1996

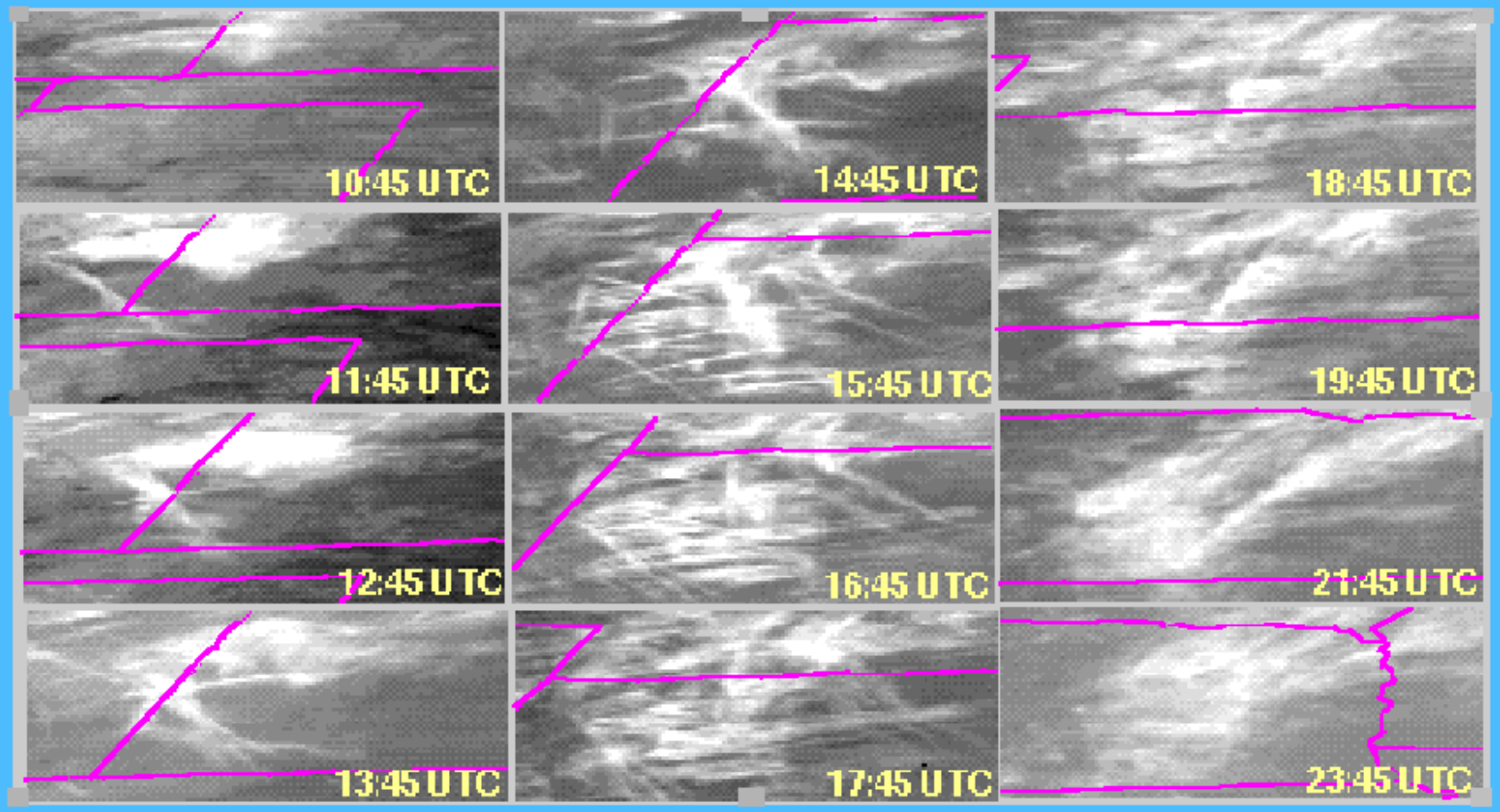

Minnis et al., *Science*, 1999

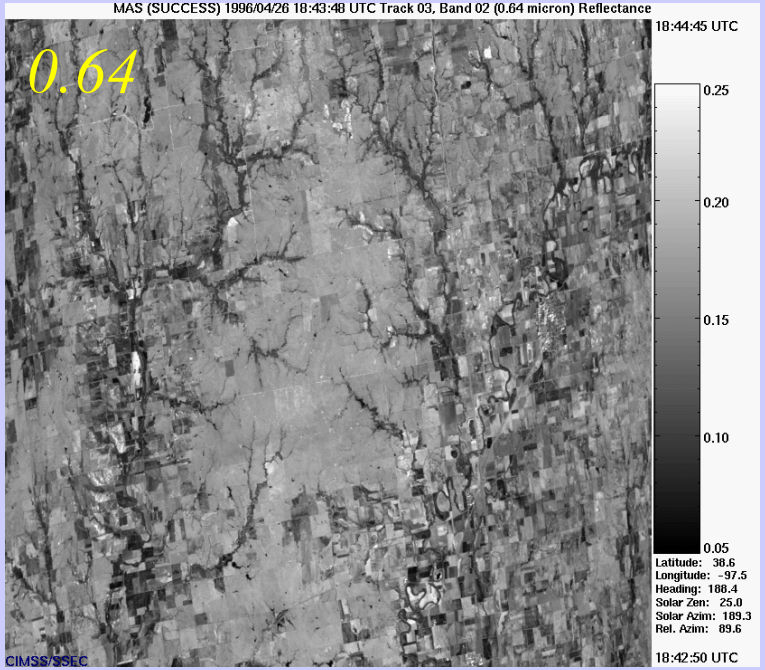
MAS (SUCCESS) 1996/04/26 18:43:48 UTC Track 03, Band 02 (0.64 micron) Reflectance
0.64
18:44:45 UTC
0.25
0.20
0.15
0.10
0.05
Latitude: 38.6
Longitude: -97.5
Heading: 188.4
Solar Zen: 25.0
Solar Azim: 189.3
Rel. Azim: 89.6
18:42:50 UTC
CIMSS/SSEC

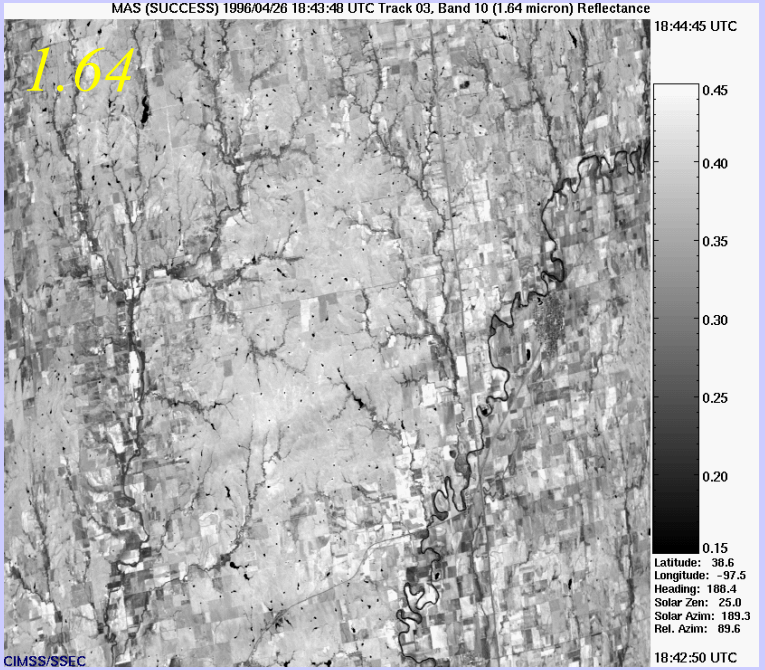
MAS (SUCCESS) 1996/04/26 18:43:48 UTC Track 03, Band 10 (1.64 micron) Reflectance
1.64
18:44:45 UTC
0.45
0.40
0.35
0.30
0.25
0.20
0.15
Latitude: 38.6
Longitude: -97.5
Heading: 188.4
Solar Zen: 25.0
Solar Azim: 189.3
Rel. Azim: 89.6
18:42:50 UTC
CIMSS/SSEC

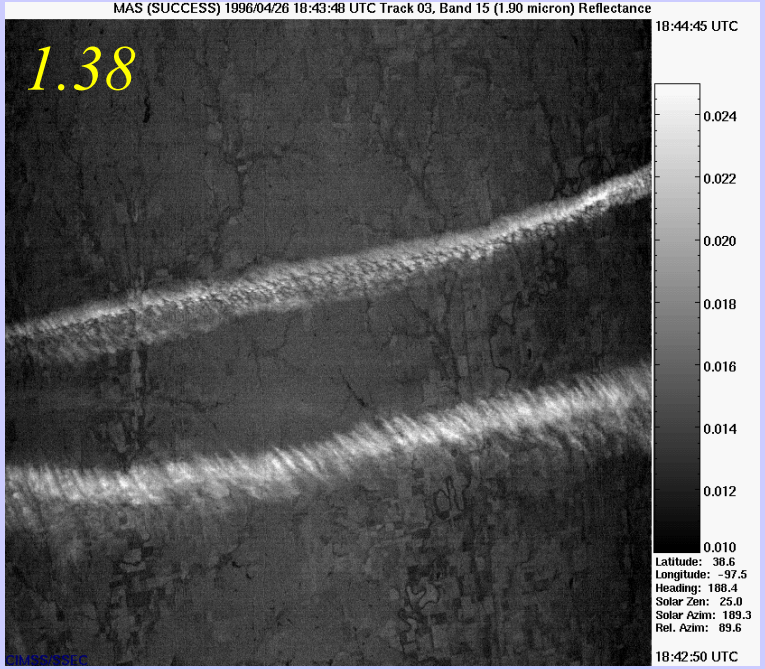
MAS (SUCCESS) 1996/04/26 18:43:48 UTC Track 03, Band 15 (1.90 micron) Reflectance
1.38
18:44:45 UTC
0.024
0.022
0.020
0.018
0.016
0.014
0.012
0.010
Latitude: 38.6
Longitude: -97.5
Heading: 188.4
Solar Zen: 25.0
Solar Azim: 189.3
Rel. Azim: 89.6
18:42:50 UTC
CIMSS/SSEC

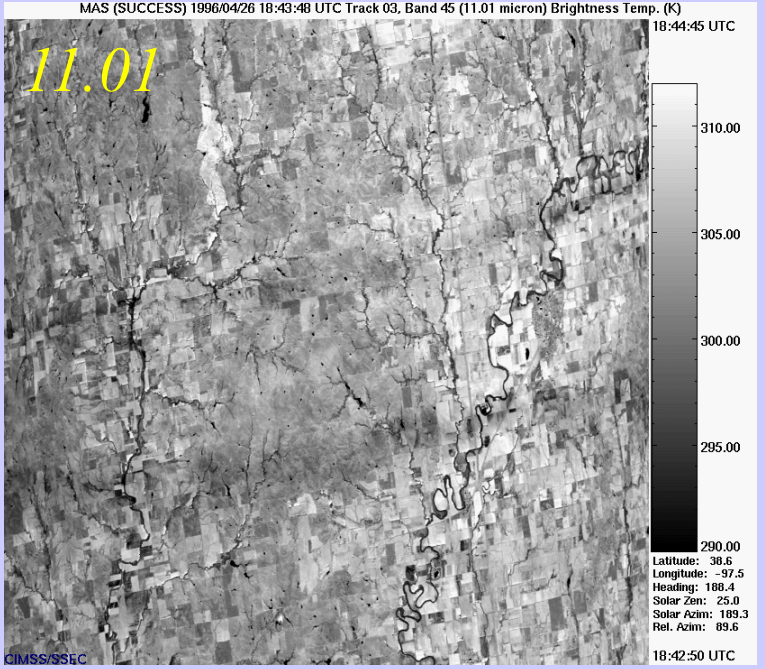
MAS (SUCCESS) 1996/04/26 18:43:48 UTC Track 03, Band 45 (11.01 micron) Brightness Temp. (K)
11.01
18:44:45 UTC
310.00
305.00
300.00
295.00
290.00
Latitude: 38.6
Longitude: -97.5
Heading: 188.4
Solar Zen: 25.0
Solar Azim: 189.3
Rel. Azim: 89.6
18:42:50 UTC
CIMSS/SSEC

Is cirrus related to air traffic?

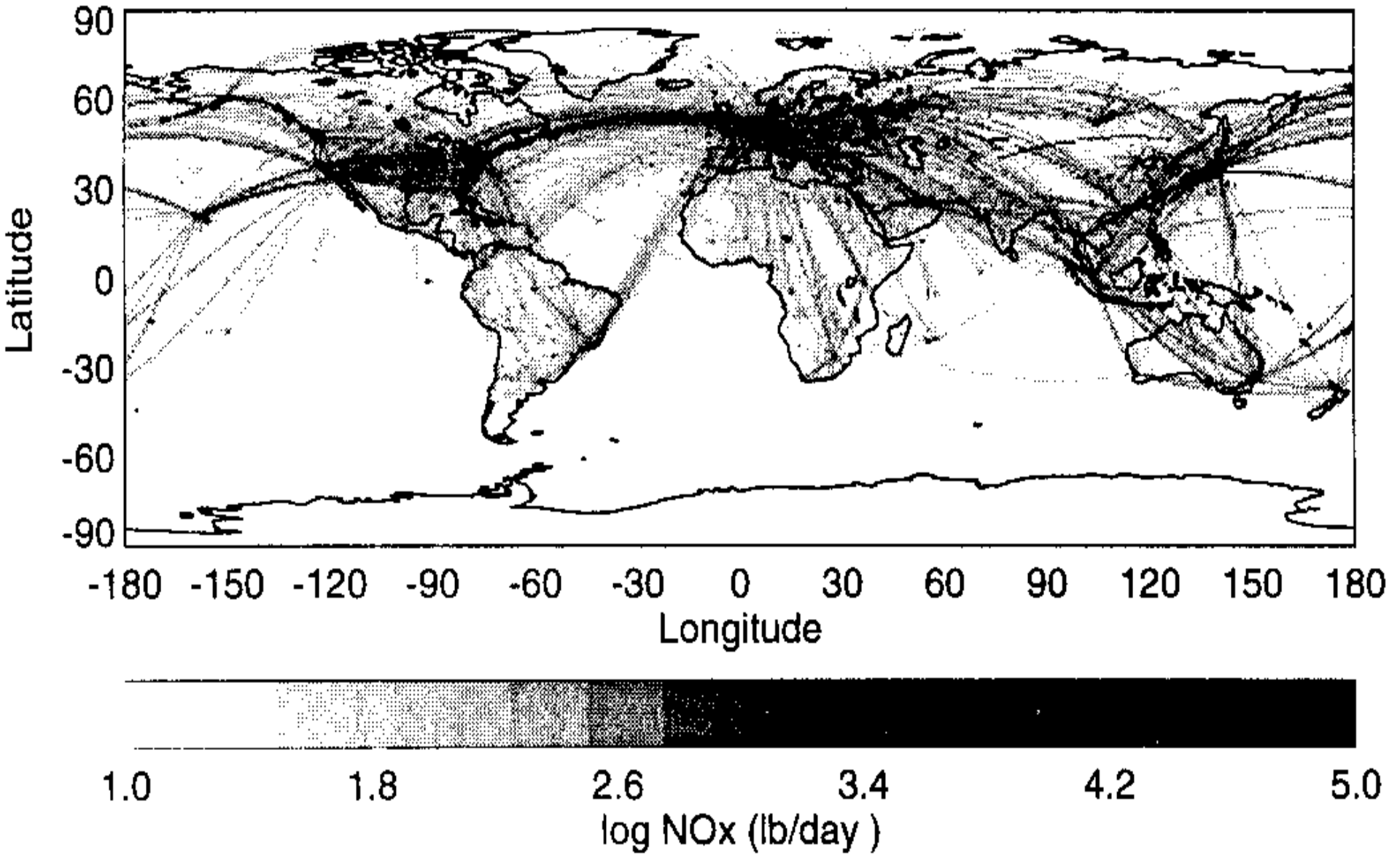

Ice Clouds have particles of many sizes and shapes

3 layer model

*1 km 10 to 50 um spheres

*1 km 300 um columns

*2 km 150 um aggregates and bullet rosettes.

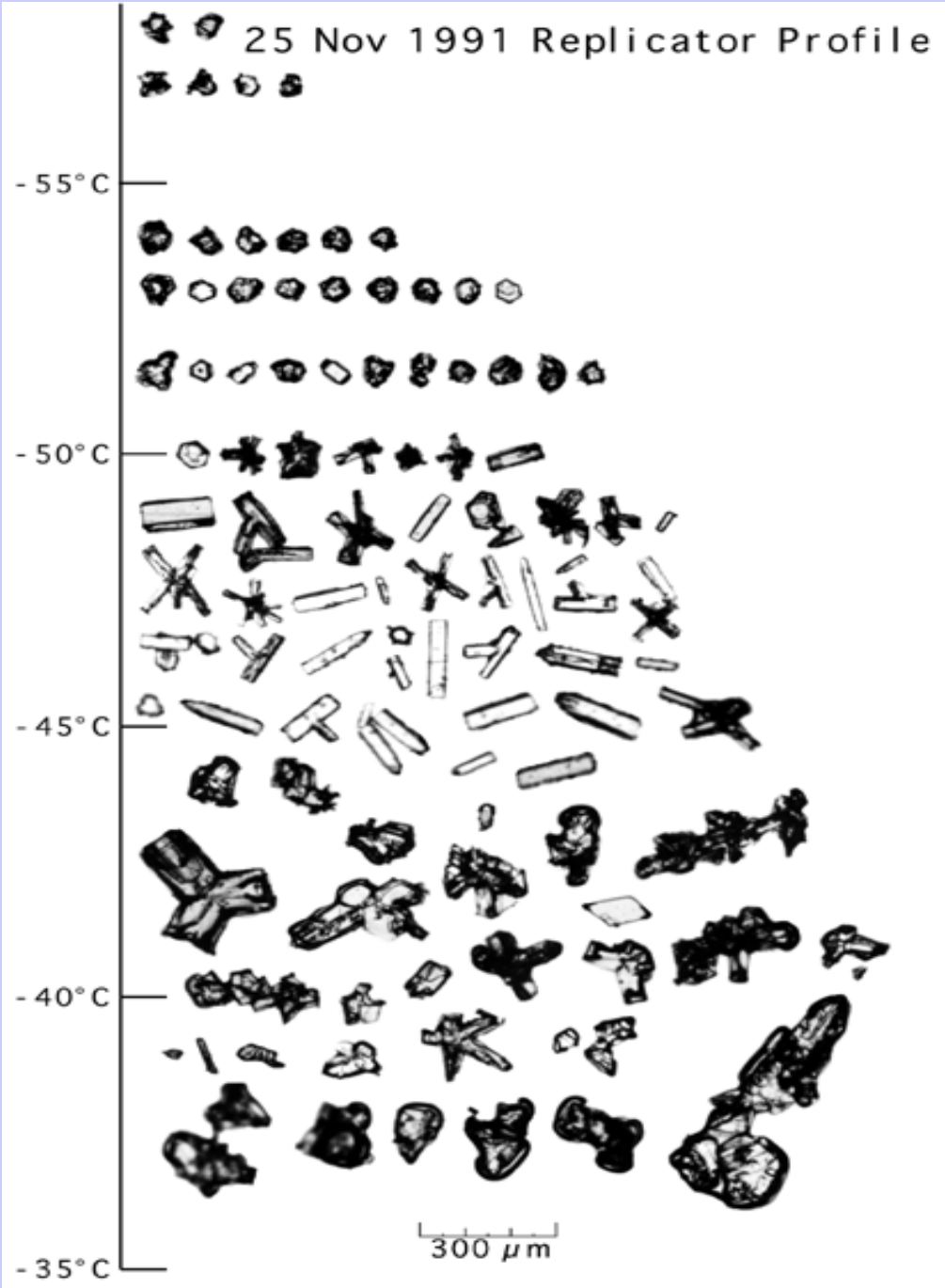

MODIS detects ship tracks

Ship Tracks occur in marine stratocumulus regions of the globe

- California, Azores, Namibia, and Peru

Conditions for formation

- High humidity
- Small air-sea temperature difference
- Low wind speed
- Boundary layer between 300 and 750 m deep

Enhanced reflectance of clouds at 3.7 μm

- Larger number of small droplets arising from particulate emission from ships

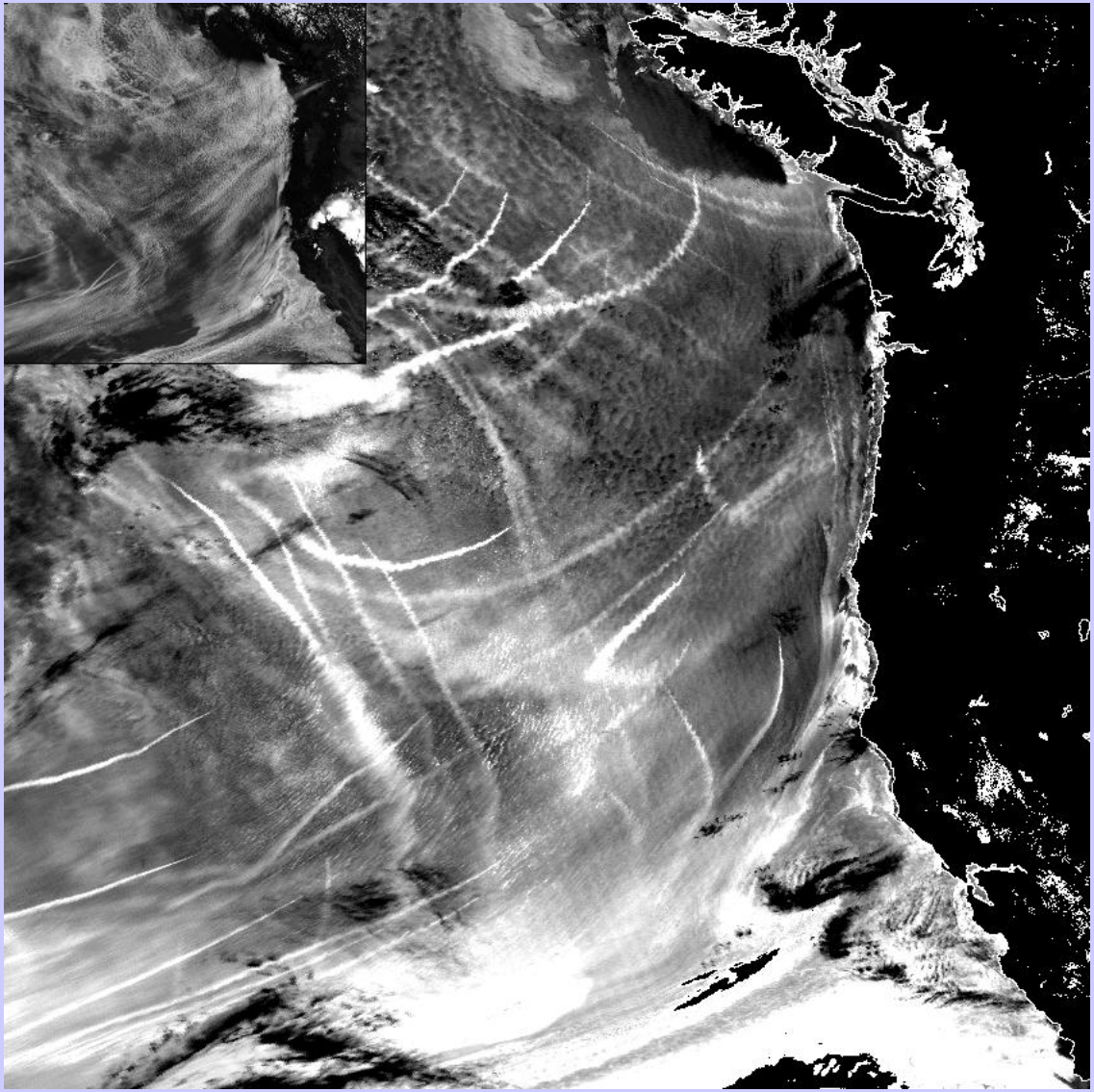

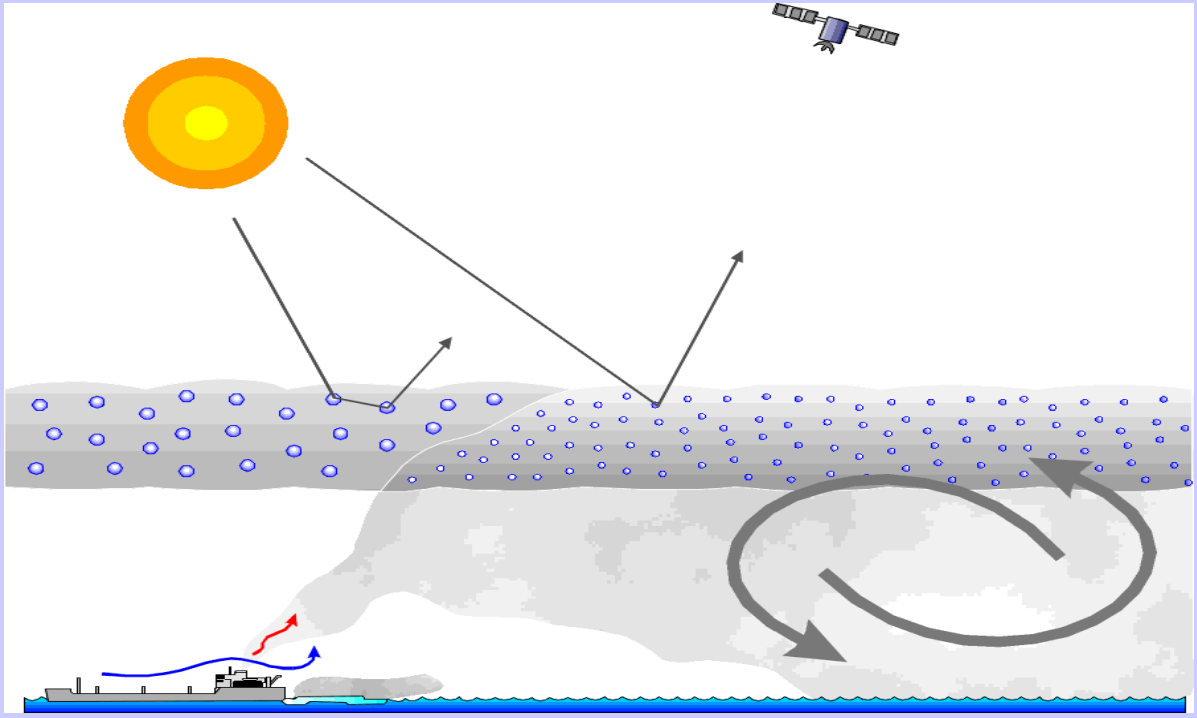

* Particles emitted by ships increase concentration of cloud condensation nuclei (CCN) in the air
* Increased CCN increase concentration of cloud droplets and reduce average size of the droplets
* Increased concentration and smaller particles reduce production of drizzle (100 μm radius) droplets in clouds
* Liquid water content increases because loss of drizzle particles is suppressed
* Clouds are *optically thicker* and brighter along ship track

Cloud Clearing

For a single layer of clouds, radiances in one spectral band vary linearly with those of another as cloud amount varies from one field of view (fov) to another

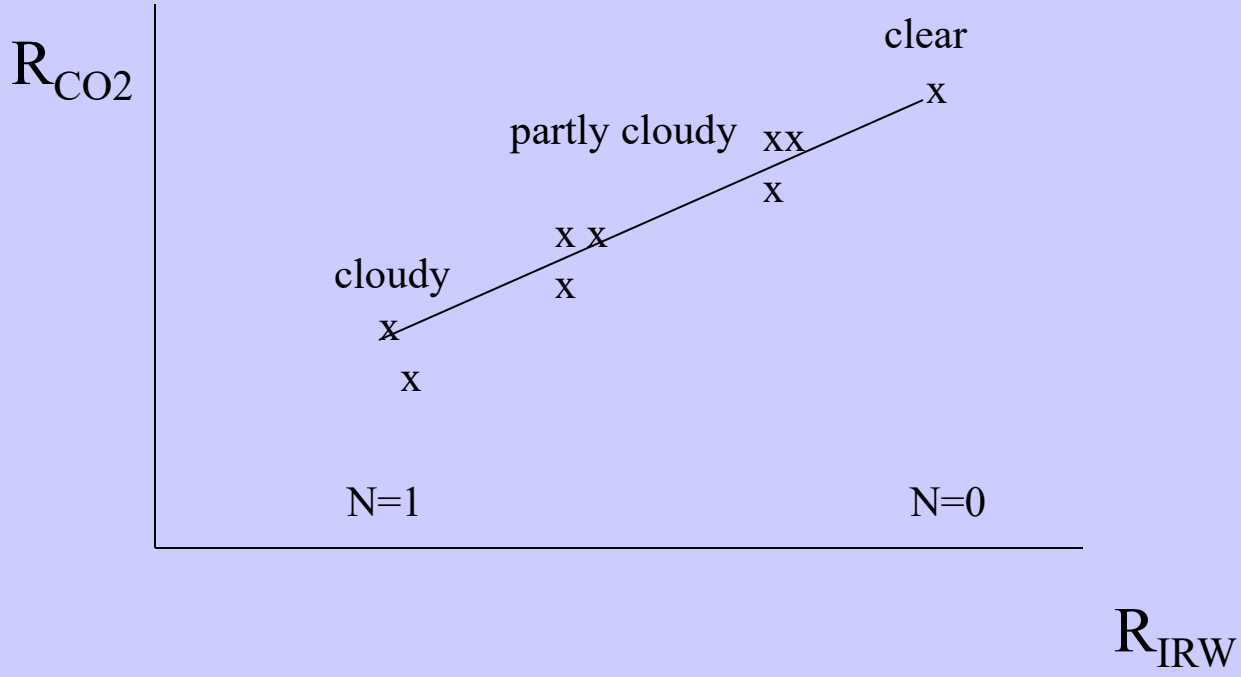

Clear radiances can be inferred by extrapolating to cloud free conditions.

Paired field of view proceeds as follows. For a given wavelength λ, radiances from two spatially independent, but geographically close, fields of view are written

$$I_{\lambda,1} = \eta_1 I_{\lambda,1}^{cd} + (1 - \eta_1) I_{\lambda,1}^{c} \quad ,$$

$$I_{\lambda,2} = \eta_2 I_{\lambda,2}^{cd} + (1 - \eta_2) I_{\lambda,2}^{c} \quad ,$$

If clouds are at uniform altitude, and clear air radiance is in each FOV

$$I_\lambda^{cd} = I_{\lambda,1}^{cd} = I_{\lambda,2}^{cd}$$

$$I_\lambda^{c} = I_{\lambda,1}^{c} = I_{\lambda,2}^{c}$$

$$\frac{\eta_1 \ (I_\lambda^{cd} - I_\lambda^{c})}{\eta_2 \ (I_\lambda^{cd} - I_\lambda^{c})} = \frac{\eta_1}{\eta_2} = \eta^* = \frac{I_{\lambda,1} - I_\lambda^{c}}{I_{\lambda,2} - I_\lambda^{c}} \ ,$$

where η^* is the ratio of the cloud amounts for the two geographically independent fields of view of the sounding radiometer. Therefore, the clear air radiance from an area possessing broken clouds at a uniform altitude is given by

$$I_\lambda^{c} = [\, I_{\lambda,1} - \eta^* I_{\lambda,2}] \,/[1 - \eta^*]$$

where η^* still needs to be determined. Given an independent measurement of surface temperature, T_s, and measurements $I_{w,1}$ and $I_{w,2}$ in a spectral window channel, then η^* can be determined by

$$\eta^* = [I_{w,1} - B_w(T_s)] \,/\, [I_{w,2} - B_w(T_s)]$$

and I_λ^c for different spectral channels can be solved.

Applications with Multispectral Remote Sensing Data

Satellite Remote Sensing

Energy Balance

VIS, IR, and MW Radiative Transfer

EOS Terra & Aqua MODIS

Multispectral Signatures

*(Ocean Color, SST, Snow/Ice, Vegetation, Aerosols, Clouds, **Moisture**, Fires, Volcanic Ash)*

Detecting Climate Trends

Water vapour evaluated in multiple infrared window channels where absorption is weak, so that

$$\tau_w = \exp[-k_w u] \sim 1 - k_w u \text{ where w denotes window channel}$$

and

$$d\tau_w = -k_w du$$

What little absorption exists is due to water vapour, therefore, u is a measure of precipitable water vapour. RTE in window region

$$I_w = B_{sw}(1-k_w u_s) + k_w \int_o^{u_s} B_w du$$

u_s represents total atmospheric column absorption path length due to water vapour, and s denotes surface. Defining an atmospheric mean Planck radiance, then

$$I_w = B_{sw}(1-k_w u_s) + k_w u_s \bar{B}_w \text{ with } \bar{B}_w = \int_o^{u_s} B_w du \Big/ \int_o^{u_s} du$$

Since B_{sw} is close to both I_w and B_w, first order Taylor expansion about the surface temperature T_s allows us to linearize the RTE with respect to temperature, so

$T_{bw} = T_s(1-k_w u_s) + k_w u_s \bar{T}_w$, where T_w is mean atmospheric temperature corresponding to B_w.

For two window channels (11 and 12um) the following ratio can be determined.

$$\frac{T_s - T_{bw1}}{T_s - T_{bw2}} = \frac{k_{w1} u_s (T_s - \bar{T}_{w1})}{k_{w1} u_s (T_s - \bar{T}_{w2})} = \frac{k_{w1}}{k_{w2}}$$

where the mean atmospheric temperature measured in the one window region is assumed to be comparable to that measured in the other, $T_{w1} \sim T_{w2}$,

Thus it follows that

$$T_s = T_{bw1} + \frac{k_{w1}}{k_{w2} - k_{w1}} [T_{bw1} - T_{bw2}]$$

and

$$u_s = \frac{T_{bw} - T_s}{k_w (\bar{T}_w - T_s)} .$$

Obviously, the accuracy of the determination of the total water vapour concentration depends upon the contrast between the surface temperature, T_s, and

the effective temperature of the atmosphere $\bar{T}_w$

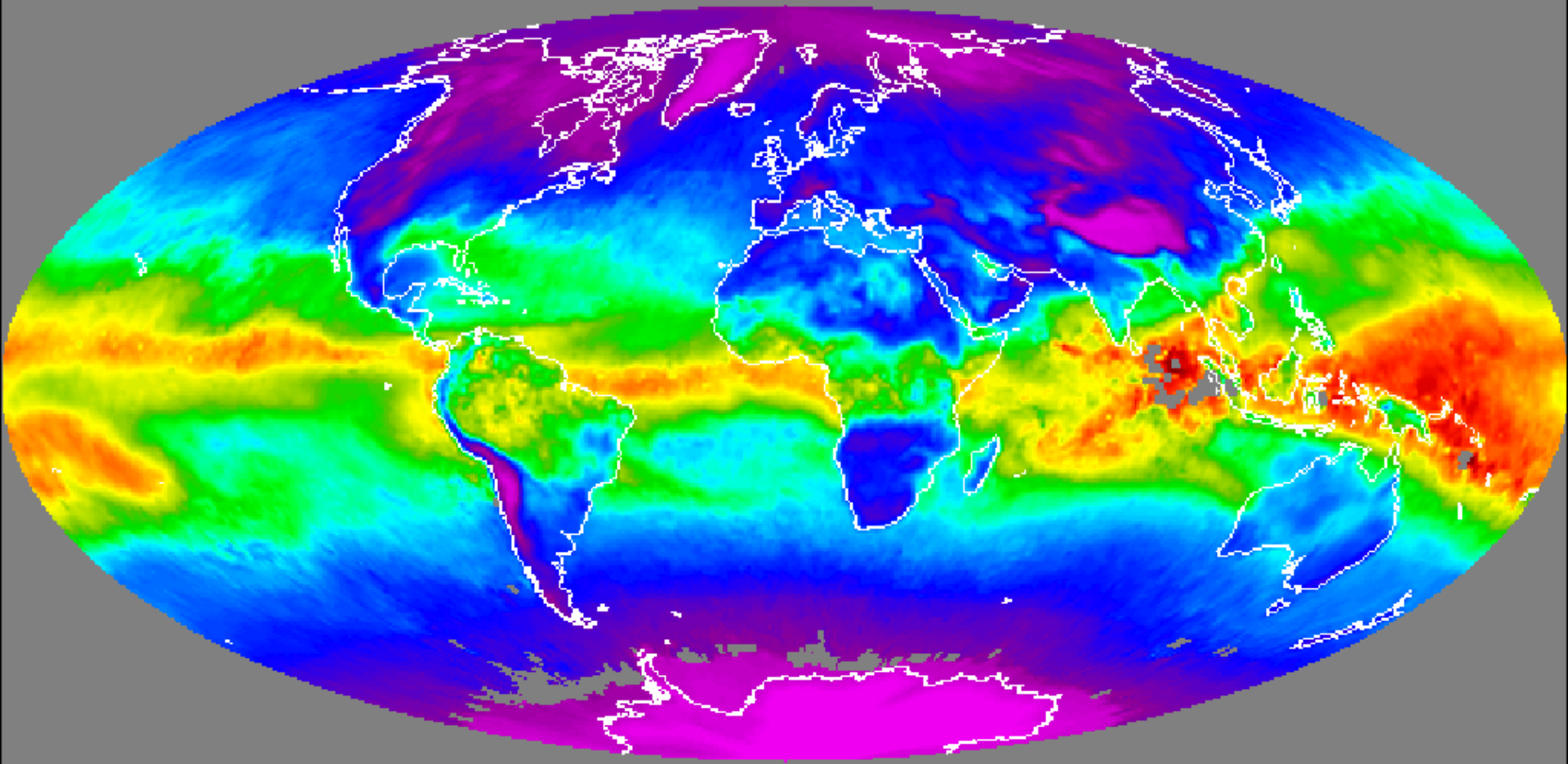

Global TPW from Seemann

T(p)

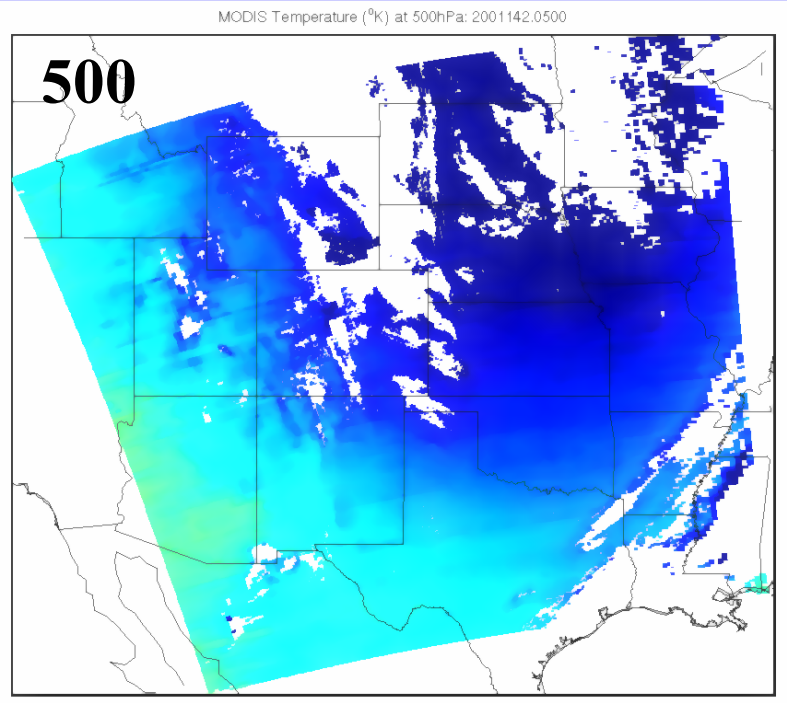
MODIS Temperature (°K) at 500hPa: 2001142.0500
500

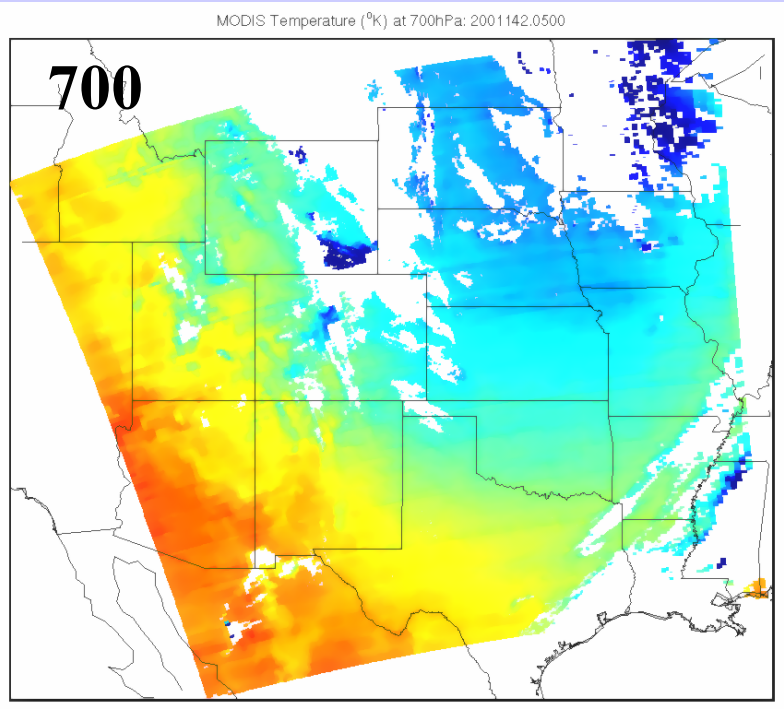
MODIS Temperature (°K) at 700hPa: 2001142.0500
700

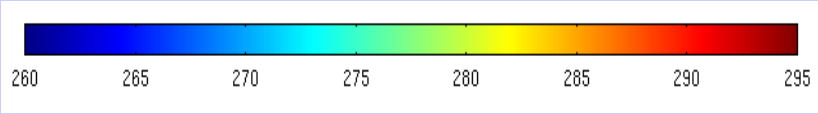
260
265
270
275
280
285
290
295

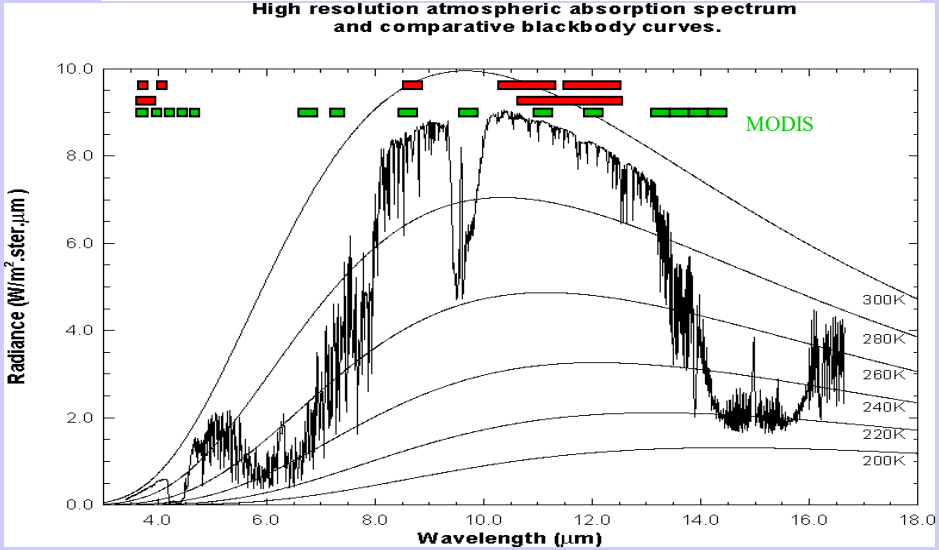
High resolution atmospheric absorption spectrum
and comparative blackbody curves.
MODIS
Radiance (W/m².ster.μm)
Wavelength (μm)
300K
280K
260K
240K
220K
200K

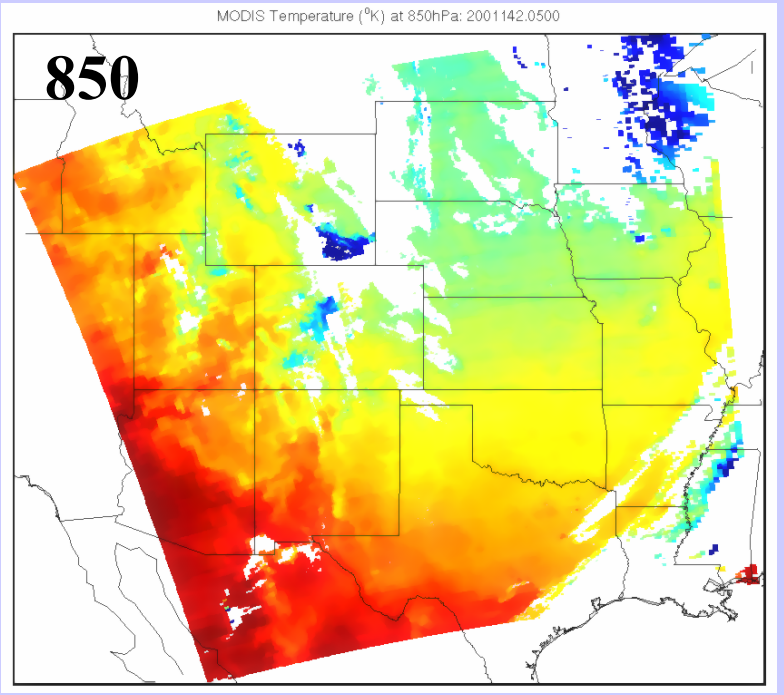
MODIS Temperature (°K) at 850hPa: 2001142.0500
850

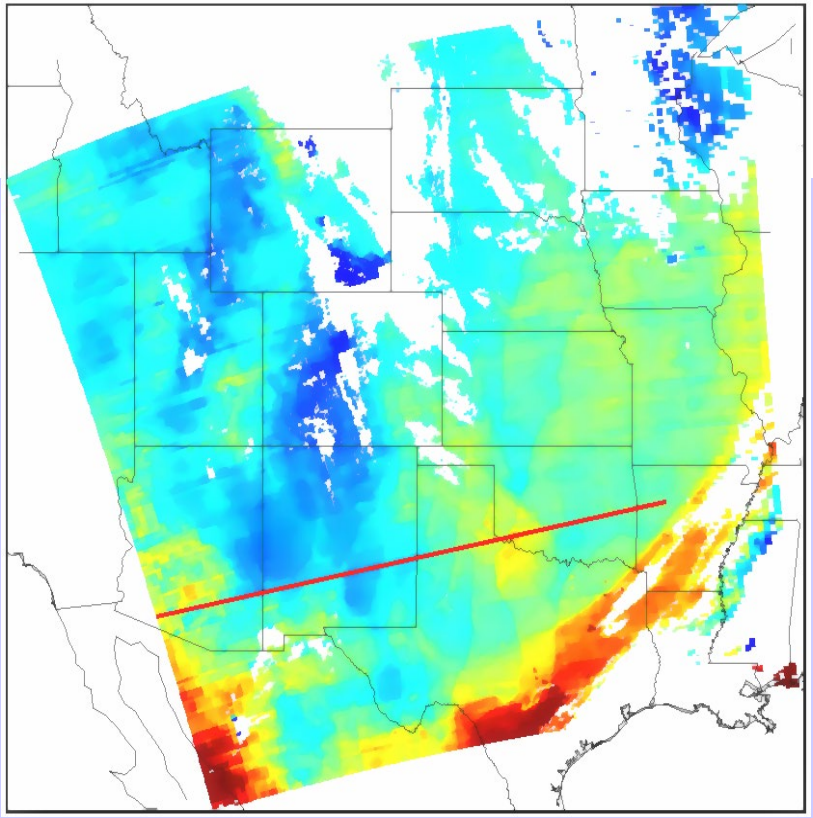

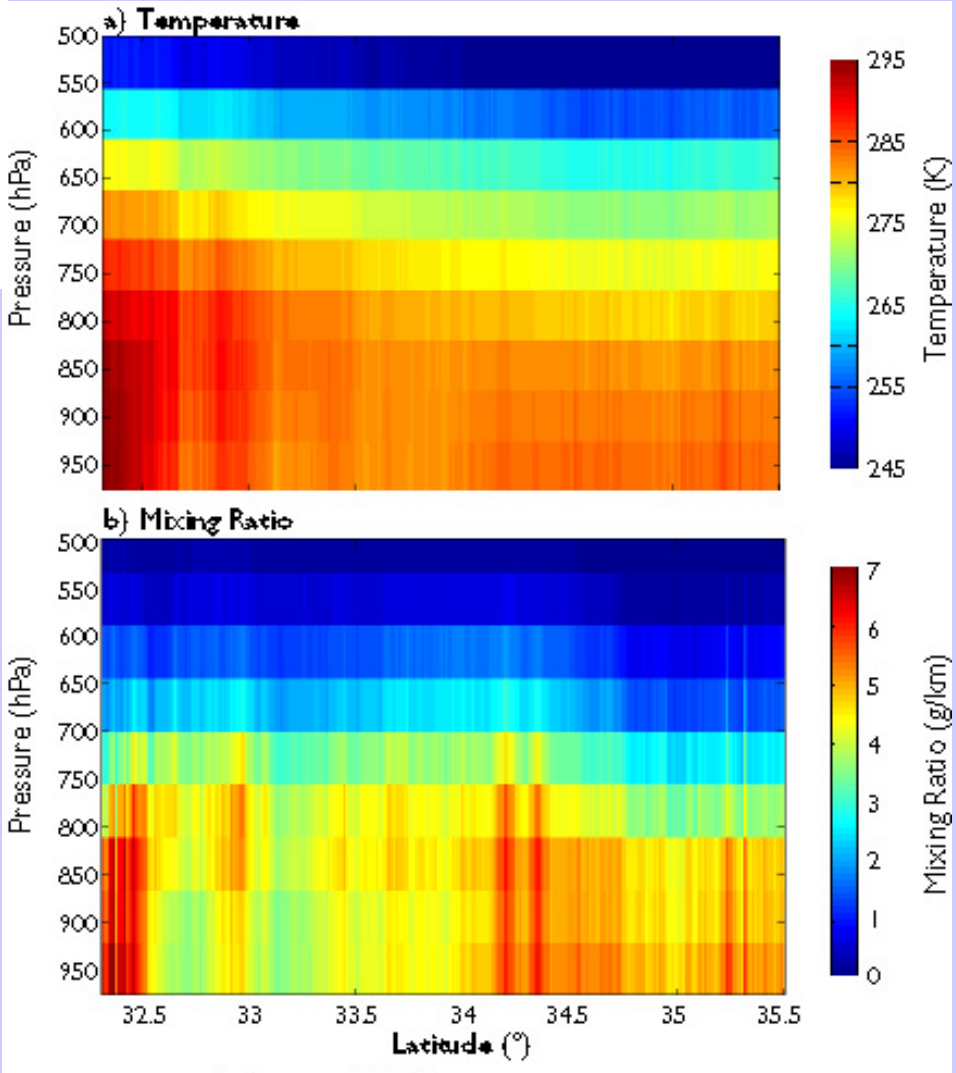

Clear sky layers of temperature and moisture

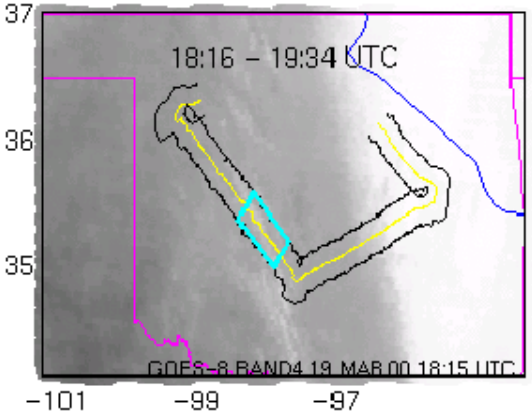
NASTI on Proteus, 19–Mar–2000
18:16 – 19:34 UTC
GOES–8 BAND4 19 MAR 00 18:15 UTC
37
36
35
–101
–99
–97


670–680 cm^{-1}

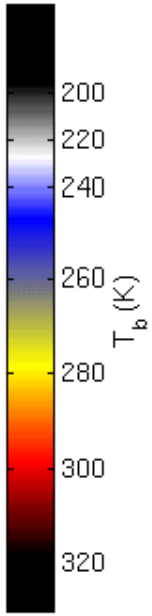
200
220
240
260
280
300
320
T_b (K)

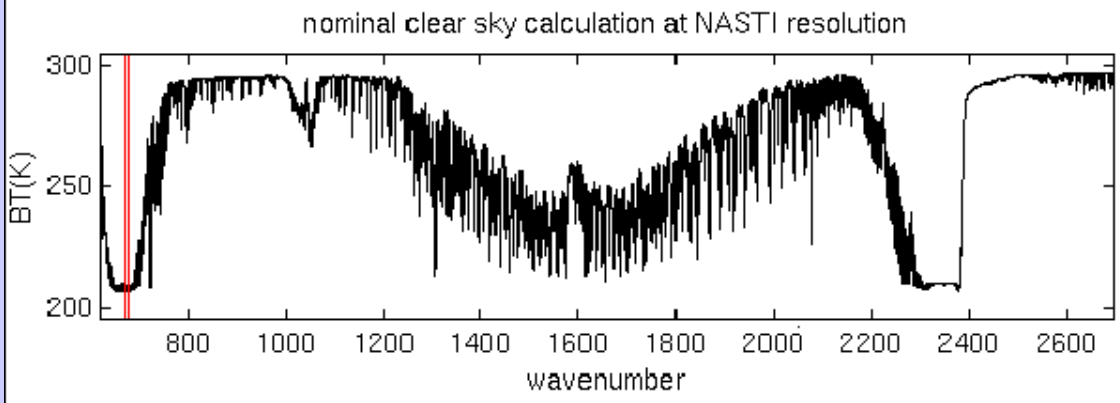
nominal clear sky calculation at NASTI resolution
BT(K)
300
250
200
800
1000
1200
1400
1600
1800
2000
2200
2400
2600
wavenumber

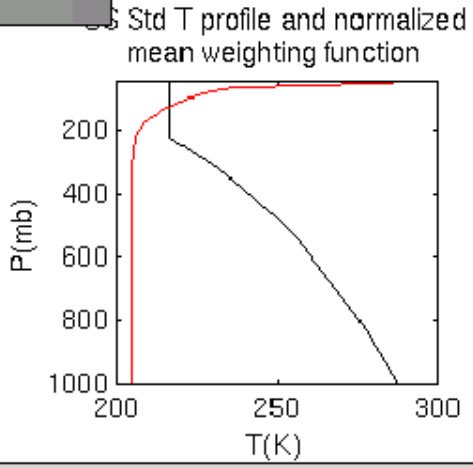
Std T profile and normalized
mean weighting function
P(mb)
200
400
600
800
1000
200
250
300
T(K)

Applications with Multispectral Remote Sensing Data

Satellite Remote Sensing

Energy Balance

VIS, IR, and MW Radiative Transfer

EOS Terra & Aqua MODIS

Multispectral Signatures

(Ocean Color, SST, Snow/Ice, Vegetation, Aerosols, Clouds, Moisture, ***Fires, Volcanic Ash****)*

Detecting Climate Trends

Active Fire Detection

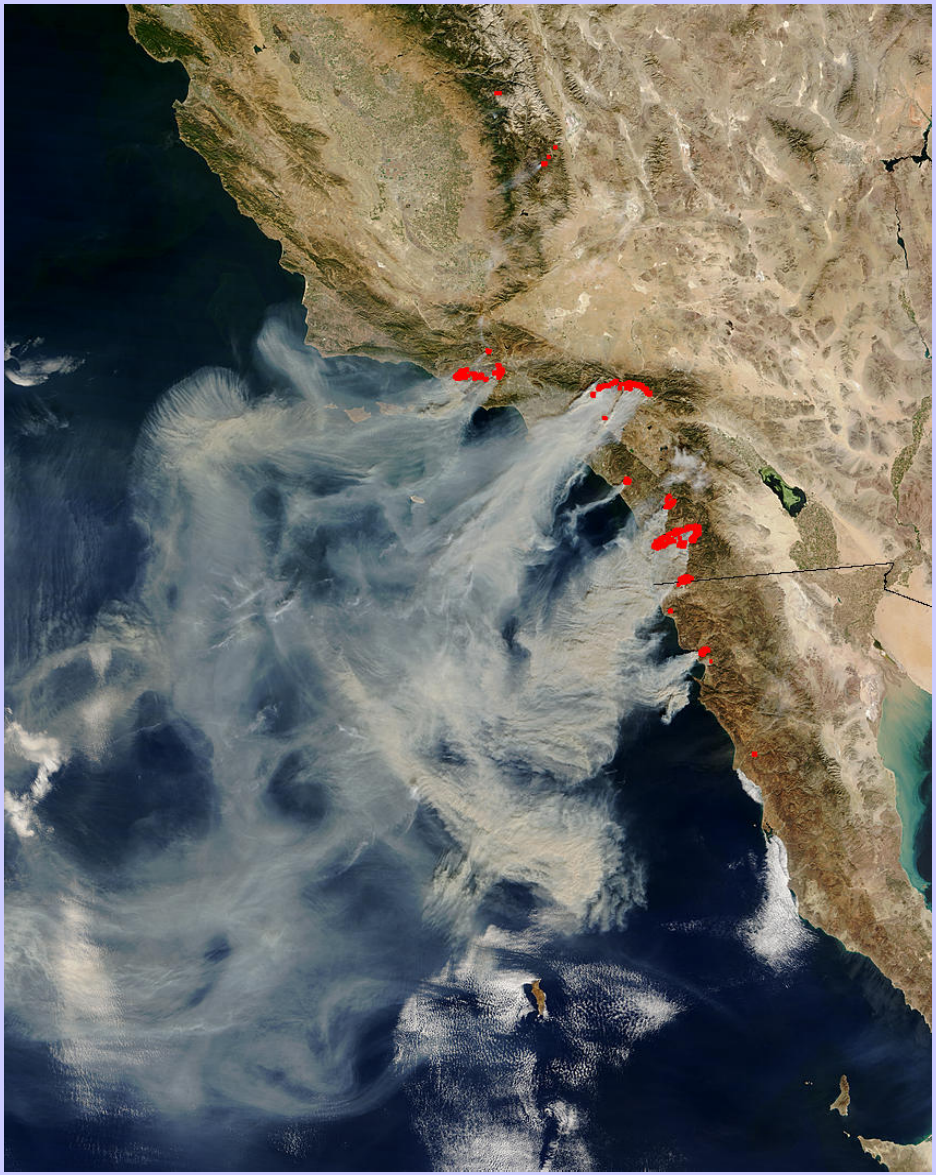

California – 10/26/03

- Same code as the "offical" MOD14 thermal anomalies product
- Contextual algorithm (Giglio et al., 2003)
- The algorithm considers the spectral signature (in middle and thermal infrared) of each pixel and compares it to the non-burning surrounding pixels
- The natural variability of the surrounding background is taken into account
- Fewer false detections than traditional threshold-based algorithms
- Sensitive enough to detect small fires
- Current version: v4.3.2 (March 2003)

The fire extent and temperature within a field of view can be determined by considering the upwelling thermal radiance values obtained by both channels (Matson and Dozier, 1981; Dozier, 1981). For a given channel, λ, the radiative transfer equation indicates

$$R_\lambda(T) = \varepsilon_\lambda B_\lambda(Ts)\, \tau_\lambda(s) + \int_0^1 B_\lambda(T)\, d\tau_\lambda$$

When the GOES radiometer senses radiance from a pixel containing a target of blackbody temperature T_t occupying a portion p (between zero and one) of the pixel and a background of blackbody temperature T_b occupying the remainder of the pixel (1-p), the following equations represent the radiance sensed by the instrument at 4 and 11 micron.

$$R_4(T_4) = p\, R_4(T_t) + \varepsilon_4\, (1-p)\, R_4\, (T_b) + (1-\varepsilon_4)\, \tau_4(s)\, R_4(solar)$$

$$R_{11}(T_{11}) = p\, R_{11}(T_t) + \varepsilon_{11}\, (1-p)\, R_{11}(T_b)$$

The observed short wave window radiance also contains contributions due to solar reflection that must be distinguished from the ground emitted radiances; solar reflection is estimated from differences in background temperatures in the 4 and 11 micron channels. Once T_b is estimated from nearby pixels, these two nonlinear equations can be solved for T_t and p. In this study, the solution to the set of equations is found by applying a globally convergent bisection technique followed by Newton's method.

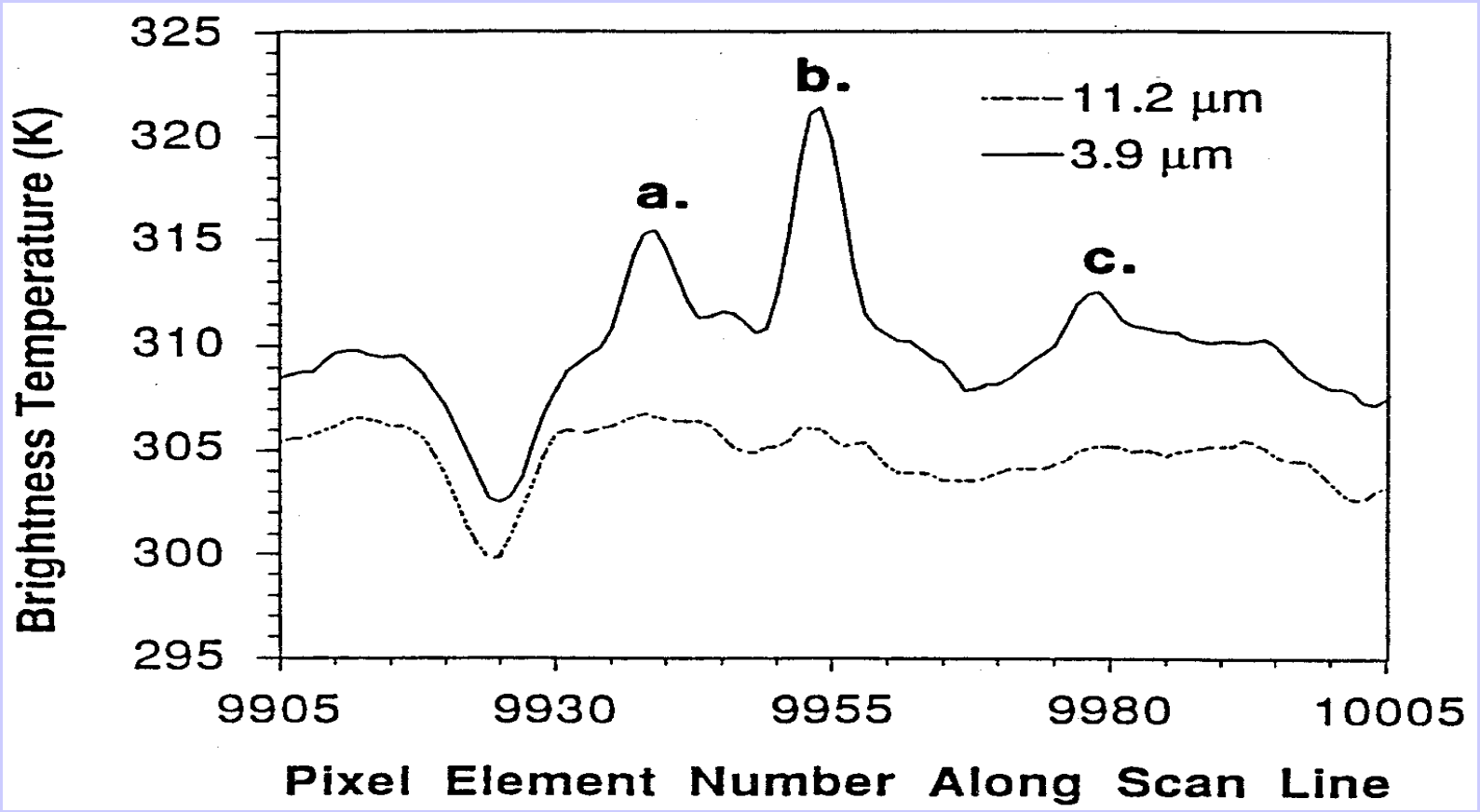

3.9 and 11.2 microns plotted for one scan line over grassland burning in South America; fires are likely at a, b, and c.

Ash Plume Detection

Mt. Cleveland Eruption 19 Feb 2001

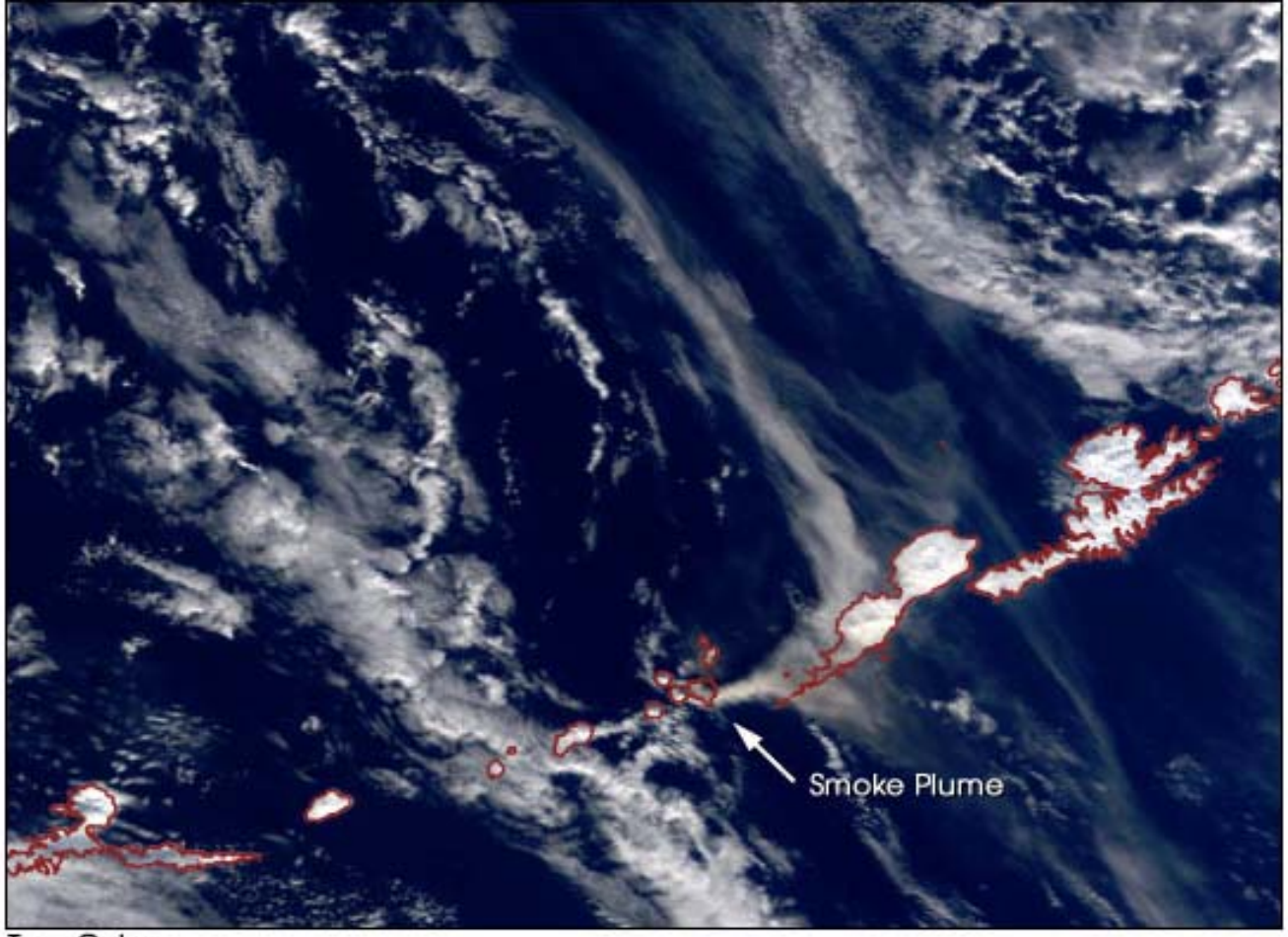

True Color

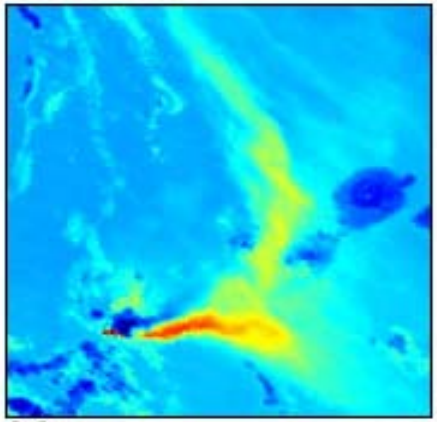

3.9μm

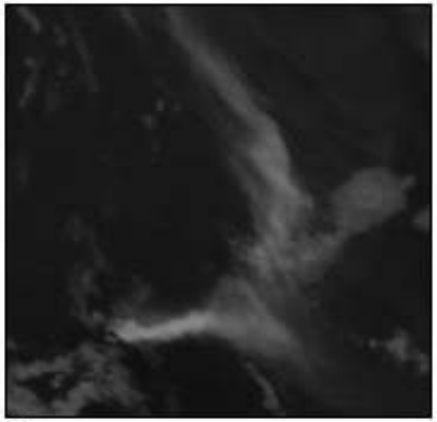

11μm

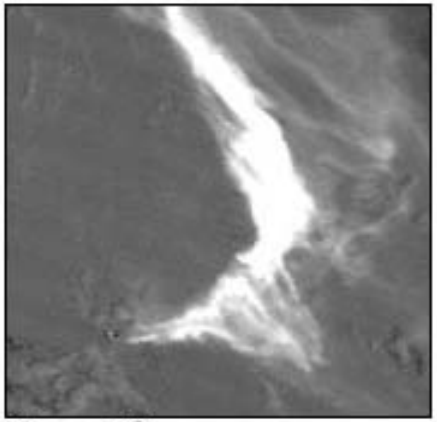

11μm - 12μm

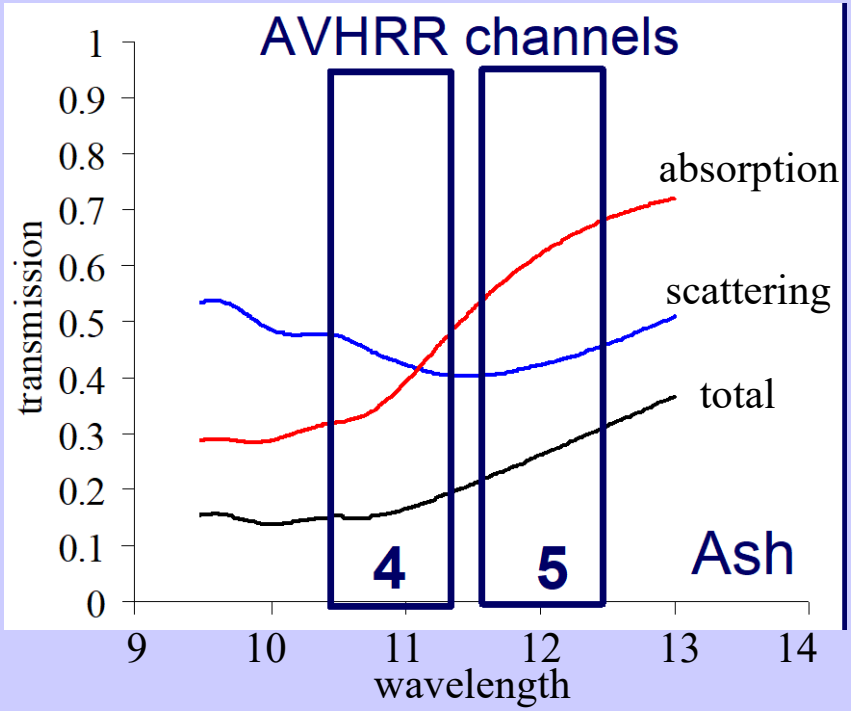

Investigating with Multi-spectral Combinations

Given the spectral response of a surface or atmospheric feature

Select a part of the spectrum where the reflectance or absorption changes with wavelength

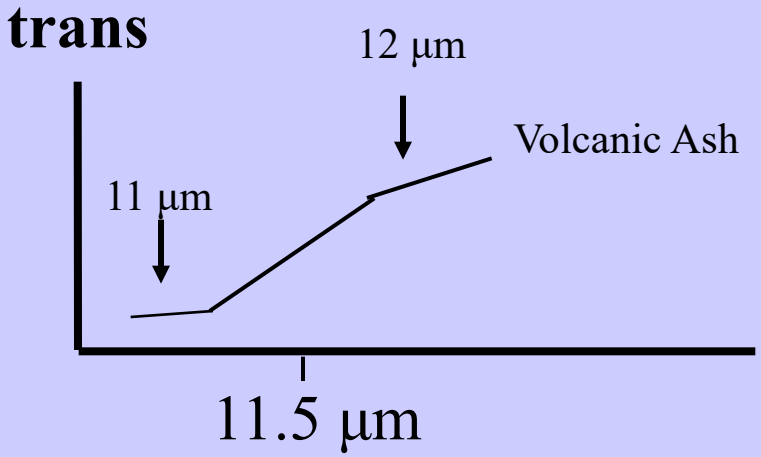

e.g. transmission through ash

If 11 μm sees the same or higher BT than 12 μm the atmosphere viewed does not contain volcanic ash; if 12 μm sees considerably higher BT than 11 μm then the atmosphere probably contains volcanic ash

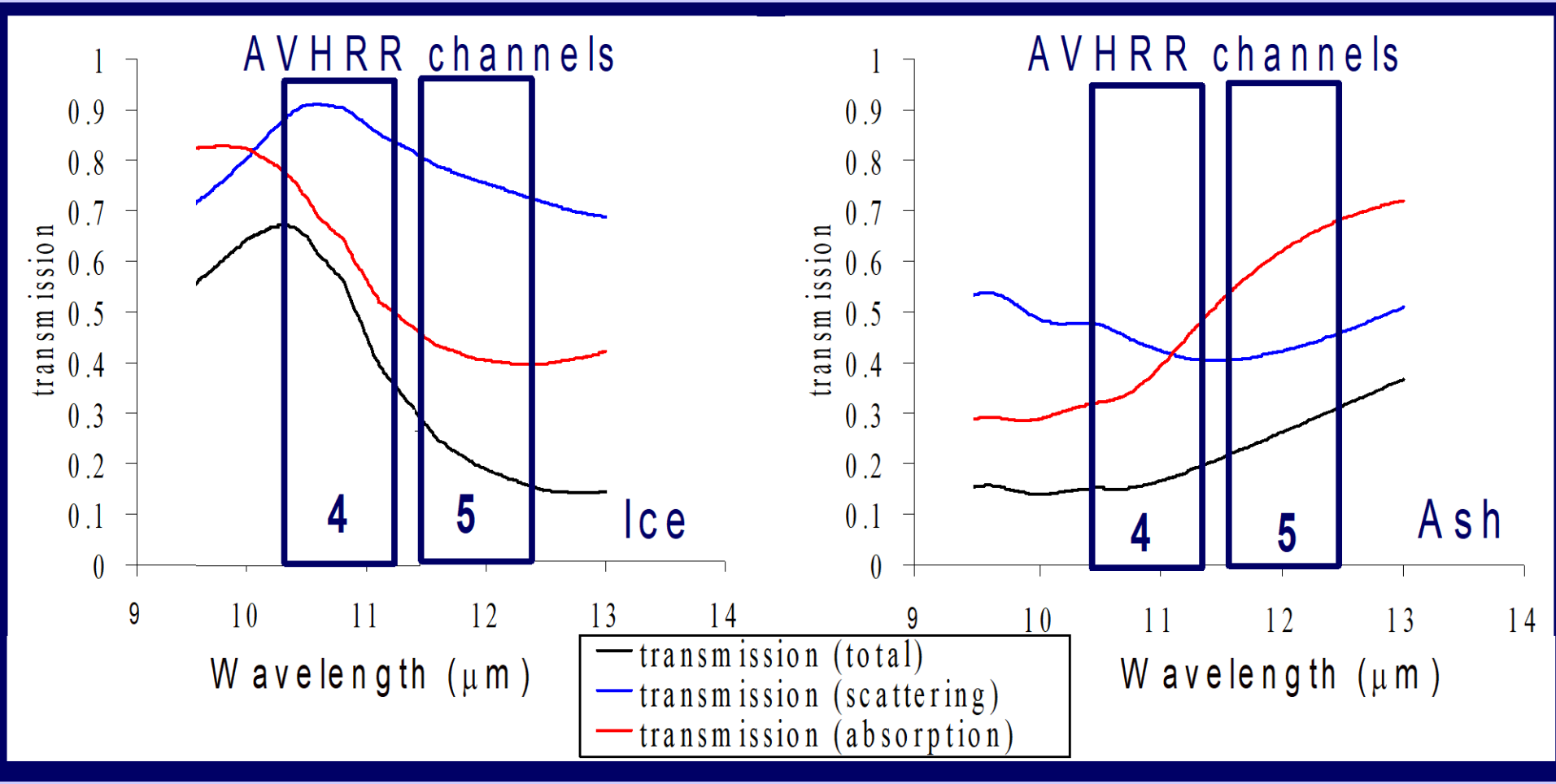

BT11-BT12 > 0 for ice
BT11-BT12 < 0 for volcanic ash

Frank Honey 1980s

Applications with Multispectral Remote Sensing Data

Satellite Remote Sensing

Energy Balance

VIS, IR, and MW Radiative Transfer

EOS Terra & Aqua MODIS

Multispectral Signatures

(Ocean Color, Snow/Ice, Vegetation, Aerosols, Clouds, Moisture, Fires, Volcanic Ash)

Detecting Climate Trends

Climate System Energy Balance

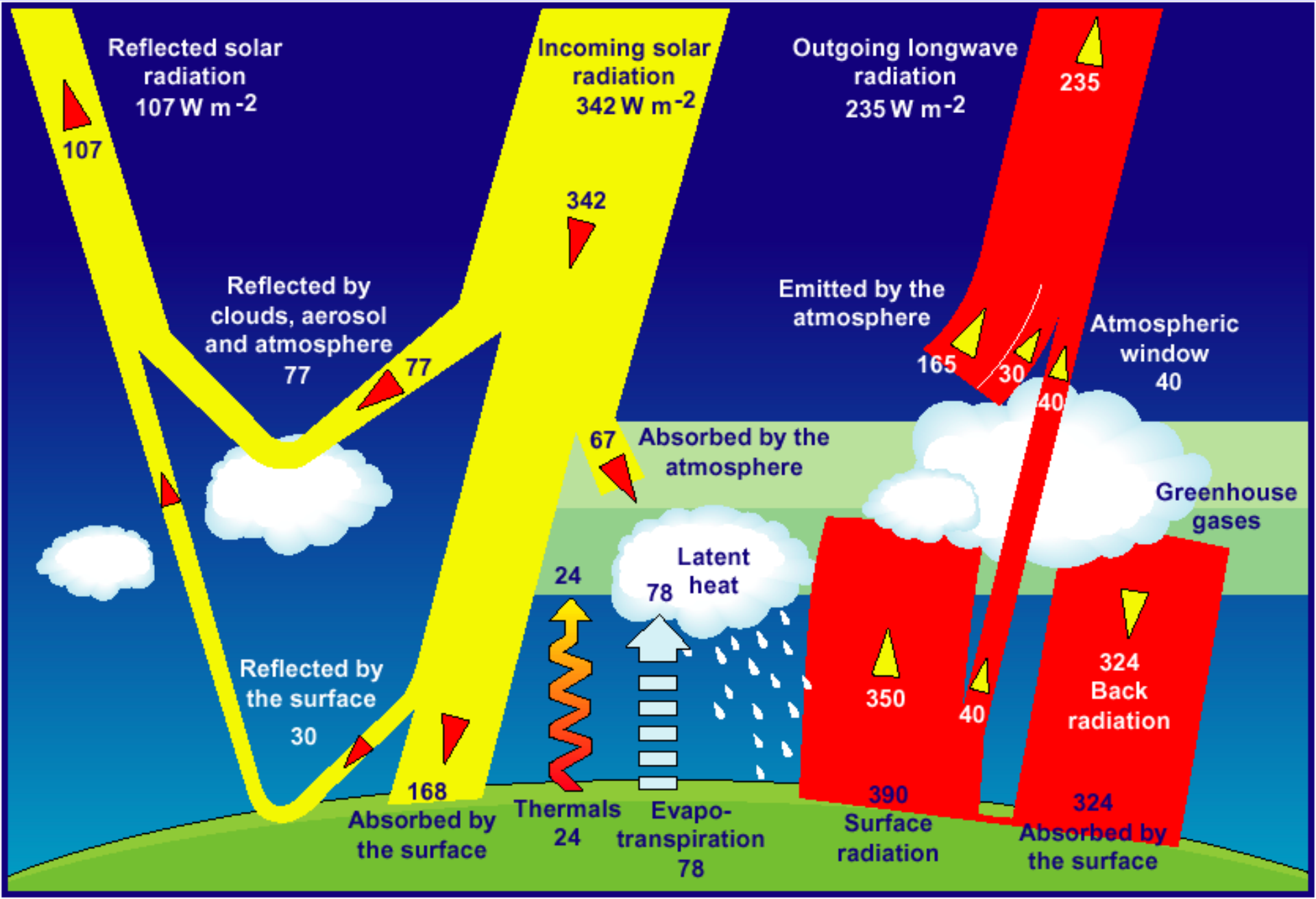

Major Climate System Elements

Carbon Cycle

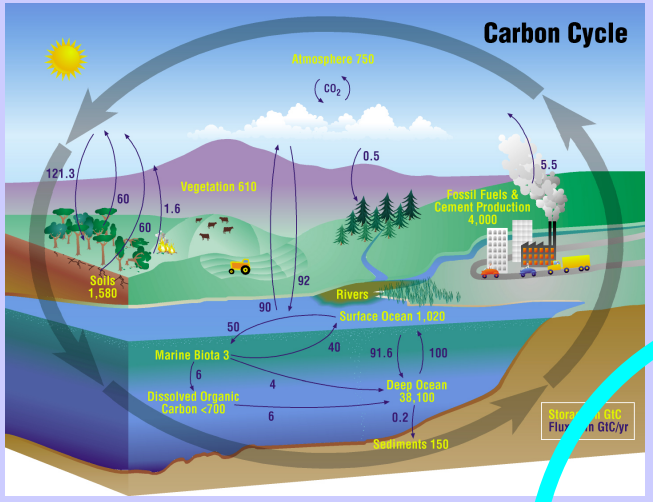

Water & Energy Cycle

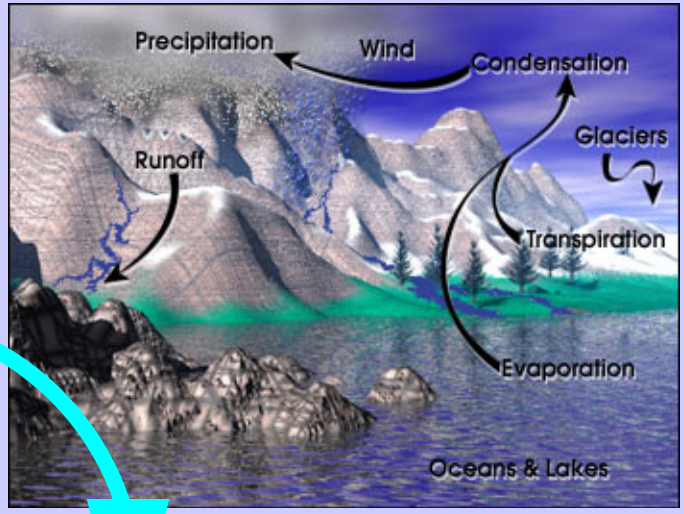

Coupled Chaotic Nonlinear

Atmospheric Chemistry

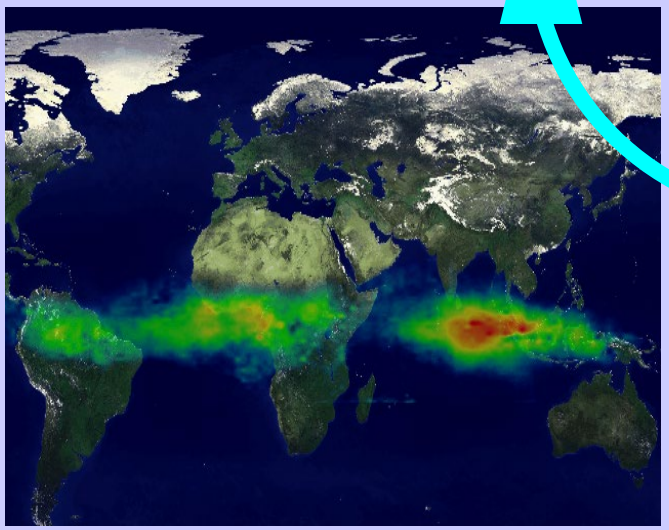

Atmosphere and Ocean Dynamics

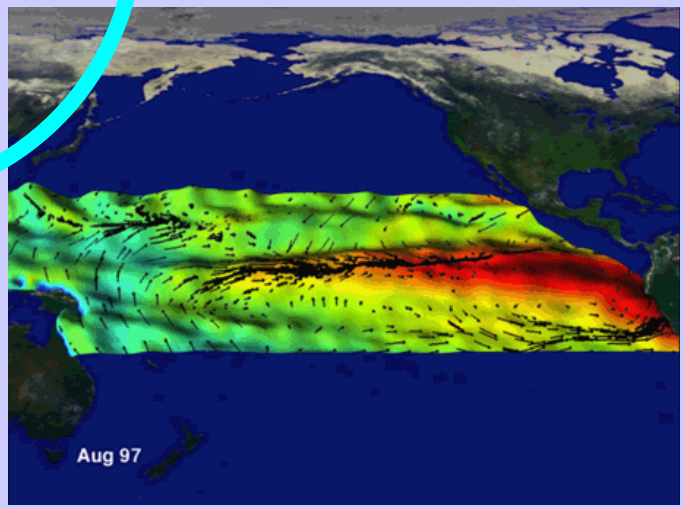

What global surface temperature change has occurred so far?

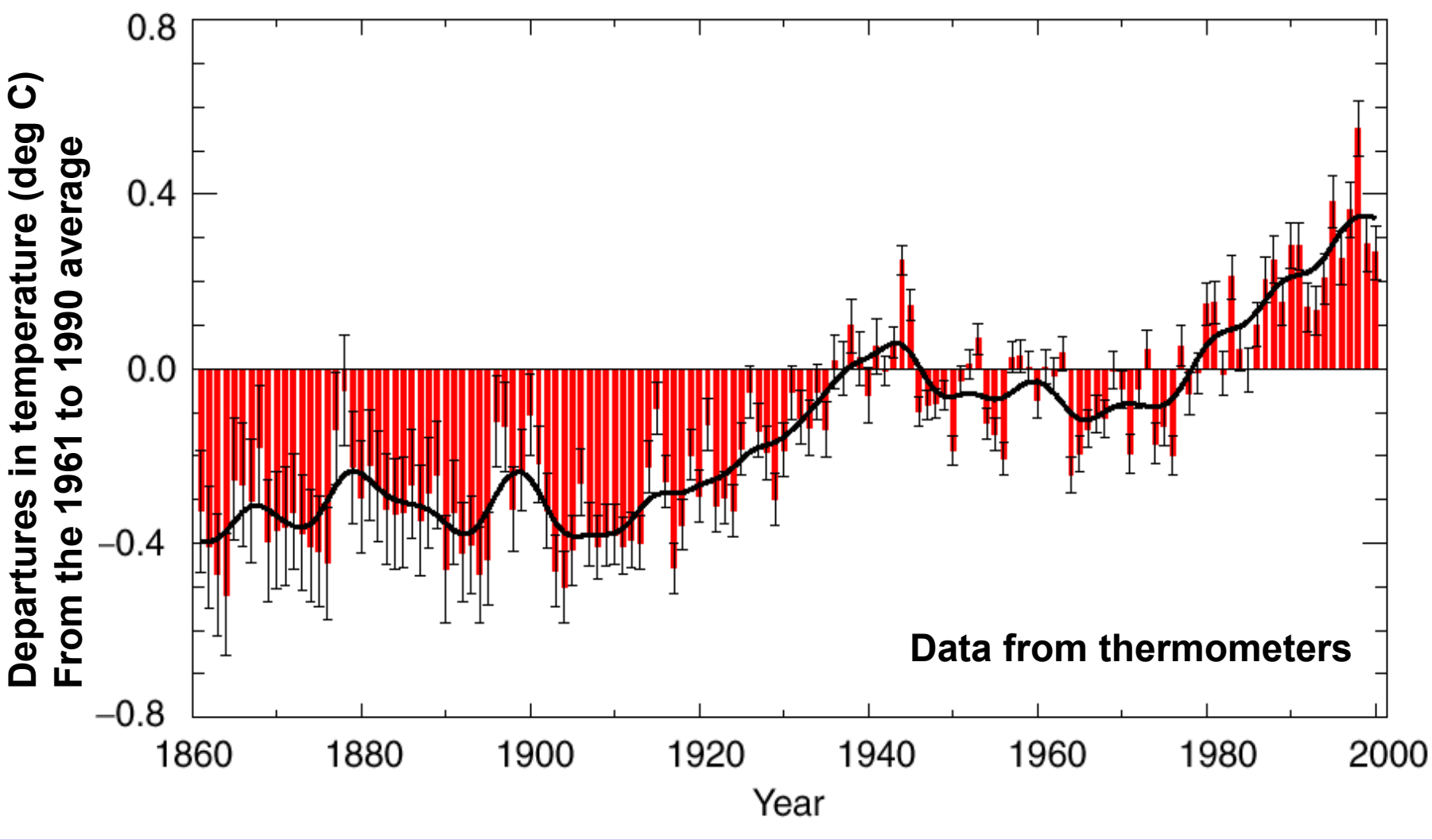

IPCC 2001

Human Influence on Climate

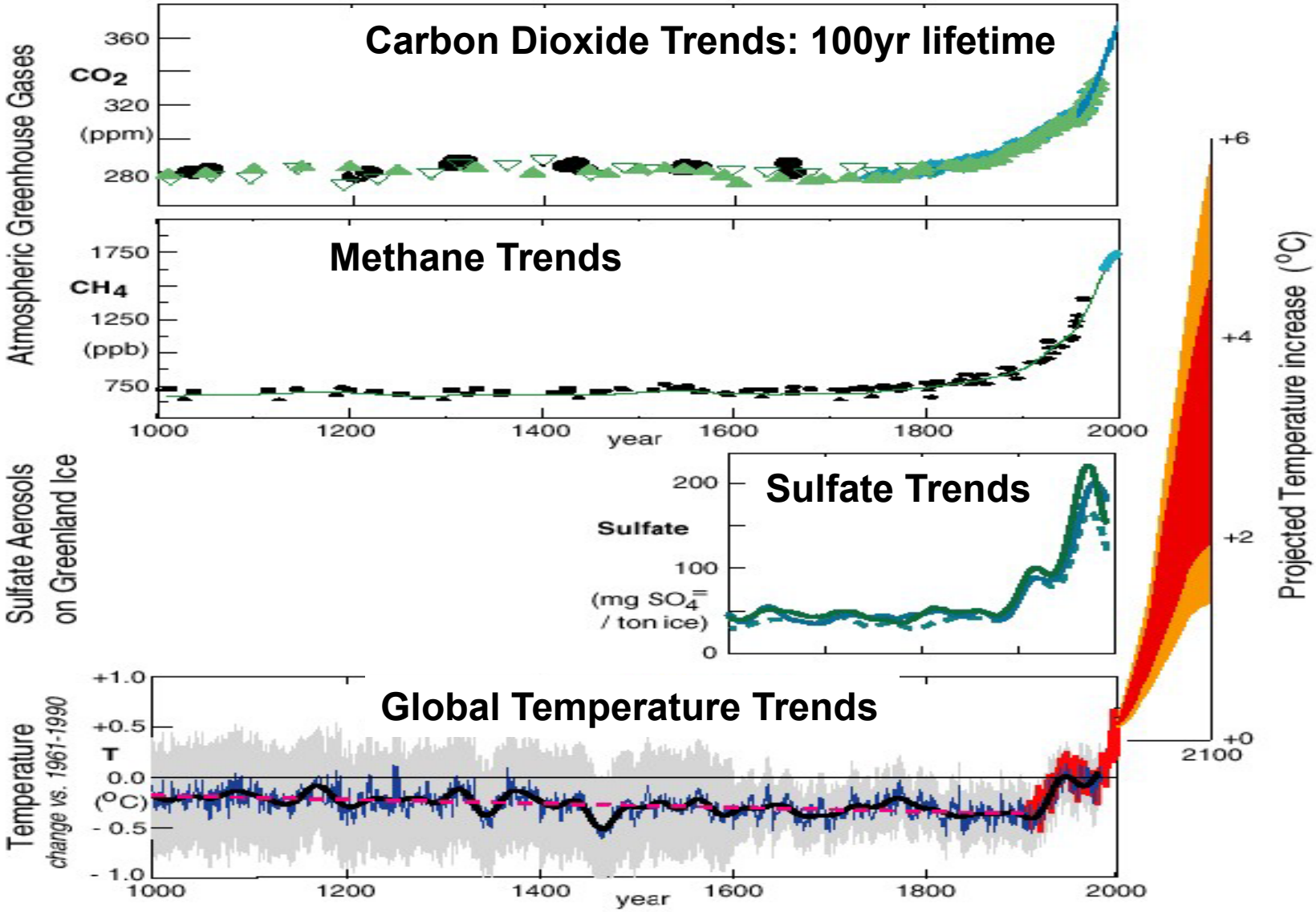

From M. Prather University of California at Irvine

Cloud Feedback is a key unknown

Stephens et al, 2005

•Climate Variability is key NOAA mission. It supports our mission for real-time cloud remote sensing.

•Clouds are major uncertainty in climate models. Satellite records are now long enough to begin to offer some relevant constraints if they are credible.

•The scientific relevance of the cloud climate records from EOS and NPOESS will be much larger if we can extend selected time series back in time using the AVHRR data.

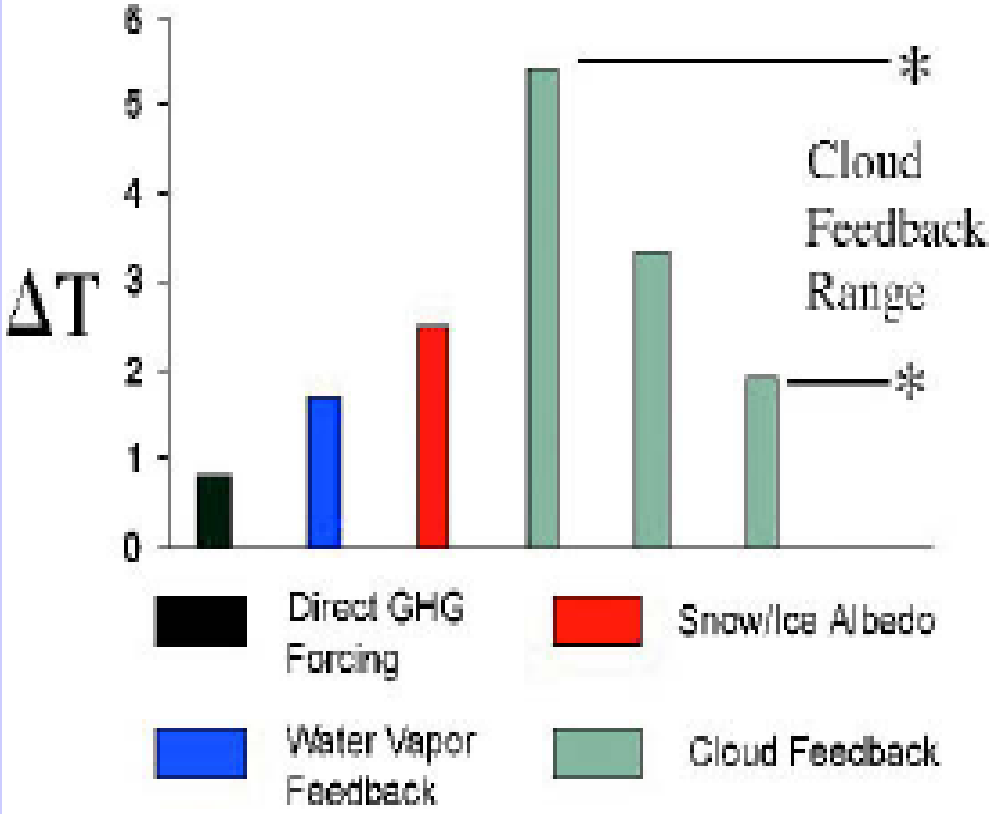

FIG. 13. The response of a single climate model to an imposed doubling of CO_2 as different feedbacks are systematically added in the model (adapted from Senior and Mitchell 1993). Different treatments of cloud processes in the model produce a large spread in predicted surface temperature due to CO_2 doubling.

Annual Cycle of Total Cloud Amount

0-30N Ocean

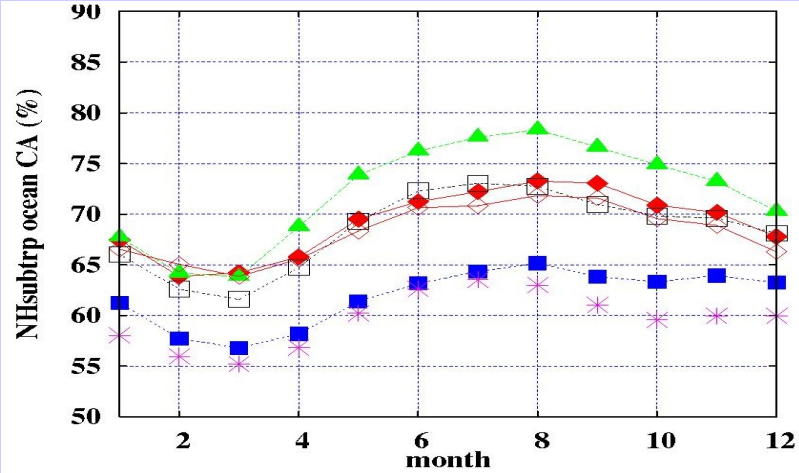

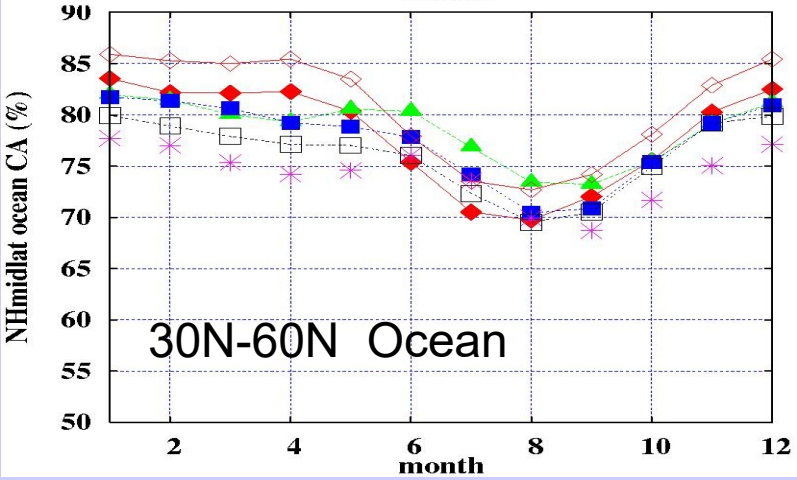

30S – 0N Ocean

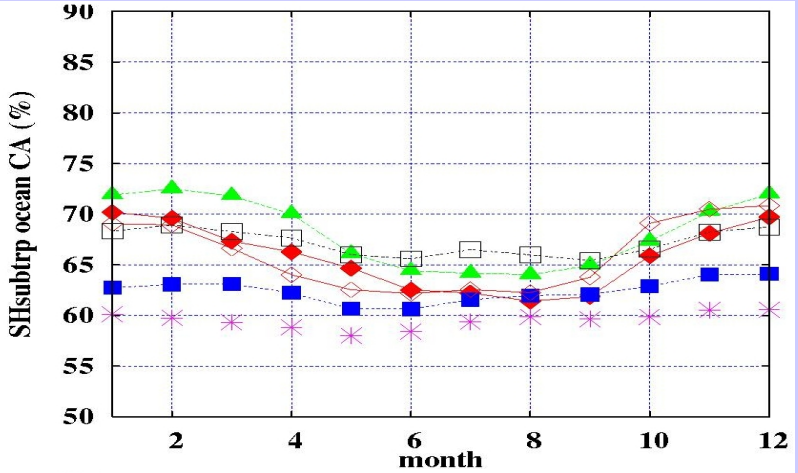

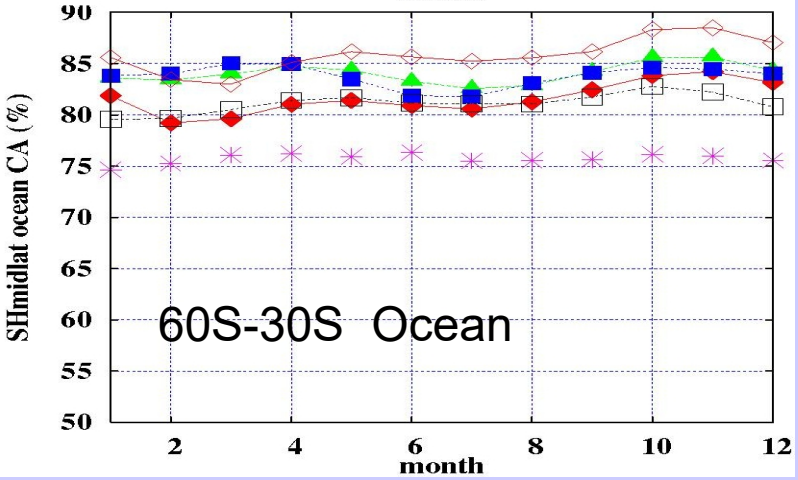

ISCCP, SOBS, UW/HIRS, TOVS/HIRS, PATMOS-x, MODIS

Seasonal cycles all agree through 10% spread on magnitudes.

Detection of High Cloud Differs Appreciably

A series of GEWEX workshops to assess the state of the various satellite cloud climatologies (ISCCP, HIRS, PATMOS-x, MODIS) found large disagreement in the high cloud long-term time-series. Work remains to be done.

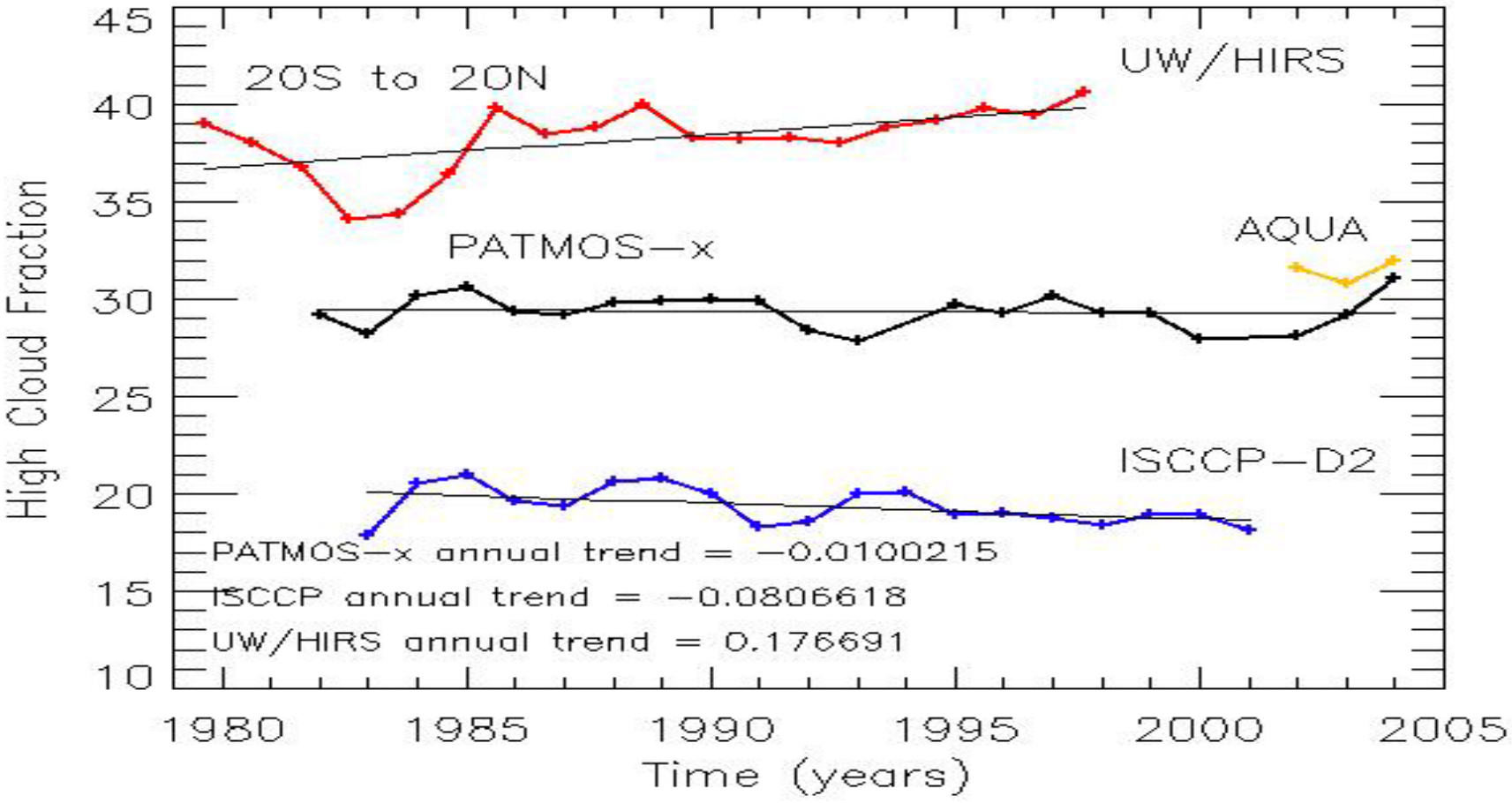

Striving for the Sustainable Society

"A place where humans and their use of the environment are in balance with nature"

"living in harmony with the environment and having resilience to natural hazards"